1-1-2018

Effect of Maternal Melatonin Levels during Late Gestation on the Programming and Metabolic Disposition of Adipose Tissue and Skeletal Muscle in Bovine Offspring

Robyn Carl Thompson

Effect of maternal melatonin levels during late gestation on the programming and metabolic disposition of adipose tissue and skeletal muscle in bovine offspring

By

Robyn Carl Thompson

A Thesis
Submitted to the Faculty of
Mississippi State University
in Partial Fulfillment of the Requirements
for the Degree of Master of Science
in Agriculture
in the Department of Animal and Dairy Sciences

Mississippi State, Mississippi

August 2018

Effect of maternal melatonin levels during late gestation on the programming and metabolic disposition of adipose tissue and skeletal muscle in bovine offspring

By

Robyn Carl Thompson

Approved:

_____

Derris D. Burnett
(Major Professor)

_____

Caleb O. Lemley
(Committee Member)

_____

Trent Smith
(Committee Member)

_____

Mark A. Crenshaw
(Committee Member)

_____

Jamie Larson
(Graduate Coordinator)

_____

George Hopper
Dean
College of Agriculture and Life Sciences

Name: Robyn Carl Thompson

Date of Degree: August 10, 2018

Institution: Mississippi State University

Major Field: Agriculture

Major Professor: Derris D. Burnett

Title of Study: Effect of maternal melatonin levels during late gestation on the programming and metabolic disposition of adipose tissue and skeletal muscle in bovine offspring

Pages in Study 158

Candidate for Degree of Master of Science

The objectives of this study were to determine: the effects of maternal melatonin (**MEL**) supplementation during late gestation on the histological and molecular regulation in the Longissimus dorsi (**LM**) muscle of fetal bovine offspring, composition and gene expression of fetal perirenal (**PR**) adipose tissue, and LM gene expression in postnatal offspring at birth and d 195 of age. Maternal supplementation of MEL during late gestation resulted in no difference in calf fetal body weight or birth weight. However, at d 195 of age, calves from MEL treated dams had an average body weight increase of 20 kg. Fetal LM weight and length tended to be increased in calves from MEL treated dams. Fetal gene expression of calves from MEL treated dams resulted in: increased LM adenosine monophosphate-activated protein kinase-α (**AMPK**) and decreased PR adiponectin (**ADIPOQ**), CCAAT enhancer binding protein alpha (**CEBPA**), proliferator activated receptor gamma (**PPARg**), and stearoyl-CoA desaturase (**SCD**). The improved metabolic status of LM coupled with the decrease in adipogenic gene expression, could result in calves from MEL treated dams having improved lean muscle accretion and reduced overall adiposity during postnatal development.

ACKNOWLEDGEMENTS

First, I would like to acknowledge my committee members, Dr.'s Derris Burnett, Caleb Lemley, Trent Smith and Mark Crenshaw, for their contributions to my research project. I'd especially like to thank Dr. Derris Burnett who has given me the opportunity to grow as a scientist through his guidance and support. I would like to give a special thanks to Dr. Caleb Lemley for helping me anytime that I needed extra support. I'd like to thank all the graduate students who have helped me along this journey. Lastly, I would like to thank my fiancé, Jamee Moran, for helping me countless hours on my research project and for encouraging me to always do my best, no matter how daunting the task.

TABLE OF CONTENTS

LIST OF TABLES

LIST OF FIGURES

CHAPTER I

INTRODUCTION

Prenatal myogenic and adipogenic development are a large determinant of a livestock animal's future postnatal production potential. Changes in the uterine environment during fetal development can alter offspring future growth potential and result in impaired growth with increased risk of diseases (Barker, 1997, 2004, 2007; Nathanielsz et al., 2007). This manipulation of the fetus leads to the concept of fetal programming. Fetal programming, also known as developmental programming, is a change in the growth and/or developmental trajectory due to a stimulus or insult during a critical time in development for the fetus resulting in persistent effects to development and production (Nathanielsz et al., 2007). Growth of livestock can be broken into various phases that roughly coincide with the putative stages of production. The phases for livestock growth consist of: conception to birth, birth to puberty, and puberty to maturity, with harvesting of animals preceding maturity. The first critical time point in growth for livestock is during prenatal development. The fetus at this point is completely dependent on the dam for nutrients. These nutrients are in maternal circulation and must cross over to the fetus through the placenta. The flux of nutrient substrates from dam to fetus is

dependent on the activity and accessibility of nutrient-specific transporters (Brett et al., 2014) as well as uterine blood flow (Reynolds and Redmer, 1995). Maternal uteroplacental blood flow increase exponentially throughout gestation in both sheep and cattle to sustain a growing fetus (Reynolds and Redmer, 1995; Meschia, 1983). In sheep with compromised pregnancies, both over- and undernutrition led to decreased placental vascularity and reduced fetal weight (Chandler et al., 1985; Leury et al., 1990; Newnham et al., 1991; Kelly, 1992; Arnold et al., 2001; Wallace et al., 2002; Redmer et al., 2004; Luther et al., 2005; Lemley et al., 2013). In rats, decreasing placental blood flow in the last trimester of gestation led to reduced placental weight, fetal weight, and litter size, confirming the role of placental blood flow in fetal growth restriction (Anderson et al., 2005). Several studies have shown that as blood flow increases throughout gestation, nutrient transport increases (Reynolds and Redmer, 1995; Reynolds et al., 2010). This increase in nutrient transport is not an increase in nutrient extraction per unit of blood, but due to an increase in placental perfusion and umbilical blood flow (Reynolds et al., 2010).

As previously mentioned, nutritional status of the dam and uteroplacental blood flow to fetus during gestation are scenarios that can lead to developmental programming of the offspring's long term metabolic efficiency and productivity. Research on nutritional effects on fetal development has shown overnutrition of dams during gestation to increase adipogenesis and fibrogenesis in fetal skeletal muscle (Duarte et al., 2014). Likewise, undernutrition has shown to decrease myofibril number and increase myofibril cross-sectional area (Funston et al., 2010). These scenarios indicate that muscle and adipose tissues are prone to manipulation during prenatal development and can be altered

to effect carcass quality and value. Based on these findings, providing optimal levels of nutrition to the dam and trying to enhance uteroplacental blood flow or counter restricted blood flow during gestation can lead to increased nutrient transport to the fetus, supporting proper development.

Since the dam is the sole source of nutrients to the developing fetus, strategies to maximize nutrient delivery and blood flow are needed in normal and compromised pregnancies to ensure proper development. Therapeutic supplements such as phosphodiesterase 5-specific inhibitors, have shown success in increasing blood flow. The vasodilatory action of these agents occurs through the action of nitric oxide (**NO**) inhibiting the breakdown of cyclic guanosine monophosphate (**cGMP**), resulting in relaxation of vascular smooth muscle (Michel, 2006). However, current literature is lacking data on the effects therapeutic blood flow supplements on uteroplacental hemodynamics in models of rescuing fetal growth restriction. Supplementation of melatonin (**MEL**) is currently being investigated as a novel approach on increasing uteroplacental blood flow (Richter et al., 2009; Lemley et al., 2012; Brockus et al., 2016b).

Melatonin is a natural hormone produced from the pineal gland and derived from tryptophan acting as a vasodilator, strong antioxidant, and signaling molecule for regulating natural circadian rhythm (Richter et al., 2009). Melatonin has also been shown to play a significant role in promoting the recruitment of brown adipose tissue (**BAT**) in newborn sheep (Seron-Ferre et al., 2015) as well as the browning of inguinal white adipose tissue in juvenile rats (Jimenez-Aranda et al., 2013). Brown adipose is extremely important in newborns due to its thermogenic properties. However, the fetal pineal gland

does not produce MEL, so all melatonin must come from maternal circulation. With the supplementation of MEL to the dam during gestation, maternal concentrations will increase thus increasing fetal concentrations. This increase in MEL leads to increased blood flow of the dam, thus amount of nutrients available to the fetus and with increased BAT recruitment can result in decreased newborn mortality (Carstens et al., 1997). A study conducted by Brockus and colleagues (2016a) found that Holstein calves from dams supplemented MEL during their last trimester of gestation, had significantly higher body weights at 8 to 9 weeks of age. They hypothesized that MEL supplementation to dams during late gestation possibly led to a response in the offspring resulting in developmental changes in skeletal muscle (Brockus et al., 2016a).

Therefore, the objectives of this study were to determine: the effects of maternal MEL supplementation during late gestation on the histological and molecular regulation in the Longissimus dorsi (**LM**) muscle of fetal bovine offspring, composition and gene expression of fetal perirenal (**PR**) adipose tissue, and LM gene expression in postnatal offspring at birth and d 195 of age.

1.1 References

Anderson, C. M., F. Lopez, H. Y. Zhang, K. Pavlish, and J. N. Benoit. 2005. Reduced uteroplacental perfusion alters uterine arcuate artery function in the pregnant Sprague-Dawley rat. Biol. Reprod. 72:762–766.

Arnold, D. R., A. N. Scheaffer, D. A. Redmer, J. S. Caton, and L. P. Reynolds. 2001. Effect of nutrient restriction on placental vascularity and fetal growth in sheep. Biol. Reprod. 64:352.

Barker, D. J. and P. M. Clark. 1997. Fetal undernutrition and disease in later life. Rev. Reprod. 2:105–112.

Barker, D. J. 2004. Developmental origins of well being. Philos. Trans. R. Soc. Lond. 359:1359–1366.

Barker, D. J. 2007. Introduction: The window of opportunity. Symposium: Novel concepts in the developmental origins of adult health and disease. J. Nutr. 137:1058–1059.

Brett, K. E., Z. M. Ferraro, J. Yockell-Lelievre, A. Gruslin, and K. B. Adamo. 2014. Maternal–Fetal Nutrient Transport in Pregnancy Pathologies. Int. J. Mol. Sci. 15:16153-16185.

Brockus, K. E., C. G. Hart, B. O. Fleming, T. Smith, S. H. Ward, C. O. Lemley. 2016a. Effects of Supplementing Holstein Heifers with Dietary Melatonin during Late Gestation on Growth and Cardiovascular Measurements of their Offspring. Reprod. Dom. Anim. 51: 240-247; doi: 10.1111/rda.12672.

Brockus, K. E., C. G. Hart, C. L. Gilfeather, B. O. Fleming, and C. O. Lemley. 2016b. Dietary melatonin alters uterine artery hemodynamics in pregnant Holstein heifers. Dom. Ani. Endo. 55:1-10.

Carstens, G. E., P. C. Mostyn, M. A. Lammoglia, R. C. Vann, R. C. Apter, and R. D. Randel. 1997. Genotypic effects on norepinephrine-induced changes in thermogenesis, metabolic hormones, and metabolites in newborn calves. J. Anim. Sci. 75:1746–1755.

Chandler, K.D., B. J. Leury, A. R. Bird, and A. W. Bell. 1985. Effects of undernutrition and exercise during late pregnancy on uterine, fetal and uteroplacental metabolism in the ewe. Br. J. Nutr. 53:625–635.

Duarte, M. S., M. P. Gionbelli, P. V. R. Paulino, N. V. L. Serão, C. S. Nascimento, M. E. Botelho, T. S. Martins, S. C. V. Filho, M. V. Dodson, S. E. F. Guimarães, and M. Du. 2014. Maternal overnutrition

enhances mRNA expression of adipogenic markers and collagen deposition in skeletal muscle of beef cattle fetuses. J. Anim. Sci. 92:3846–3854. https://doi.org/10.2527/jas.2014-7568.

Funston, R. N., D. M. Larson, and K. A. Vonnahme. 2010. Effects of maternal nutrition on conceptus growth and offspring performance: Implications for beef cattle production. J. Anim. Sci. 88:E205-E215. doi:10.2527/jas.2009-2351.

Jimenez-Aranda, A., G. Fernandez-Vazquez, D. Campos, M. Tassi, L. Velasco-Perez, D. X. Tan, R. J. Reiter, and A. Agil. 2013. Melatonin induces browning of inguinal white adipose tissue in Zucker diabetic fatty rats. J. Pineal. Res. 55:416-423. Doi:10.1111/jpi.12089.

Kelly, R. W. 1992. Nutrition and placental development. Proc. Nutr. Soc. Au. 17:203–211.

Lemley, C. O., A. M. Meyers, L. E. Camacho, T. L. Neville, D. J. Newman, J. S. Caton, and K. A. Vonnahme. 2012. Melatonin supplementation alters uteroplacental hemodynamics and fetal development in an ovine model of intrauterine growth restriction. Am. J. Physiol. Regul. Integr. Comp. Physiol. 302: 454–467; doi:10.1152/ajpregu.00407.2011.

Lemley, C. O., L. E. Camacho, and K. A. Vonnahme. 2013. Uterine Infusion of Melatonin or Melatonin Receptor Antagonist Alters Ovine Feto-Placental Hemodynamics During Midgestation. Bio. of Repro. 89:41-49.

Leury, B.J., A. R. Bird, K. D. Chandler, and A. W. Bell. 1990. Glucose partitioning in the pregnant ewe: effects of undernutrition and exercise. Br. J. Nutr. 64:449–462.

Luther, J. S., D. A. Redmer, L. P. Reynolds, and J. M. Wallace. 2005. Nutritional paradigms of ovine fetal growth restriction: implications for human pregnancy. Human. Fertil. 8:179–187.

Meschia, G. 1983. Circulation to female reproductive organs. In Handbook of Physiology, Sect. 2, Vol. III, part 1, ed. Shepherd JT & Abboud FM, pp. 241–269. American Physiological Society, Bethesda, MD.

Michel, T. 2006. Treatment of myocardial ischemia. Pages 823–844 in Goodman & Gilman's The Pharmacological Basis of Therapeutics. 11th ed. L. L. Brunton, J. S. Lazo, and K. L. Parker, ed. McGraw-Hill, New York, NY.

Nathanielsz, P. W., L. Poston, and P. D. Taylor. 2007. In utero exposure to maternal obesity and diabetes: Animal models that identify and

characterize implications for future health. Clin. Perinatol. 34:515–526.18063102

Newnham JP, Kelly RW, Patterson L & James I. 1991. The influence of maternal undernutrition in ovine twin pregnancy on fetal growth and Doppler flow-velocimetry waveforms. J Dev Physiol16, 277–282.

Redmer, D. A., R. P. Aitken, J. S. Milne, P. P. Borowicz, M. A. Borowicz, K. D. Kraft, L. P. Reynolds, J. S. Luther, and J. M. Wallace. 2004. Influence of maternal nutrition on placental vascularity during late pregnancy in adolescent ewes. *Biol. Reprod.* 70**:**(Suppl 1), 150.

Reynolds, L. P., and D. A. Redmer. 1995. Utero-placental vascular development and placental function. J. Anim. Sci. 73:1839–1851.7545661

Reynolds, L. P., P. P. Borowicz, J. S. Caton, K. A. Vonnahme, J. S. Luther, D. S. Buchanan, S. A. Hafez, A. T. Grazul-Bilska, and D. A. Redmer. 2010. Utero-placental vascular development and placental function: An update. Invited review. Special Issue: Placental Developmental Biology. J. Dev. Biol. 54:355–366.

Richter, H. G., J. A. Hansell, S. Raut, and D. A. Giussani. 2009. Melatonin improves placental efficiency and birth weight and increases the placental expression of antioxidant enzymes in undernourished pregnancy. J. Pineal. Res. 46:357–364.

Seron-Ferre, M., H. Reynolds, N. A. Mendez, M. Mondaca, F. Valenzuela, R. Ebensperger, G. J. Valenzuela, E. A. Herrera, A. J. Llanos, and C. Torres-Farfan. 2015. Impact of maternal melatonin suppression on amount and functionality of brown adipose tissue (BAT) in newborn sheep. Fendo. 5:1-11; doi: 10.3389/fendo.2014.00232

Wallace, J.M., D. A. Bourke, R. P. Aitken, N. Leitch, and W. W. Hay. 2002. Blood flows and nutrient uptakes in growth-restricted pregnancies induced by overnourishing adolescent sheep. Am. J. Physiol. 282**:**R1027–R1036.

CHAPTER II

LITURATURE REVIEW

2.1 Fetal Programming in Humans and Livestock

The time and prevailing environmental conditions that humans and animals are subjected to while *in utero* leads to long term developmental and economic consequences. In child health and development, fetal growth restriction resulting in low birth weight infants' effects on average over 350,000 infants a year in the U.S. totaling approximately $363,000 per child in long term medical bills (Luther et al., 2005; Wallace et al., 2006; NVSR, 2009). The effects of low birth weight not only impact the neonate's short-term chances of survival, it extends into adolescence and adulthood potentially impacting their long-term quality of life. Lifelong consequences of developmental programming can be linked to increased risk of cardiovascular disease, obesity, diabetes, immune dysfunction, stunted growth, and more (Barker, 2004, 2007). Fetal programming due to growth restriction is not only an issue in humans, but in livestock species as well.

In livestock, long-term health consequences resulting from a compromised uterine environment are not as impactful due to their relatively short lifespan. Instead, livestock animals affected by fetal programming can have dramatically altered carcass composition which results in increased adiposity and reduced meat yield and quality. This decrease is

production potential leads to inferior animals that take more resources to reach market. Fetal growth restriction in livestock occurs commonly from poor nutritional environment of the dam during gestation. Factors that influence the nutritional environment of the dam consist of: animals that have multiple fetuses or litters; genetically selecting for greater milk production; and the breeding of livestock during warm seasons with higher temperatures and poor-quality forage with no supplementation (Wu et al., 2006). As researches have witnessed with humans, fetal programming in livestock results in increased neonatal mortality and morbidity. A larger issue with livestock is the reduced production of affected offspring that consist of: decreased growth rate due to reduced efficiency and ADG, poor carcass composition that contain higher amounts of adipose tissue with reduced myofibril numbers and increased connective tissue that results in inferior meat quality, and many diseases and other disorders (Wu et al., 2006; Reynolds et al., 2006).

Environmental stressors such as nutrition of the dam can impact proper placental development, leading to reduced placental vascular function and compromised fetal growth. These stressors without maternal adaptation during gestation can reduce uteroplacental blood flow by hampering proper vascular bed formation resulting in fetal growth restriction or death (Vandenbosche and Kirchner, 1998; Funston et al., 2010; Vonnahme et al., 2013). Nutrient restriction of the dam during early to mid-embryonic development in cattle may appear to be unimportant due to size and requirements of the fetus during this time and research has shown that 75% of fetal growth and development occurs in the last 2 months gestation (Robinson et al., 1977). This, however, is a very important time as maximal placental growth, differentiation, and vascularization, along

with fetal organogenesis is occurring which lays the foundation for long-term future development of the fetus (Funston et al., 2010). Restrictions during this phase could reduce the size of the placenta and capacity for nutrient transfer influencing fetal growth and development resulting in reduced birth weight and inferior growth and production (Robinson et al., 2014). A study by Long and colleagues in 2010 found that restricting heifers at 55% of NRC recommendations for early gestation resulted in no change to birth weight, postnatal growth, or carcass characteristics (Long et al., 2010). However, the offspring from this study exhibited larger myofiber cross-sectional area (Long et al., 2010). Overall findings of early gestation nutrient restriction show a tendency for the offspring to have reduced myofiber number due to intrauterine growth retardation (Robinson et al., 2013).

Mid to late-gestational nutrient restriction can occur with rising nutritional demands of the fetus. Restrictions in cattle at this point in fetal development can lead to increased perinatal mortality, reduced birthweights, and reduced postnatal growth (Kroker and Cummins, 1979). Fetal muscle development in cattle initially occurs within the first 2 months post-conception, though very few muscle fibers are formed during this time, the impact from nutrient restriction isn't as detrimental (Russell and Oteruelo, 1981). Most of muscle cell formation occurs between 2 and 8 months of gestation with insults to growth resulting in detrimental effects to muscle fiber number leading to irreversible effects on meat composition throughout life (Russell and Oteruelo, 1981; Zhu et al., 2006, Du et al., 2010). Developmental programming not only impacts yield of meat due to reduction of muscle fiber numbers, but also negatively impacts meat quality.

Meat tenderness and palatability are very important to consumers, with tenderness rated as the most important contributor to beef palatability in the United States (Koohmaraie et al., 2002). The tenderness of meat is made up of a contribution of several effects that include muscle fiber size and density, solubility of connective tissue (mainly collagen), and the amount and distribution of marbling. Understanding the critical time point in development for the muscle, adipose, and connective tissue components within skeletal muscle and how they can be altered, is imperative for the economics of the meat industry. Each tissue and their fetal development will be discussed in further detail below.

2.2 Muscle Development in Cattle

In the livestock industry, animals raised for their skeletal muscle provide meat for consumer demands. Skeletal muscle is a heterogeneous tissue made up of myocytes, adipocytes, and fibroblasts, with the ratio of the cells determining muscle composition, product yield, and meat quality. During fetal development, muscle accretion is accomplished through myofiber hyperplasia and hypertrophy. This differs from postnatal muscle accretion since the total number muscle fibers are determined before birth and myofibers can no longer undergo hyperplasia; therefore, postnatal muscle accretion is the result of hypertrophy of existing fibers (Du et al., 2010). The developmental foundation for each skeletal muscle group begins with a finite pool of multipotent mesenchymal stem cells that differentiate into mostly myocytes, with the remainder committing to either adipocytes for intramuscular fat accumulation sites, or fibroblasts for structural connective tissue (Dodson et al., 2010; Du et al., 2010; Yan et al., 2012). The number of cells that commit to each of these lineages can be altered by environmental stressors such

as nutritional status of the dam, however, primary muscle fiber number seems to be resistant to such influences (Dwyer et al., 1994; Zhu et al., 2006; Duarte et al., 2014). Skeletal muscle development initiates via mesenchymal stem cells receiving signals from neighboring tissue promoting their differentiation into myoblasts (Kollias and McDermott, 2008; Du et al., 2010). These signals consist of Wingless and Int (**Wnt**) and Sonic hedgehog which regulate the expression of paired box 3 and 7 (**Pax3, Pax7**). The activation of Pax3 and Pax7 then leads to the activation of myogenic regulatory factors such as myogenic factor 5 (**Myf5**), myogenic differentiation 1 (**MyoD**), and myogenin (**MyoG**) (Buckingham, 2001; Kassar-Duchossoy et al., 2005; Du et al., 2010). Various myogenic regulatory factors work together to promote differentiation of proliferating myoblast into multinucleated myotubules, eventually forming mature muscle fibers through a process known as myogenesis (Keren et al., 2006; Kollias and McDermott, 2008; Du et al., 2010). Fetal muscle development, or myogenesis, can be broken up into two stages. First stage of myogenesis begins in early embryonic development with myocytes proliferating into primary muscle fibers (Du et al., 2010). These primary fibers are the foundation to which muscle groups form, acting as scaffolding for muscle fibers to replicate. The second stage of myogenesis is responsible for the majority of myofibers that make up skeletal muscle. This is especially important since secondary myogenesis ends before birth, resulting in the offspring's total muscle fiber number and future production potential being established before birth (Stickland, 1978; Karuatatne et al., 2005; Du et al., 2010).

In cattle, primary muscle fibers begin developing within the first 2 months and roughly ends by 4 months post conception. Secondary muscle fibers begin forming

between 2 to 8 months post conception (Russell and Oteruelo, 1981). Since the majority of muscle fibers are established at this time, maternal nutritional insults during this mid- to late-gestational period can lead to irreversible reduction in myofiber numbers (Zhu et al., 2006). In sheep, maternal nutrient restriction during mid- to late-gestation resulted in reduced total secondary muscle fibers (Zhu et al., 2004). In pigs, maternal undernutrition from days 20 to 90 of pregnancy reduced piglet birth weight and muscle fiber number (Dwyer et al., 1994).

Another factor controlling prenatal and postnatal metabolism and muscle development is the insulin-like growth factor signaling system (Bass et al., 1999; Holt et al., 2012; Gonzalez et al., 2013). In this system, insulin-like growth factor 2 (**IGF2**) is mainly responsible for fetal growth and muscle development as insulin-like growth factor 1 (**IGF1**) is mainly responsible for postnatal growth and muscle development (Florini et al., 1991; Haig and Graham, 1991; Braxton et al., 1993; Bass et al., 1999; Le Roith et al., 2001; Gluckman and Pinal, 2003; Gonzalez et al., 2013). Liu et al. in 1993, looked at the effects of IGF1, IGF1 receptor (**IGF1R**), and IGF2 on fetal growth and development. They found that knocking out IGF1R led to dwarfism and neonatal lethality, and that the reduced body weight was attributed to suppressed muscle fiber hypoplasia rather than hypertrophy in mice (Liu et al., 1993). Adams and Haddad (1996) found that rats with increased IGF1 resulted in increased muscle mass, fiber size, and protein-to-body weight ratio, and that IGF1 expression preceded muscle fiber hypertrophic phase.

As stated above, restricted offspring have permanent changes to muscle fiber number and size. They develop with lower muscle fiber numbers with each fiber being larger than normal (Foxcroft el al., 2006; Alvarenga et al., 2013). This is due to the

inverse relationship between muscle fiber size and number (Rehfeldt and Kuhn, 2006). This permanent reduction in muscle fiber number inhibits the potential for postnatal catch-up of low birth weight offspring with those born without restrictions. Hypertrophy of existing muscle fibers is the only form of postnatal muscle accretion. Reduced muscle fiber numbers reduce meat yield and increased myofibril size that leads to reduced meat quality (Klosowska et al., 1979; Fiedler et al., 1999). These data indicate that livestock species in mid- to late-gestation are susceptible to fetal programming that can result in the permanent reduction in muscle cell number and growth trajectory ultimately reducing productivity and efficiency.

2.3 Adipose Development in Cattle

In addition to superior muscle development, producers would like to increase intramuscular fat deposition (marbling) within skeletal muscle without wasting excessive resources into undesirable adipose depots such as visceral, subcutaneous, and intermuscular adipose depots. This is due to marbling contributing to the flavor and juiciness of meat, increasing economic value as marbling increases (Crouse et al., 1983; Hausman et al., 2009; Du et al., 2017). The extent of adipogenesis during fetal development is critical for determining the amount of marbling that can develop postnatally. Adipose accumulation in visceral, subcutaneous, and intermuscular depots lowers the efficiency and economic value of livestock. This leaves researchers with the task of selectively enhancing marbling deposition, which is the last adipose depot to accumulate fat, while limiting formation and accretion of adipose tissue in the higher metabolic priority, yet more undesirable depots (Crouse et al., 1983; Mir et al., 2002;

Hausman et al., 2009; Du et al., 2017). The fetal period is an underappreciated window to selectively impact these depots.

The total mass or volume of adipose tissue is determined by the number of adipocytes and their respective size (Spalding et al., 2008). During the fetal stage, adipogenesis starts with mesenchymal stem cells that can either differentiate into myocytes, adipocytes, or fibroblasts. When mesenchymal stem cells commit to the adipogenic lineage, starting around mid-gestation, they become future sites for adipose tissue accretion and lipid accumulation. Permanent differentiation into adipocytes requires self-reinforcing regulation of transcription factors CCAAT enhancer binding protein (**CEBP**) and peroxisome proliferator activated receptor gamma (**PPARg**) (Clarke et al., 1997; Wu et al., 1999). When CEBP alpha (**CEBPA**) is induced and binds to the promoter of PPARg, it activates the expression of PPARg which further stimulates the expression of CEBPA (Clarke et al., 1997; Wu et al., 1999). With the activation and expression of PPARg, terminal adipogenic differentiation is achieved through the induction of many genes that are important for triglyceride uptake and storage (Frohnert et al., 1999; Rosen and MacDougald, 2006).

Maternal manipulation strategies can be applied during early fetal development, to alter mesenchymal stem cell commitment into adipocytes to enhance adipogenesis (Feve, 2005). This can result in improved intramuscular fat and meat quality; however, it can also lead to over fattening, decreased feed efficiency, and lower retail yield. Studies with nutrient-restricted mothers have shown adipose tissue development impaired, but due to adipose tissue plasticity, offspring born to restricted mothers often have compensatory gain of adipose tissue leading to fatter offspring with decreased feed

efficiency and lower muscle mass (Zhu et al., 2006; Wang et al., 2017). The overnutrition of pregnant ewes fed 150% of NRC requirements (NRC, 1985) has shown to increase adipogenesis in skeletal muscle (Tong et al., 2008, 2009). This increased adiposity in skeletal muscle can result in higher quality grades increasing the value of the carcass, though it increases external fat as well due to intramuscular deposition being last in priority. This increase in other fat depots lowers the yield grade of carcasses due to trim loss resulting in a decrease in closely trimmed retail cuts. However, in cases of maternal undernutrition, adipose tissue development is impaired, but due to adipose tissue plasticity, offspring born to restricted mothers often have compensatory gain of adipose tissue (Zhu et al., 2006; Wang et al., 2017). The chronological formation of adipose depots may still hold the key to enhancing marbling while limiting overall adiposity. Intramuscular adipocyte development primarily occurs during late gestation up to 250 days of age (Du et al., 2017). In beef cattle, providing high-energy supplementation to early weaning calves before 250 days of age will enhance intramuscular formation resulting in increased marbling during fattening stages (Corah and McCully, 2007; Du et al., 2013). While postnatal feeding strategies can be used to enhance the accretion of these depots, the initial foundation of cells and lipid accumulation within begins during fetal development (Corah and McCully, 2007; Du et al., 2013).

In livestock, dietary energy that is above the metabolic needs of the animal is stored as adipose tissue and can lead to obesity if left uncontrolled. Though in some mammalian species, excessive energy storage during specific times of the year is needed to survive. These mammals exhibit seasonal changes in adiposity that are induced either by changes in photoperiod or an endogenous clock (Bartness et al., 2002). These seasonal

changes effect lipid storage in white adipose tissue (**WAT**; the major storage of energy in mammals) and brown adipose tissue (**BAT**; responsible for heat production via thermogenesis). These environmental ques are critical for the secretion of melatonin, a naturally produced hormone that is secreted by the pineal gland, and its role with maintaining natural circadian rhythm.

2.4 Intramuscular Fibrogenesis in Cattle

Connective tissue not only plays a role with muscle physiology but is a major determinant of consumer perception of meat tenderness which reported to be the single most desirable characteristic of beef to consumers (Huffman et al., 1996). The connective tissue that underlies this meat quality trait arises from fibroblast during early development and begins with commitment of mesenchymal stem cells to the myogenic, adipogenic, or firbogenic lineage (Aguiari et al., 2008; Kuang et al., 2008; Yablonka-Reuveni et al., 2008). These connective tissues in various types of muscles serve as structural support by binding muscle cells together and insuring proper alignment, or to contract providing motion (Borg and Caulfield, 1980). There are three layers of connective tissues within skeletal muscle: epimysium surrounds the entire muscle, perimysium is a sheath surrounding bundles of muscle fibers, and endomysium surrounds individual muscle cells (Borg and Caulfield, 1980). These connective tissues are made up in large part by collagen and collagen cross-links, that provides a strong and elastic support. Connective tissue development is also influenced by growth retardation that results in increased collagen content along with an increase in adipogenesis within fetal skeletal muscle (Duarte et al., 2014). Studies investigating fibrogenesis in overfed ewes and malnutrition sows have both shown that insults to the nutrient environment of the

dam can program the fetus to have increased fibrosis which impairs muscle function and increase meat toughness (Huang et al., 2010; Karunaratne et al., 2005).

2.5 Therapeutic Melatonin Supplementation in Normal and Compromised Pregnancies

In compromised pregnancies, reduced uterine blood flow and placental vascularity leads to reduced umbilical blood flow with inferior nutrient delivery resulting in fetal growth restriction (Thureen et al., 1992; Rigano et al., 2001; Wallace et al., 2002; Regnault et al., 2003; Kwon et al., 2004; Reynolds et al., 2005). Low birth weight offspring born to dams with compromised pregnancies have slower growth rates, increased chances of diseases, and increased postnatal adiposity (Barker and Clark, 1997; Zhu et al., 2006). Therefore, studies have experimented with therapeutic treatment of compromised pregnancies and blood flow with the use of vasodilators.

Melatonin (**MEL**) is a highly conserved compound that exhibits numerous receptor mediated and receptor independent physiological effects. Melatonin is produced by the pineal gland in the mammalian brain and in addition to its best-known effects on circadian rhythm (Reiter, 2003), it is a powerful scavenger of free radicals (Reiter et al., 1995; Manchester et al., 2015), involved in vasodilation (Lemley et al., 2012; Brockus et al., 2016b), and tissue level metabolism (Ha et al., 2006; Torres-Farfan et al., 2008; Stratos et al., 2012). Our understanding of the function of MEL begins with its discovery and isolation by Aaron Lerner and colleagues at Yale University (Lerner et al., 1958) who hoped to use it as a treatment for reversing the darkening effects of melanocyte stimulating hormone on skin (Lerner et al., 1958). Melatonin was later suggested to play a role in affecting the brain, gonads, and other neuroendocrine systems (Wurtman et al.,

1968; Reiter et al., 1978). The pineal gland secretes melatonin during the absence of light induced stimulus (Axelrod et al., 1964). Light is first detected by retinal ganglion cells and transmitted via a multisynaptic pathway to the pineal gland (Larsen et al., 1998). This neurochemical signal of photoperiod is delivered by the sympathetic nervous system (**SNS**) and causes pinealocytes to secrete an endocrine signal into the bloodstream, MEL. Light stimulus causes an interruption in the negative feedback loop needed for MEL secretion, blocking the effects on short-day seasonal reproduction systems and seasonal changes in adiposity (Bartness et al., 1984; Vitale et al., 1985; Moore, 1996).

The potential for MEL to prevent or rescue compromised pregnancies has gained interest in recent years. Studies in MEL supplementation to sheep with compromised pregnancies has shown to alter uteroplacental hemodynamics and fetal development (Lemley et al., 2012, 2013). Likewise, in pregnant Holstein heifers, blood flow was improved with supplemental MEL during late gestation resulting up to a 25% increase in uterine blood flow of MEL treated heifers compared to control (Brockus et al., 2016b). Offspring born to MEL supplemented Holstein heifers exhibited significantly greater body weights at 8 to 9 weeks of age (Brockus et al., 2016a).

Once secreted, MEL exhibits its direct effects through binding to MEL receptors on various tissues (Bartness et al., 2002). The known MEL receptors include MT1 and MT2 (Dubocovich et al., 1998, 2010) and their presence has been detected on peripheral tissues including muscle (Stratos et al., 2012) and adipose tissue (Le Gouic et al., 1997). In skeletal muscle, binding of MEL to these receptors stimulates glucose transport into muscle cells (Ha et al., 2006), increases the number of satellite cells, reduces inflammation, and inhibits apoptosis by modulating associated signaling pathways

allowing for cell regeneration (Stratos et al., 2012). Melatonin increased insulin receptor substrate-1 is phosphorylated and the activity of phosphatidylinositol 3-kinase is increased, resulting in increased glucose uptake (Ha et al., 2006). In adipose tissue, a study supplementing rats with 0.4 μg/ml of MEL in water bi-weekly found a reduction in intra-abdominal adiposity by 20%, plasma leptin (ng/ml) by 33%, and plasma insulin (ng/ml) by 25% (Wolden-Hanson et al., 2000). Seasonal studies show a positive correlation between increased adiposity and MEL levels (Bartness et al., 1984; Wade et al., 1984; Bartness et al., 1985). This increase in the sympathetic drive causes an increase in release of norepinephrine, which effects WAT and BAT. Melatonin indirectly effects WAT through increased norepinephrine and epinephrine which results in increased lipolysis (Youngstrom and Bartness, 1998; Demas and Bartness, 2001). Norepinephrine stimulates increased BAT thermogenesis through cAMP-PKA signaling cascade that causes the phosphorylation of PKA to activate hormone sensitive lipase (**HSL**) (Townsend and Tseng, 2012). Hormone sensitive lipase cleaves triglycerides into free fatty acids that are shuttled into the mitochondria to undergo β-oxidation for ATP production or activate uncoupling protein 1 (**UCP1**) to produce heat via thermogenesis (Townsend and Tseng, 2012). Thermogenesis is important for heat production in newborns, increasing survival and homeothermy (Himms-Hagen, 1990). This links BAT thermogenesis to newborn mortality rate, in which potentially increasing BAT recruitment or thermogenic properties could lead to a decrease in newborn loss due to hypothermia (Carstens et al., 1997). Studies in various species have shown MEL to increase the amount of BAT (Jimenez-Aranda et al., 2013; Seron-Ferre et al., 2015),

however MEL's mechanism of action on BAT recruitment is still unknown (Bartness et al., 2002).

Given its widespread role in central and peripheral metabolism and physiological function, MEL has shown promise as a potential therapeutic agent to prevent or rescue compromised pregnancies. In addition, given its role in directly modulating muscle growth and repair as well as modulating brown and white adipose tissue metabolism, MEL supplementation during gestation has the potential to improve the development of these economically important tissues to improve efficiency and quality of beef production. The underlying tissue level responses in fetal carcass tissues to maternal MEL supplementation mechanisms have not been thoroughly investigated which is the objective of the current research. The operational hypothesis is that maternal supplementation of MEL during mid- to late-gestation programs the fetus for superior postnatal development and improved skeletal muscle growth through a combination of direct and indirect mechanisms.

2.6 References

Adams, G. R. and F. Haddad. 1996. The relationships among IGF-1, DNA content, and protein accumulation during skeletal muscle hypertrophy. App. Physio. 81: 2509-2516

Aguiari, P., S. Leo, B. Zavan, V. Vindigni, A. Rimessi, K. Bianchi, C. Franzin, R. Cortivo, M. Rossato, R. Vettor, G. Abatangelo, T. Pozzan, P. Pinton, and R. Rizzuto. 2008. High glucose induces adipogenic differentiation of muscle-derived stem cells. Proc. Natl. Acad. Sci. USA 105:1226–1231.

Alvarenga, A. L. N., H. Chiarini-Garcia, P. C. Cardeal, L. P. Moreira, G. R. Foxcroft, D. O. Fontes, and F. R. C. L. Almeida. 2013. Intra-uterine growth retardation affects birthweight and postnatal development in pigs, impairing muscle accretion, duodenal mucosa morphology and carcass traits. Repro. Fert. Develop. 25:387:395

Axelrod J, Wurtman RJ, Winget CM: Melatonin synthesis in the hen pineal and its control by light. Nature 210:1134, 1964

Barker DJ, Clark PM. Fetal undernutrition and disease in later life. Rev Reprod 2: 105–112, 1997.

Barker, D. J. 2004. Developmental origins of well being. Philos. Trans. R. Soc. Lond. 359:1359–1366

Barker, D. J. 2007. Introduction: The window of opportunity. Symposium: Novel concepts in the developmental origins of adult health and disease. J. Nutr. 137:1058–1059

Bartness TJ, Wade GN. Photoperiodic control of body weight and energy metabolism in Syrian hamsters (Mesocricetus auratus): role of pineal gland melatonin gonads and diet. Endocrinology 114:492–498, 1984.

Bartness TJ, Wade GN. Body weight food intake and energy regulation in exercising and melatonin-treated Siberian hamsters (Phodopus sungorus sungorus). Physiol Behav 35:805–808, 1985.

Bartness, T. J., G. E. Demas, C. K. Song. 2002. Seasonal Changes in Adiposity: the Roles of the Photoperiod, Melatonin and Other Hormones, and Sympathetic Nervous System. Exp. Biol. Med. 227: 363-376

Bass, J., J. Oldham, M. Sharma, and R. Kambadur. 1999. Growth factors controlling muscle development. Dom. Ani. Endo. 17: 191-197

Borg, T. K. and J. B. Caulfield. 1980. Morphology of connective tissue in skeletal muscle. Tissue & Cell. 12:197-207

Braxton, L., Hollingshead P, Warburton C, Dowd M, Pitts-Meek S, Dalton D, Gillett N, Stewart T A. 1993. IGF-I is required for normal embryonic growth in mice. Genes Dev 7:2609–2617, pmid:8276243

Brockus, K. E., C. G. Hart, B. O. Fleming, T. Smith, S. H. Ward, C. O. Lemley. 2016a. Effects of Supplementing Holstein Heifers with Dietary Melatonin during Late Gestation on Growth and Cardiovascular Measurements of their Offspring. Reprod. Dom. Anim. 51: 240-247; doi: 10.1111/rda.12672

Brockus, K. E., C. G. Hart, C. L. Gilfeather, B. O. Fleming, and C. O. Lemley. 2016b. Dietary melatonin alters uterine artery hemodynamics in pregnant Holstein heifers. Dom. Ani. Endo. 55:1-10

Buckingham, M. 2001. Skeletal muscle formation in vertebrates. Curr. Opin. Genet. Dev. 11:440–448.

Carstens, G. E., P. C. Mostyn, M. A. Lammoglia, R. C. Vann, R. C. Apter, and R. D. Randel. 1997. Genotypic effects on norepinephrine- induced changes in thermogenesis, metabolic hormones, and metabolites in newborn calves. J. Anim. Sci. 75:1746–1755.

Clarke, S. L., C. E. Robinson, and J. M. Gimble. 1997. CAAT/ enhancer binding proteins directly modulate transcription from the peroxisome proliferator-activated receptor γ 2 promoter. Biochem. Biophys. Res. Commun. 240:99–103.

Corah, L., and M. McCully. 2007. Declining quality grades: A review of factors reducing marbling deposition in beef cattle. Certified Angus Beef LLC. http://www. cabpartners.com/news/research/declining_quality_grades.pdf.

Crouse, J. D., H. R. Cross, and S. C. Seideman. 1983. effects of a grass or grain diet on the quality of three beef muscles. J. Anim. Sci. 58:619-625

Demas GE, Bartness TJ. Direct innervation of body fat and adrenal medullary catecholamines mediate photoperiodic changes in body fat. Am J Physiol 281:1499–1505, 2001.

Dodson, M. V., G. J. Hausman, L. Guan, M. Du, T. P. Rasmussen, S. P. Poulos, P. Mir, W. G. Bergen, M. E. Fernyhough, D. C. McFarland, R. P. Rhoads, B. Soret, J. M. Reecy, S. G. Velleman, and Z. Jiang. 2010. Skeletal muscle stem cells from animals I. Basic cell biology. Int. J. Biol. Sci. 6:465–474.

Du., M., J. Tong, J. Zhao, K. R. Underwood. M. Zhu, S. P. Ford, and P. W. Nathanielsz. 2010. Fetal programming of skeletal muscle development in ruminant animals. J. Anim. Sci. 88:E51–E60. doi:10.2527/jas.2009-2311

Du, M., Y. Huang, A.K. Das, Q. Yang, M.S. Duarte, M.V. Dodson, and M.-J. Zhu. 2013. Meat science and muscle biology symposium: Manipulating mesenchymal progenitor cell differentiation to optimize performance and carcass value of beef cattle. J. Anim. Sci. 91:1419–1427. doi:10.2527/jas.2012-5670

Du., M., S. P. Ford, and M. J. Zhu. 2017. Optimizing livestock production efficiency through maternal nutritional management and fetal developmental programming. Animal Frontiers. 7:5–11. https://doi.org/10.2527/af.2017-0122

Duarte, M. S., M. P. Gionbelli, P. V. R. Paulino, N. V. L. Serão, C. S. Nascimento, M. E. Botelho, T. S. Martins, S. C. V. Filho, M. V. Dodson, S. E. F. Guimarães, and M. Du. 2014. Maternal overnutrition enhances mRNA expression of adipogenic markers and collagen deposition in skeletal muscle of beef cattle fetuses. J. Anim. Sci. 92:3846–3854. https://doi.org/10.2527/jas.2014-7568

Dubocovich ML, Cardinali DP, Guardiola-Lemaitre B, Hagan RM, Krause DN, Sugden D, Vanhoutte PM and Yocca FD (1998) Melatonin receptors, in The IUPHAR Compendium of Receptor Characterization and Classification pp 187– 193, IUPHAR Media, London.

Dubocovich, M.L., Delagrange, P., Krause, D.N., Sugden, D., Cardinali, D.P., Olcese, J. 2010. International Union of Basic and Clinical Pharmacology. LXXV. Nomenclature, classification, and pharmacology of G protein-coupled melatonin receptors. Pharmacol. Rev. 62, 343–380.

Dwyer, C. M., N. C. Stickland, and J. M. Fletcher. 1994. The influence of maternal nutrition on muscle fiber number development in the porcine fetus and on subsequent postnatal growth. J. Anim. Sci. 72:911–917.

Feve, B. 2005. Adipogenesis: Cellular and molecular aspects. Best Pract. Res. Clin. Endocrinol. Metab. 19:483–499.

Fiedler, I., K. Ender, M. Wicke, S. Maak, G. Lengerken, and W. Meyer. 1999. Structural characteristics of muscle fibers in pigs with different malignant hyperthermia susceptibility and different meat quality. Meat Sci. 53:9–15.

Florini, J. R., K. A. Magri, D. Z. Ewton, P. L. James, K. Grindstaff, and P. S. Rotwein. 1991. "Spontaneous" differentiation of skeletal myoblasts is dependent upon autocrine secretion of insulin-like growth factor-II. J. Biol. Chem. 266:15917–15923

Foxcroft, G. R., W. T. Dixon, S. Novak, C. T. Putman, S. C. Town, M. D. A. Vinsky; The biological basis for prenatal programming of postnatal performance in pigs', Journal of Animal Science, Volume 84, Issue suppl_13, 1 April 2006, Pages E105–E112, https://doi.org/10.2527/2006.8413_supplE105x

Frohnert, B. I., T. Y. Hui, and D. A. Bernlohr. 1999. Identification of a functional peroxisome proliferator-responsive element in the murine fatty acid transport protein gene. J. Biol. Chem. 274:3970–3977.

Funston, R. N., D. M. Larson, and K. A. Vonnahme. 2010. Effects of maternal nutrition on conceptus growth and offspring performance: Implications for beef cattle production. J. Anim. Sci. 88:E205-E215. doi:10.2527/jas.2009-2351

Gluckman, P. D., Catherine S. Pinal; Regulation of Fetal Growth by the Somatotrophic Axis, The Journal of Nutrition, Volume 133, Issue 5, 1 May 2003, Pages 1741S–1746

Gonzalez, J. M., L. E. Camacho, S. M. Ebarb, K. C. Swanson, K. A. Vonnahme, AA. M. Stelzleni, and S. E. Johnson. 2013. Realimentation of nutrient restricted pregnant beef cows supports compensatory fetal muscle growth. J Anim. Sci. 91:4797–4806

Ha., E., S. Yim, J. Chung, K. Yoon, I. Kang, Y. H. Cho, and H. H. Baik. 2006. Melatonin stimulates glucose transport via insulin receptor substrate-1/phosphatidylinositol 3-kinase pathway in C2C12 murine skeletal muscle cells. J. Pineal Res. 14:67-72

Haig, D., and C. Graham. 1991. Genomic imprinting and the strange case of the insulin-like growth factor II receptor. Cell. 64:1045–1046

Hausman, J. G., M. V. Dodson, K. Ajuwon, M. Azain, K. M. Barnes, L. L. Guan, Z. Jiang, S. P. Poulos, R. D. Sainz, S. Smith, M. Spurlock, J. Novakofski, M. E. Fernyhough, W. G. Bergen; board-invited review:

The biology and regulation of preadipocytes and adipocytes in meat animals,, Journal of Animal Science, Volume 87, Issue 4, 1 April 2009, Pages 1218–1246, https://doi.org/10.2527/jas.2008-1427

Himms-Hagen, J. 1990. Brown adipose tissue thermogenesis: Interdisciplinary studies. FASEB J. 4:2890–2898.

Holt, L. J., N. Turner, N. Mokbel, S. Trefely, T. Kanzleiter, W. Kaplan, C. J. Ormandy, R. J. Daly, and G. J. Cooney. 2012. Grb10 regulates the development of fiber number in skeletal muscle. FASEB J. 26:3658–3669

Huang Y. Yan X. Zhu M. J. McCormick R. J. Ford S. P. Nathanielsz P. W. Du M. 2010. Enhanced transforming growth factor-β signaling and fibrogenesis in ovine fetal skeletal muscle of obese dams at late gestation. Am. J. Physiol. Endocrinol. Metab. 298:E1254–E1260.

Huffman K. L., M.F. Miller, L.C. Hoover, C.K.Wu, H.C. Brittin, C.B. Ramsey. 1996. Effect of beef tenderness on consumer satisfaction with steaks consumed in the home and restaurant J. Ani. Sci. 74:91-97

Jimenez-Aranda, A., G. Fernandez-Vazquez, D. Campos, M. Tassi, L. Velasco-Perez, D. X. Tan, R. J. Reiter, and A. Agil. 2013. Melatonin induces browning of inguinal white adipose tissue in Zucker diabetic fatty rats. J. Pineal. Res. 55:416-423. Doi:10.1111/jpi.12089

Karunaratne, J. F., C. J. Ashton, and N. C. Stickland. 2005. Fetal programming of fat and collagen in porcine skeletal muscles. J Anat. 207: 763-768

Kassar-Duchossoy, L., E. Giacone, B. Gayraud-Morel, A. Jory, D. Gomes, and S. Tajbakhsh. 2005. Pax3/Pax7 mark a novel population of primitive myogenic cells during development. Genes Dev. 19:1426–1431.

Keren, A., Y. Tamir, and E. Bengal. 2006. The p38 MAPK signaling pathway: A major regulator of skeletal muscle development. Mol. Cell. Endocrinol. 252:224–230.

Klosowska, D., A. Niewarowicz, B. Klosowski, and M. Trojan.1979. Histochemische und histologische Untersuchungen am M. pectoralis superficialis mit beschleunigter, normaler und verzögerter Glykolyserate in Broilern. Fleischwirtschaft 7:1004–1008.

Kollias, H. D., and J. C. McDermott. 2008. Transforming growth factor-β and myostatin signaling in skeletal muscle. J. Appl. Physiol. 104:579–587.

Koohmaraie, M., M. P. Kent, S. D. Shackelford, E. Veiseth, and T. L. Wheeler. 2002. Meat tenderness and muscle growth: is there any relationship? Meat Sci. 62:345–352.

Kroker, G. A., and L. J. Cummins. 1979. The effect of nutritional restriction on Hereford heifers in late pregnancy. Aust. Vet. J. 55:467–474.

Kuang, S., M. A. Gillespie, and M. A. Rudnicki. 2008. Niche regulation of muscle satellite cell self-renewal and differentiation. Cell Stem Cell 2:22–31

Kwon H, Ford SP, Bazer FW, Spencer TE, Nathanielsz PW, Nijland MJ, Hess BW, Wu G. Maternal nutrient restriction reduces concentrations of amino acids and polyamines in ovine maternal and fetal plasma and fetal fluids. Biol Reprod 71: 901–908, 2004.

Larsen PJ, Enquist LW, Card JP. Characterization of the multisynaptic neuronal control of the rat pineal gland using viral transneuronal tracing. Eur J Neurosci 10:128–145, 1998.

Le Gouic, S, Atgie, C, Viguerie-Bascands, N, Hanoun, N, Larrouy, D, Ambid, L, Raimbault, S, Ricquier, D, Delagrange, P, Guardiola-Lemaitre, B, Penicaud, L, Casteilla, L. 1997. Characterization of a melatonin binding site in Siberian hamster brown adipose tissue. Eur J Pharmacol339:271–278

Le Roith, D., C. Bondy, S. Yakar, J. L. Liu, and A. Butler. 2001. The somatomedin hypothesis: 2001. Endocr. Rev. 22:53-57

Lerner AB, Case JD, Takahashi Y, Lee TH, Mori W: Isolation of melatonin, the pineal gland factor that lightens melanocytes. J Amer Chem Soc 80:2587, 1958

Lemley, C. O., A. M. Meyers, L. E. Camacho, T. L. Neville, D. J. Newman, J. S. Caton, K. A. Vonnahme. 2012. Melatonin supplementation alters uteroplacental hemodynamics and fetal development in an ovine model of intrauterine growth restriction. Am. J. Physiol. Regul. Integr. Comp. Physiol. 302: 454–467; doi:10.1152/ajpregu.00407.2011

Lemley, C. O., L. E. Camacho, and K. A. Vonnahme. 2013. Uterine Infusion of Melatonin or Melatonin Receptor Antagonist Alters Ovine Feto-Placental Hemodynamics During Midgestation. Bio. of Repro. 89:41-49

Liu, J. P., J. Baker, A. S. Perkins, E. J. Robertson, and A. Efstratiadis. 1993. Mice carrying null mutations of the genes encoding insulin-like growth factor I (IGF-I) and type 1 IGF receptor (Igf1r). Cell. 75:59-72.

Long, N. M., M. J. Prado-Cooper, C. R. Krehbiel, U. DeSilva, and R. P. Wettermann. 2010. Effects of nutrient restriction of bovine dams during early-gestation on postnatal growth, carcass and organ characteristics, and gene expression in adipose tissue and muscle. J. Anim. Sci. 88:3251–3261.

Luther, J. S., D. A. Redmer, L. P. Reynolds, and J. M. Wallace. 2005. Nutritional paradigms of ovine fetal growth restriction: Implications for human pregnancy. Hum. Fertil. 8:179–187.

Manchester LC, Coto-Montes A, Boga JA, Andersen LP, Zhou Z, Galano A, Vriend J, Tan DX, Reiter RJ, 2015: Melatonin: an ancient molecule that makes oxygen metabolically tolerable. J Pineal Res 59, 403–419.

Mir, P. S., Z. Mir, P. S. Kuber, C. T. Gaskins, E. L. Martin, M. V. Dodson, J. A. Elias Calles, K. A. Johnson, J. R. Busboom, A. J. Wood, G. J. Pittenger, J. J. Reeves; Growth, carcass characteristics, muscle conjugated linoleic acid (CLA) content, and response to intravenous glucose challenge in high percentage Wagyu, Wagyu × Limousin, and Limousin steers fed sunflower oil-containing diets,, Journal of Animal Science, Volume 80, Issue 11, 1 November 2002, Pages 2996–3004, https://doi.org/10.2527/2002.80112996x

Moore RY. Neural control of the pineal gland. Behav Brain Res 73:125–130, 1996.

NRC. 1985. Nutrient Requirements of Sheep. 6th ed. Natl. Acad. Press, Washington, DC.

NVSR (National Vital Statistics Reports). 2009. Vol. 57, No. 12. Births: Preliminary Data for 2007. National Center for Health Statistics, Centers for Disease Control and Prevention, DHHS.

Regnault TR, de Vrijer B, Galan HL, Davidsen ML, Trembler KA, Battaglia FC, Wilkening RB, Anthony RV. The relationship between transplacental oxygen diffusion and placental expression of PlGF, VEGF and their receptors in a placental insufficiency model of fetal growth restriction. J Physiol 550: 641–656, 2003.

Rehfeldt, C. and Kuhn, G. Consequences of birth weight for postnatal growth performance and carcass quality in pigs as related to myogenesis. J. Anim. Sci. 2006; 84: 113–123

Reiter RJ, et al: Melatonin: Reproductive effects. J Neur Trans 13 (Suppl):209-223, 1978

Reiter RJ, Melchiorri D, Sewerynek E, Poeggeler B, Barlow-Walden L, Chuang J, Ortiz GG, Acu~naCastroviejo D, 1995: A review of the evidence supporting melatonin's role as an antioxidant. J Pineal Res 18,1 –11

Reiter, R. J. 2003. Melatonin: clinical relevance. Endo & Metab. 17:273-285

Reynolds LP, Borowicz PP, Vonnahme KA, Johnson ML, Grazul-Bilska AT, Redmer DA, Caton JC. 2005. Placental angiogenesis in sheep models of compromised pregnancy. J Physiol 565: 43–58

Reynolds, L. P., J. S. Caton, D. A. Redmer, A. T. Grazul-Bilska, K. A. Vonnahme, P. B. Borowicz, J. S. Luther, J. M. Wallace, G. Wu, and T. E. Spencer. 2006. Evidence for altered placental blood flow and vascularity in compromised pregnancies. J. Physiol. 572:51–58.

Rigano S, Bozzo M, Ferrazzi E, Belloti M, Battaglia FC, Galan HL. Early and persistent reduction in umbilical vain blood flow in the growthrestricted fetus: a longitudinal study. Am J Obstet Gynecol 185: 834–838,2001.

Robinson, J. J., I. McDonald, C. Fraser, and I. McHattie. 1977. Studies on reproduction in prolific ewes. I. Growth of the products of conception. J. Agric. Sci. Camb. 88:539–552.

Robinson, D. L., L. M. Cafe, P. L. Greenwood; Meat Science And Muscle Biology Symposium: Developmental programming in cattle: Consequences for growth, efficiency, carcass, muscle, and beef quality characteristics,, Journal of Animal Science, Volume 91, Issue 3, 1 March 2013, Pages 1428–1442, https://doi.org/10.2527/jas.2012-5799

Robinson, D. L., L. M. Cafe, and P. L. Greenwood. 2014. Developmental programming in cattle: Consequences for growth, efficiency, carcass, muscle, and beef quality characteristics. J. Anim. Sci. 91:1428–1442. doi:10.2527/jas2012-5799

Rosen, E. D., and O. A. MacDougald. 2006. Adipocyte differentiation from the inside out. Nat. Rev. Mol. Cell Biol. 7:885–896.

Russell, R. G., and F. T. Oteruelo. 1981. An ultrastructural study of the differentiation of skeletal muscle in the bovine fetus. Anat. Embryol. 162:403–417

Seron-Ferre, M., H. Reynolds. N. A. Mendez, M. Mondaca, F. Valenzuela, R. Ebensperger, G. J. Valenzuela, E. A. Herrera, A. J. Llanos, and C. Torres-Farfan. 2015. Impact of maternal melatonin suppression on amount and functionality of brown adipose tissue (BAT) in newborn sheep. Fendo. 5:1-11; doi: 10.3389/fendo.2014.00232

Spalding, K.L., E. Arner, P.O. Westermark, S. Bernard, B.A. Buchholz, O. Bergmann, L. Blomqvist, J. Hoffstedt, E. Naslund, T. Britton, H. Concha, M. Hassan, M. Ryden, J. Frisen, and P. Arner. 2008. Dynamics of fat cell turnover in humans. Nature 453:783–787. doi:10.1038/nature06902

Stickland, N. C. 1978. A quantitative study of muscle development in the bovine foetus (Bos indicus). Anat. Histol. Embryol. 7:193–205.

Stratos I, Richter N, Rotter R. 2012. Melatonin restores muscle regeneration and enhances muscle function after crush injury in rats. J Pineal Res. 52:62–70.

Thureen PJ, Trembler KA, Meschia G, Makowski EL, Wilkening RB. Placental glucose transport in heat-induced fetal growth retardation. Am J Physiol Regul Integr Comp Physiol 263: R578–R585, 1992.

Tong, J., M. J. Zhu, K. R. Underwood, B. W. Hess, S. P. Ford, and M. Du. 2008. AMP-activated protein kinase and adipogenesis in sheep fetal skeletal muscle and 3T3–L1 cells. J. Anim. Sci. 86:1296–1305.1834429

Tong, J. F., X. Yan, M. J. Zhu, S. P. Ford, P. W. Nathanielsz, and M. Du. 2009. Maternal obesity downregulates myogenesis and β-catenin signaling in fetal skeletal muscle. Am. J. Physiol. Endocrinol. Metab. 296:E917–E924.19176350

Torres-Farfan, C., F. J. Valenzuela, M. Mondaca, G. J. Valenzuela, B. Krause, E. A. Herreral, R. Riquelme, A. J. Llanos, and M. Seron-Ferre. 2008. Evidence of a role for melatonin in fetal sheep physiology: Direct actions of melatonin on fetal cerebral artery, brown adipose tissue and adrenal gland. J. Physiol. 586:4017–4027

Townsend, K., Y. Tseng. 2012. Brown adipose tissue. Adipocyte. 1: 13-24

Vandenbosche, R. C., and J. T. Kirchner. 1998. Intrauterine growthretardation. Am. Fam. Physician 58:1384–1390.

Vitale PM, Darrow JM, Duncan MJ, Shustak CA, Goldman BD. Effects of photoperiod pinealectomy and castration on body weight and daily torpor in Djungarian hamsters (Phodopus sungorus). J Endocrinol 106:367–375, 1985.

Vonnahme, K. A., C. O. Lemley, P. Shukla, S. T. O'Rourke; 2011 AND 2012 EARLY CAREERS ACHIEVEMENT AWARDS: Placental programming: How the maternal environment can impact placental function,, Journal of Animal Science, Volume 91, Issue 6, 1 June 2013, Pages 2467–2480, https://doi.org/10.2527/jas.2012-5929

Wade GN, Bartness TJ. Seasonal obesity in Syrian hamsters: effects of age diet photoperiod and melatonin. Am J Physiol 247:R328– R334, 1984.

Wallace JM, Bourke DA, Aitken RP, Leitch N, Hay WW Jr. Blood flows and nutrient uptakes in growth-restricted pregnancies induced by overnourishing adolescent sheep. Am J Physiol Regul Integr Comp Physiol 282: R1027–R1036, 2002.

Wallace, J. M., J. S. Luther, J. S. Milne, R. P. Aitken, D. A. Redmer, L. P. Reynolds, and W. W. Hay Jr. 2006. Nutritional modulation of adolescent pregnancy outcome—A review. Placenta. 27: S61–S68.

Wang, B., X. Fu, X. Liang, Z. Wang, Q. Yang, W. Nie, J. Zhao, P. Gao, M.J. Zhu, J.M. De Avila, J.W. Maricelli, B.D. Rodger, and M. Du. 2017. Maternal retinoids increase PDGFRα progenitor population and beige adipogenesis in progeny by stimulating vascular development. E. Bio. Medicine. 18:288–299. doi:10.1016/j.ebiom.2017.03.041

Wolden-Hanson, T., D. R. Mitton, R. L. McCants, S. M. Yellon, C. W. Wilkinson, A. M. Matsumoto, D. D Rasmussen; Daily Melatonin Administration to Middle-Aged Male Rats Suppresses Body Weight, Intraabdominal Adiposity, and Plasma Leptin and Insulin Independent of Food Intake and Total Body Fat, Endocrinology, Volume 141, Issue 2, 1 February 2000, Pages 487–497

Wu, Z., E. D. Rosen, R. Brun, S. Hauser, G. Adelmant, A. E. Troy, C. McKeon, G. J. Darlington, and B. M. Spiegelman. 1999. Cross-regulation of C/EBPα and PPARγ controls the transcriptional pathway of adipogenesis and insulin sensitivity. Mol. Cell 3:151–158.

Wu, G., F. W. Bazer, J. M. Wallace, and T. E. Spencer. 2006. BOARD-INVITED REVIEW: Intrauterine growth retardation: Implications for the animal sciences. J. Anim. Sci. 84:2316–2337.16908634

Wurtman RJ, Axelrod J, Kelly DE: The Pineal. New York, Academic Press, 1968

Yablonka-Reuveni, Z., K. Day, A. Vine, and G. Shefer. 2008. Defining the transcriptional signature of skeletal muscle stem cells. J. Anim. Sci. 86:E207–E216.

Yan, X., M. Zhu, M. V. Dodson, and M. Du. 2012. Developmental programming of fetal skeletal muscle and adipose tissue development. J. Genomics 1:29–38.

Youngstrom TG, Bartness TJ. White adipose tissue sympathetic nervous system denervation increases fat pad mass and fat cell number. Am J Physiol 275:R1488–R1493, 1998.

Zhu, M. J., S. P. Ford, P. W. Nathanielsz, and M. Du. 2004. Effect of maternal nutrient restriction in sheep on the development of fetal skeletal muscle. Biol. Reprod. 71:1968–1973.

Zhu, M. J., S. P. Ford, W. J. Means, B. W. Hess, P. W. Nathanielsz, and M. Du. 2006. Maternal nutrient restriction affects properties of skeletal muscle in offspring. J. Physiol. 575:241–250.16763001

CHAPTER III

EFFECT OF MATERNAL MELATONIN SUPPLEMENTATION DURING LATE GESTATION ON MUSCLE AND ADIPOSE TISSUE HISTOLOGY, GENE EXPRESSION IN 240 DAY OLD BOVINE FETUSES

3.1 Abstract

Melatonin is a natural hormone that is secreted by the pineal gland and has effects on economically important reproductive and carcass tissues including muscle and adipose tissue. There is evidence to suggest that supplemental melatonin to dams during late gestation may alter skeletal muscle development in fetal calves as documented by an increased postnatal weight of calves starting at 8 weeks of age (Brockus et al., 2006a). The objectives of this study were to determine the effects of maternal melatonin supplementation during late gestation on the histological and molecular regulation in the Longissimus dorsi (**LM**) of fetal bovine offspring and to determine the effects of maternal melatonin on composition and gene expression of perirenal (**PR**) adipose tissue. Beef heifers (n = 32) and cows (n = 25) consisting of purebred Angus, purebred Hereford, or crossbred genetics, were bred via timed-artificial insemination and assigned to one of two treatment groups. The treatment groups consisted of melatonin supplementation (**MEL**) or without supplementation (**CON**). Supplementation of MEL

was delivered via two- 24 mg implants with the CON receiving two placebo implants at days 180, 210, and 240 of gestation. After day 240 of gestation, dams received no further treatments and a subset of twelve crossbred heifers (n = 6 MEL; n = 6 CON) underwent cesarean section on day 243 ± 2 of gestation to collect fetal tissue samples. Samples consisted of LM, PR, umbilical artery and vein plasma, fetal trunk plasma, and maternal plasma. In this study, there was no difference ($P > 0.05$) in fetal body weight between calves from MEL treated dams compared to CON dams. Calves from MEL treated dams tended to have increased LM weight and length than that of calves from CON treated dams. Immunohistochemistry (**IHC**) analysis of fetal LM showed calves from dams treated with MEL having a tendency for increased PAX7 activated nuclei to total nuclei ratio. Relative gene expression of fetal LM identified calves from MEL treated dams to have increased adenosine monophosphate-activated protein kinase-α (**AMPK**). Maternal MEL supplementation during late gestation lead to no difference in fetal PR weight compared to CON treated dams. However, relative gene expression of fetal PR showed decreased adiponectin (**ADIPOQ**), CCAAT enhancer binding protein alpha (**CEBPA**), stearoyl-CoA desaturase (**SCD**), peroxisome proliferator activated receptor gamma (**PPARg**), insulin-like growth factor 1 (**IGF1**), and a tendency for decreased insulin-like growth factor 2 (**IGF2**). Maternal MEL supplementation during late gestation resulted in fetal programming of LM muscle and PR adipose tissues in the bovine offspring.

3.2 Introduction

With the rapidly increasing global population, the need for improving the efficiency of livestock and meat production is vital. Prenatal myogenic and adipogenic development are a large determinant of the animal's future postnatal production potential.

Economically important tissues such as muscle and adipose are of a lower developmental priority compared to vital organs and nervous tissues (Zhu et al., 2006; Du et al., 2010). This leaves muscle and adipose tissue development particularly susceptible to the prevailing nutritional environment *in utero* (Zhu et al., 2006; Du et al., 2010). Stimuli and/or insults during the development of these tissues can set the stage for increased production efficiency, maximal growth, and superior carcasses, or lead to impaired growth, inferior carcass composition, and increased risk of morbidity and mortality. Fetal programming is a change in the growth trajectory due to a stimulus or insult during a critical time in development for the fetus resulting in persisting effects into the postnatal phases of life or production (Nathanielsz et al., 2007). The first of these critical time points in growth for livestock is during prenatal development, at which point the fetus is completely dependent on the dam for nutrients. Nutrients for the fetus are in maternal circulation and must cross over to the fetus through the placenta. The nutritional status of the dam can have long lasting effects on fetal development by permanently altering the development of adipogenesis, fibrogenesis, and myogenesis (Karunaratne et al., 2005; Rehfeldt and Kuhn, 2006; Zhu et al., 2006; Funston et al., 2010; Huang et al., 2010; Duarte et al., 2014; Wang et al., 2017). However, even with sufficient nutrients in circulation, the flux of nutrient substrates from dam to fetus is dependent on the activity and accessibility of nutrient-specific transporters (Brett et al., 2014) as well as uterine blood flow (Reynolds and Redmer, 1995). In humans and sheep, decrease placental blood flow in mid- to late-gestation reduced placental weight and fetal weight (Reynolds and Redmer, 1995; Ferrazzi et al., 2000; Konje et al., 2003; Reynolds, et al., 2005; Vonnahme et al., 2013; Eifert et al., 2015) while decreasing litter size in rats (Anderson et al., 2005).

The tissue level impacts in the fetus under these scenarios have not been as thoroughly discussed.

Approaches to prevent or rescue compromised pregnancies include identifying agents and mechanisms to improve uteroplacental nutrient exchange and in turn augment the *in utero* nutritional environment experienced by the fetus. Among these, supplementation of melatonin has been investigated as a novel therapeutic approach to increase uteroplacental blood flow (Juaniaux et al., 2006; Paulis and Simko, 2007; Richter et al., 2009; Lemley et al., 2012 and 2013; Vonnahme et al., 2013; Eifert et al., 2015; Brockus et al., 2016a and 2016b). Melatonin is a natural hormone produced from the pineal gland and derived from tryptophan. Melatonin has been described as having pleiotropic properties acting as a vasodilator, strong antioxidant, and signaling molecule for regulating natural circadian rhythm (Richter et al., 2009). The known melatonin receptors include MT1 and MT2 (Dubocovich et al., 1998, 2010) and their presence has been detected on peripheral tissues including muscle (Stratos et al., 2012) and adipose tissue (Le Gouic et al., 1997). In skeletal muscle, binding of melatonin to these receptors stimulates glucose transport into muscle cells (Ha et al., 2006), increases the number of satellite cells, reduces inflammation, and inhibits apoptosis by modulating associated signaling pathways (Stratos et al., 2012). Melatonin increased insulin receptor substrate-1 is phosphorylated and the activity of phosphatidylinositol 3-kinase is increased, resulting in increased glucose uptake (Ha et al., 2006). Melatonin has decreased intraabdominal adiposity in rats (Wolden-Hanson et al., 2000). Melatonin has also been shown to play a significant role in promoting the recruitment of brown adipose tissue (**BAT**) in newborn sheep (Seron-Ferre et al., 2015) as well as the browning of inguinal white adipose tissue

(**WAT**) in juvenile rats (Jimenez-Aranda et al., 2013). Brown adipose is extremely important in newborns due to its thermogenic properties which can decrease newborn mortality (Carstens et al., 1997). Studies have found melatonin to cause increased hair follicle growth in goats (Nixon et al.,1993), cardiovascular influence (Pechanova et al.,2014), and decreased core body temperature in humans (Krauchi et al.,1997). However, studies looking at similar effects in cattle are lacking. A study conducted by Brockus et al. (2016a) supplemented Holstein heifers with melatonin to look at effects on offspring blood pressure, heart rate, liver blood flow, skin temperature, and hair growth. They found that calves from dams supplemented with melatonin during their last trimester of gestation, had significantly higher body weights at 8 to 9 weeks of age (Brockus et al., 2016a). They hypothesized that melatonin supplementation could have altered skeletal muscle development of the calves, providing impetus for the current study (Brockus et al., 2016a).

Therefore, our hypothesis was that increased maternal melatonin concentration during late gestation alters the metabolic program of fetal skeletal muscle and adipose tissue. Additionally, the increased uterine blood flow will improve postnatal growth by programming increased myogenic mRNA gene expression in fetal skeletal muscle. The specific objectives of this study were to determine the effects of maternal melatonin supplementation on the histological and molecular regulation in the Longissimus dorsi (**LM**) of fetal bovine offspring and to determine the effects of maternal melatonin on composition and gene expression of perirenal (**PR**) adipose tissue.

3.3 Materials and Methods

3.3.1 Animal Care and Treatment

The current study was conducted under an approved Mississippi State University Institutional Animal Care and Use Committee protocol (#16-036).

As part of a larger study, a total of 87 heifers and 65 cows that consisted of purebred Angus, purebred Hereford, or crossbred genetics, were bred via timed-artificial insemination (**AI**) at the H. H. Leveck Animal Research Center, Mississippi State University, MS. Heifers were bred on December 10, 2015, and cows were bred on December 21, 2015. At d 120 post-AI, heifers and cows were examined via ultrasonography to confirm pregnancy. This resulted in 32 heifers and 25 cows with confirmed conception. Then dams were blocked by bodyweight and randomly assigned to one of 2 maternal treatment groups. The 2 maternal treatment groups consist of a melatonin treatment (**MEL**; n = 29) and a no melatonin treatment (**CON**; n = 28). The MEL group was administered two ear impants (MelatoninImplants.com) containing 24 mg MEL each, every 30 days starting at d 180 of gestation (baseline) and ending on d 240 of gestation. The MEL implant on d 240 of gestation was expected to provide increased maternal MEL concentration approximately till d 270 of gestation. After d 270 of gestation, all dams received no further treatments throughout the study. Furthermore, on d 180, 210, and 240 of gestation, uterine blood flow was measured via ultrasonography; with serum, plasma, hair scores, and thermal images also collected from each treatment group. Both maternal treatment groups were managed the same throughout the study and had access to similar dietary regimes with ad libitum water access. At d 240 of gestation (~85% gestation period), 12 heifers (n = 6 CON and n = 6

MEL) were randomly chosen to undergo Cesarean sections for collection of fetuses and fetal tissues.

3.3.2 Cesarean Section

Cesarean surgeries were performed by veterinarians from the Mississippi State University College of Veterinary Medicine. Once removed from the uterus, each fetal calf was weighed, exsanguinated, and then weighed again to determine pre- and post-exsanguination weights. Fetal tissue samples collected consisted of: LM, PR, and blood for plasma and serum collection. For LM muscle samples, each sample was portioned into two 1 cm by 1 cm samples and stored in cryotubes, tissue embedding molds, and then stored at -80°C until further analysis. Tissue embedding consisted of a 1 cm by 1 cm section of muscle placed in Optimal Cutting Temperature (**OCT**) tissue embedding media (Fisher Scientific, Pittsburgh, PA), and frozen by submersion in supercooled isobutane. For PR adipose samples, each sample was sectioned into 500 mg samples and stored in cryotubes and sterile whirlpack bags, then stored at -80°C until further analysis. Blood was collected in red and purple top tubes for collection of serum and plasma, respectively. The samples were then spun down via centrifuge, with the supernatant layer extracted via pipetting and portioned into cryotubes and stored at -80°C until further analysis.

3.3.3 Analysis of Fatty Acids

Fatty acids were extracted from maternal plasma, fetal plasma, fetal umbilical artery and vein plasma, and fetal PR adipose tissue, then esterified using a transesterification method (O'Fallon et al., 2007). For extraction, 500 µl of plasma

samples and 0.1-g of PR samples were placed into a 20-ml flat bottom glass vial with PTFE-lined silicon septum (Fischer scientific, Waltham, MA, USA). After, 200 µl (1-ml for PR) of methyl tridecanoate (150 mg/ml in methanol; **MeOH**) was added as internal standard (Sigma Aldrich, St. Louis, MO), fat was saponified in presence of 700 µl of potassium hydroxide and 5.3-ml of methanol. Saponified FAs were then trans-esterified in 580 µl of sulfuric acid resulting in fatty acid methyl esters (**FAME**). Fatty acid methyl esters were extracted in 600 µl (3-ml for PR) of hexane, transferred into a 2-ml amber vial, and stored in -20°C freezer until being determined by gas chromatography (**GC**). For analysis, FAME were separated and quantified using a GC system (Agilent Technologies, Santa Clara, CA) equipped with an HP- 88 capillary column (30 m × 0.25 mm, 0.2 µm film thickness; Supelco Inc., Bellefonte, PA) and a flame-ionization detector. For carrier gas, hydrogen was used at 1.5 ml/min. Peaks were identified by FAME standards in Supelco® 37 Component FAME Mix (Sigma-Aldrich, St. Louis, MO), FAME #21 Mix (Restek, Bellefonte, PA), and a customized 17-component FAME mix (Nu-Chek-Prep, Elysian, MN) and were quantified by an internal standard calibration method. For each sample, concentrations (mg/g of adipose tissue) of FA was converted from the corresponding FAME concentration by using molecular weight ratios with percentages of each FA calculated by dividing its concentration (mg/g) by total FA concentration (mg/g) and then multiplying by 100. Saturation index (**SI**) was calculated by the ratio of SFA and the sum of MUFA and PUFA.

3.3.4 Longissimus dorsi Analysis of Relative Gene Expression

3.3.4.1 QuantiNova™ SYBR® Green PCR Kit

Nucleic acids were isolated from the LM biopsy samples using 700 µl of QIAzol® Lysis Reagent (QIAGEN, Hilden, Germany), followed by purification with the use of RNA using a miRNeasy® Mini Kit (QIAGEN, Hilden, Germany). Extracted total RNA was quantified using a NanoDrop One spectrophotometer (Thermo scientific, Waltham, MA). Samples exhibiting 260 nm/280 nm ratios between 1.9 and 2.1 were deemed acceptable for downstream procedures and stored at -80°C. For each sample, duplicate cDNA synthesis reactions were conducted using 100 nanograms of total RNA using QuantiNova™ Reverse Transcription Kits (QIAGEN, Hilden, Germany) according to the manufacturers protocol. The genes of interest for LM tissue included insulin-like growth factor 1 (**IGF1**), IGF1 receptor (**IGF1R**), insulin-like growth factor 2 (**IGF2**), IGF2 receptor (**IGF2R**), cystatin (**CYS**), adenosine monophosphate-activated protein kinase-α (**AMPK**), lysyl oxidase (**LOX**), bone morphogenetic protein (**BMP**). Beta actin was used as a housekeeping gene. Gene specific primers for the genes of interest (Table 3.1) were designed and validated for quantitative PCR (**qPCR**). Primer efficiencies were determined by plotting the threshold cycle versus the log of the input concentrations for 8, 10-fold serial dilutions of pooled LM muscle cDNA. Primer sets and assays with efficiencies between 0.9 and 1.1 were considered acceptable for real time PCR analysis. Each of the duplicate cDNA samples were subjected to duplicate qPCR reactions using QuantiNova™ SYBR® Green PCR Kit (QIAGEN, Hilden, Germany). A master mix containing SYBR® Green, forward and reverse primers (diluted 1:20), and ROX reference dye along with 300 ng of cDNA was pipetted into a 96-well MicroAmp® Fast Optical

Reaction Plate (Applied Biosystems, Foster City, CA). The plate was then covered with Masterclear real-time PCR Film (Eppendorf, Hamburg, Germany), briefly vortexed and centrifuged, then placed in QuantiStudio™ 3 (Applied Biosystems, Foster City, CA) for real-time qPCR analysis. Thermal cycling parameters used consisted of: a hold stage at 95°C for 2 minutes; PCR stage with step 1 at 95°C for 5 seconds followed by step 2 at 60°C for 10 seconds for 50 cycles; with a melting curve stage have step 1 at 95°C for 1 second then step 2 60°C for 20 seconds and step 3 (dissociation) at 95°C for 1 second (capturing every 0.1°C/s). Replicate threshold cycle (**CT**) values were averaged and used for relative quantification using the $2^{-\Delta\Delta C}{}_{T}$ method (Livak and Schmittgen, 2001).

3.3.4.2 TaqMan™ fast advanced master mix

Nucleic acids were isolated from the LM biopsy samples using 700 µl of QIAzol® Lysis Reagent (QIAGEN, Hilden, Germany), followed by purification with the use of RNA using a miRNeasy® Mini Kit (QIAGEN, Hilden, Germany). Extracted total RNA was quantified using a NanoDrop One spectrophotometer (Thermo scientific, Waltham, MA). Samples exhibiting 260 nm/280 nm ratios between 1.9 and 2.1 were deemed acceptable for downstream procedures and stored at -80°C. For each sample, duplicate cDNA synthesis reactions were conducted using 100 ng of total RNA using QuantiNova™ Reverse Transcription Kits (QIAGEN, Hilden, Germany) according to the manufacturer protocol. The genes of interest for LM were myogenic factor 5 (**Myf5**), myogenin (**MyoG**), myogenic differentiation 1 (**MyoD**), CCAAT enhancer binding protein alpha (**CEBPA**), stearoyl-CoA desaturase (**SCD**), peroxisome proliferator activated receptor gamma (**PPARg**), and patatin-like phospholipase domain containing 2 (**PNPLA2**). Beta actin was used as a housekeeping gene. Assays for the genes of interest

(Table 3.2) were validated for efficiency and specificity prior to qPCR. Primer efficiencies were determined by plotting the threshold cycle versus the log of the input concentrations for 8, 10-fold serial dilutions of pooled PR adipose tissue cDNA. Primer sets and assays with efficiencies between 0.9 and 1.1 were considered acceptable for real time PCR analysis. Complementary DNA was amplified in duplicate using TaqMan™ fast advanced master mix (Thermo scientific, Waltham, MA). A master mix containing TaqMan™ fast advanced master mix and gene assay was pipetted along with 100 ng of cDNA into a 96-well MicroAmp® Fast Optical Reaction Plate (Applied Biosystems, Foster City, CA). The plate was then covered with Masterclear real-time PCR Film (Eppendorf, Hamburg, Germany), briefly vortexed and centrifuged, then placed in QuantiStudio™ 3 (Applied Biosystems, Foster City, CA) for real-time qPCR analysis. Thermal cycling parameters used consisted of: a hold stage at 50°C for 2 minutes; polymerase activation hold at 95°C for 20 seconds; PCR stage with step 1 at 95°C for 1 second followed by step 2 at 60°C for 20 seconds for 40 cycles. Replicate CT values were averaged and used for relative quantification using the $2^{-\Delta\Delta C}{}_{T}$ method (Livak and Schmittgen, 2001).

3.3.5 Perirenal Adipose Analysis of Relative Gene Expression

Nucleic acids were isolated from the PR biopsy samples using 700 µl of QIAzol® Lysis Reagent (QIAGEN, Hilden, Germany), followed by purification with the use of RNA using a miRNeasy® Mini Kit (QIAGEN, Hilden, Germany). Extracted total RNA was quantified using a NanoDrop One spectrophotometer (Thermo scientific, Waltham, MA). Samples exhibiting 260 nm/280 nm ratios between 1.9 and 2.1 were deemed acceptable for downstream procedures and stored at -80°C. For each sample, duplicate

cDNA synthesis reactions were conducted using 100 ng of total RNA using QuantiNova™ Reverse Transcription Kits (QIAGEN, Hilden, Germany) according to the manufacturer protocol. The genes of interest for PR adipose tissue were IGF1, IGF1R, IGF2, IGF2R, uncoupling protein 1 (**UCP1**), adiponectin (**ADIPOQ**), CEBPA, SCD, PPARg, and PNPLA2, with beta actin serving as housekeeping gene. Assays for the genes of interest (Table 3.3) were validated for qPCR. Primer efficiencies were determined by plotting the threshold cycle versus the log of the input concentrations for 8, 10-fold serial dilutions of pooled PR adipose tissue cDNA. Primer sets and assays with efficiencies between 0.9 and 1.1 were considered acceptable for real time PCR analysis. Complementary DNA was amplified in duplicate using TaqMan™ fast advanced master mix (Thermo scientific, Waltham, MA). A master mix containing TaqMan™ fast advanced master mix and gene assay was pipetted along with 100 ng of cDNA into a 96-well MicroAmp® Fast Optical Reaction Plate (Applied Biosystems, Foster City, CA). The plate was then covered with Masterclear real-time PCR Film (Eppendorf, Hamburg, Germany), briefly vortexed and centrifuged, then placed in QuantiStudio™ 3 (Applied Biosystems, Foster City, CA) for real-time qPCR analysis. Thermal cycling parameters used consisted of: a hold stage at 50°C for 2 minutes; polymerase activation hold at 95°C for 20 seconds; PCR stage with step 1 at 95°C for 1 second followed by step 2 at 60°C for 20 seconds for 40 cycles. Replicate CT values were averaged and used for relative quantification using the $2^{-\Delta\Delta C}{}_{T}$ method (Livak and Schmittgen, 2001).

3.3.6 Analysis of Longissimus dorsi Immunohistochemistry

For each sample, the LM tissue embedded in OCT molds was sectioned into two-10 μm cryosections via CRYOSTAR NX50 (Thermo Scientific, Waltham, MA), and

collected on positively charged SUPERFROST™ PLUS microscope slides (Thermo scientific, Waltham, MA). For immunodetection, nonspecific antigen binding sites were inhibited by incubating cryosections in 100 µl of blocking solution which consisted of 5% horse serum (GE healthcare life sciences, Marlborough, MA) and 0.2% Triton-X-100 (Acros Organics, Morris, NJ) in phosphate-buffered saline (**PBS**) for 30 minutes. Next, the blocking solution was removed via pipetting and cryosections were incubated with 100 µl of the following antibodies at 4°C: 1:500 Dystrophin (Thermo Scientific, Waltham, MA), 1:10 supernatant myosin heavy chain, slow, IgG2b (BA-D5; Developmental Studies Hybridoma Bank, University of Iowa, Iowa City, IA), 1:10 hybridoma cell supernatant, IgG1 (PAX7; Developmental Studies Hybridoma Bank). After incubating for 1 hour, then primary antibodies were removed via pipetting, and the sections were washed 3 times for 5 minutes each with PBS. Next, the sections were incubated with 100 µl of secondary antibodies (1:1000) for 30 minutes: Alexa Fluor 488 goat anti-mouse H&L (CAT # A-21121; Invitrogen, Carlsbad, CA), Alexa Fluor 594 goat anti-rabbit H&L (CAT # A-11012), Alexa Fluor 633 goat anti-mouse H&L (CAT # A-21146), and Hoescht (CAT # 33342; Thermo Scientific, Waltham, MA). Secondary antibodies were then removed via pipetting, and sections were washed 3 times for 5 minutes each. A small amount of glycerol in PBS (9:1) was applied to each section and cover-slipped for imaging. Cryosections were imaged and captured using an EVOS® microscope (AMAFD1000; Life Technologies, Carlsbad, CA) with 20x magnification. Five representative photomicrographs were captured with a minimum of 500 fibers analyzed for each individual animal. Images captured with the EVOS® consisted of: GFP light cube (Alexa Fluor 488), Texas Red light cube (Alexa Fluor 594), Cy5 light cube

(Alexa Fluor 633), DAPI light cube (Hoescht 33342). Then the images were analyzed using ImageJ (https://imagej.nih.gov/ij/download.html). Total number of primary myofibers, secondary myofibers, primary myofiber cross-sectional area (**CSA**; μm^2), secondary myofiber CSA (μm^2), total number of nuclei, and total number PAX7 activated nuclei were collected and recorded. Calculations included: total primary to secondary myofiber ratio (number of primary myofibers/number of secondary myofibers), total PAX7 activated nuclei to total nuclei ratio (number of PAX7 nuclei/number nuclei), total nuclei to myofiber ratio (number of nuclei/number of myofibers), average primary myofiber CSA, and average secondary myofiber CSA.

3.3.7 Statistical Analysis

Gene expression, fatty acid analysis, immunohistochemistry, and LM morphometrics were analyzed using MIXED procedure of the Statistical Analysis System (SAS software version 9.4, SAS Institute, Cary, NC, USA). Where the model statement included: treatment, fetal sex, and their respective interactions. Data found to be nonnormally distributed were tested using the Wilcoxon rank sum test. Least square means and standard error of the means were reported. Pairwise comparisons between the least squares means of the treatment factor levels were computed using the PDIFF option of the LSMEANS statement. Statistical significance was determined at $P < 0.05$, and P-values falling within $P > 0.05$ and $P \leq 0.10$ were considered a trend.

3.4 Results

3.4.1 Fatty Acid Analysis

Total SFA did not differ ($P > 0.05$) in fetal samples: umbilical artery plasma, umbilical vein plasma, fetal trunk plasma, and PR fat from fetuses born from MEL or CON dams (Tables 3.4-3.11; Figures 3.1-3.4). Total SFA did not differ ($P > 0.05$) in maternal plasma between MEL and CON dams (Tables 3.12, 3.13; Figures 3.5). Individual SFA did not differ ($P > 0.05$) in fetal samples: umbilical artery plasma, umbilical vein plasma, fetal trunk plasma, and PR fat from fetuses born from MEL or CON dams (Tables 3.4-3.11). Individual SFA did not differ ($P > 0.05$) in maternal plasma from MEL treated dams compared to CON (Tables 3.12, 3.13).

Total MUFA did not differ ($P > 0.05$) in fetal samples: umbilical artery plasma, fetal trunk plasma, and PR fat from fetuses born from MEL or CON dams (Tables 3.4-3.11; Figures 3.1-3.4). However, maternal MEL supplementation tended to decrease ($P = 0.09$) total MUFA percentage in umbilical vein plasma from fetuses born from MEL compared to CON dams (Table 3.7). Total MUFA did not differ ($P > 0.05$) in maternal plasma between MEL and CON dams (Tables 3.12, 3.13; Figures 3.5). Individual MUFA did not differ ($P > 0.05$) in fetal samples: umbilical artery plasma, umbilical vein plasma, fetal trunk plasma, and PR fat from fetuses born from MEL or CON dams (Tables 3.4-3.11); except for Palmitoleic acid (16:1n-7) in fetal trunk plasma, which tended to be decreased ($P = 0.07$) in calves from MEL supplemented dams compared to CON (Table 3.10). Individual MUFA did not differ ($P > 0.05$) in maternal plasma between MEL and CON dams (Tables 3.12, 3.13).

Total PUFA did not differ ($P > 0.05$) in fetal samples: umbilical artery plasma, umbilical vein plasma, fetal trunk plasma, and PR fat from fetuses born from MEL or CON dams (Tables 3.4-3.11; Figures 3.1-3.4). Total PUFA did not differ ($P > 0.05$) in maternal plasma between MEL and CON dams (Tables 3.12, 3.13; Figures 3.5). Individual PUFA did not differ ($P > 0.05$) in fetal samples: umbilical artery plasma, umbilical vein plasma, fetal trunk plasma, and PR fat from fetuses born from MEL or CON dams (Tables 3.4-3.11); except for Docosahexaenoic acid (22:6) in umbilical vein plasma and trunk plasma, which tended to be increased ($P = 0.08$) and ($P = 0.06$) respectively, in calves from MEL supplemented dams compared to CON (Tables 3.6, 3.7, 3.11). Individual PUFA did not differ ($P > 0.05$) in maternal plasma between MEL and CON dams (Tables 3.12, 3.13).

3.4.2 Fetal Morphometric Analysis

Fetal body weight did not differ ($P > 0.05$) between fetuses from MEL dams compared to CON dams (Table 3.14; Figure 3.6). Fetal LM circumference and PR weight morphometrics did not differ ($P > 0.05$) between fetuses from MEL dams compared to CON dams (Table 3.14; Figures 3.8, 3.10). Fetal LM weight tended to increase ($P = 0.10$) and fetal LM length tended to increase ($P = 0.07$) between fetuses born from MEL compared to CON dams (Table 3.14; Figures 3.7, 3.9).

3.4.3 Fetal Longissimus dorsi Relative Gene Expression Analysis

Fetal LM relative gene expression did not differ ($P > 0.05$) in the following: IGF1, IGF1R, IGF2, IGF2R, BMP, LOX, Myf5, MyoG, MyoD, CEBPA, SCD, PPARg, or PNPLA2 between fetuses from MEL compared to CON dams (Tables 3.15, 3.16;

Figures 3.11-3.15, 3.17, 3.19-3.25); except for CYS and AMPK, which were increased (P = 0.02) and (P = 0.03) respectively, between fetuses born from MEL compared to CON dams (Table 3.15; Figures 3.16, 3.18).

3.4.4 Fetal Perirenal Fat Relative Gene Expression Analysis

Fetal PR relative gene expression did not differ (P > 0.05) in UCP1, PNPLA2, or IGF1R between fetuses from MEL compared to CON dams (Table 3.17; Figures 3.26, 3.31, 3.33). However, maternal treatment of MEL resulted in calves with decreased relative gene expression in the following: ADIPOQ (P = 0.01), CEBPA (P = 0.03), PPARg (P = 0.04), SCD (P = 0.02), and IGF1 (P = 0.01) compared to calves from CON dams (Table 3.17; Figures 3.27-3.30, 3.32). Also, relative gene expression of IGF2 tended to be decreased (P = 0.09) between fetuses from MEL compared to CON dams (Table 3.17; Figure 3.34).

3.4.5 Fetal Longissimus dorsi IHC Analysis

Fetal IHC did not differ (P > 0.05) in LM ratio of primary:secondary fibers (Prime:Sec), number of nuclei to muscle fiber number ratio (Nuclei:Fiber), primary muscle fiber CSA (Prime CSA), or secondary muscle fiber CSA (Sec CSA) between fetuses born from MEL compared to CON dams (Table 3.18; Figures 3.35, 3.37-3.39); except for the ratio of Pax7 activated nuclei to total nuclei (PAX7:Nuclei) which tended to increase (P = 0.07) between fetuses born from MEL compared to CON dams (Table 3.18; Figure 3.36).

3.5 Discussion

In the present study, there was no difference in fetal body weight between calves from MEL treated dams compared to CON dams. This supports the findings of Brockus and colleagues, as they found no difference in birth weight of Holstein calves from dams treated with MEL or CON (2016a). The authors found this interesting as they also reported finding a 25% increase in total uterine artery blood flow in Holstein heifers treated with MEL compared to CON (Brockus et al., 2016b). This observed increase in uterine artery blood flow lead them to expect an increase in birth weight of offspring, as reduced blood flow in compromised pregnancies results in lower birth weights (Thureen et al., 1992; Reynolds and Redmer, 1995; Ferrazzi et al., 2000; Rigano et al., 2001; Wallace et al., 2002; Konje et al., 2003; Regnault et al., 2003; Kwon et al., 2004; Reynolds et al., 2005; Vonnahme et al., 2013; Eifert et al., 2015). However, at weeks 8 and 9 of age, the Holstein calves from MEL treated dams had increased body weights compared to that of calves from CON dams (Brockus et al., 2016a). The authors believed that MEL supplementation to Holstein dams during late gestation may have caused a programmed response leading to a change to fetal skeletal muscle development that potentially contributed to the increased weight gain (Brockus et al., 2016a).

To investigate the effects of MEL supplementation on skeletal muscle, the entire fetal LM muscle was collected to look at different morphometric measurements consisting of weight, circumference, and length. Maternal supplementation of MEL during late gestation resulted in fetal LM tending to weigh more and be longer than that of calves from CON treated dams. Upon IHC analysis, fetal LM of calves from dams treated with MEL had a tendency for increased PAX7 activated nuclei to total nuclei

ratio. The activation of PAX7 is required for fetal myoblast formation as $PAX7^{+}$ progenitor cells act as a foundation and give rise to myogenic cells necessary for fetal skeletal muscle accretion (Hutcheson et al., 2009). This tendency for increased PAX7 activation in fetal LM may explain the observed tendency for increased LM weight and length. To investigate further, fetal LM tissue was also collected for relative gene expression of genes responsible for myogenesis, adipogenesis, and fibrogenesis, as well as genes responsible for muscle metabolism.

Skeletal muscle is a heterogenous tissue comprised of myocytes, adipocyte, and fibrocytes with the overall ratio and distribution of these cells determining muscle composition, product yield, and meat quality. This lead to our decision to not only look at genes responsible for myogenesis, but adipogenic and fibrogenic genes as well (Tables 3.1-3.3). Maternal supplementation of MEL during late gestation led to no difference in the examined myogenic and adipogenic genes. However, MEL supplementation lead to calves with increased CYS relative gene expression. A study conducted by Gonzalez et al. (2013) with nutrient restricting cross-bred cows from day 30 of gestation till day 85 of gestation resulted in fetuses with a tendency for CYS to be increased compared to fetuses from non-restricted dams. They concluded that the increase would result in increased numbers of connective tissue fibroblasts (Gonzalez et al., 2013)

Muscle accretion is not only influenced by myogenic genes, but also genes that influence muscle metabolism which provides the necessary energy for muscle growth. Maternal supplementation of MEL during late gestation led to an increase in AMPK relative gene expression in fetal LM compared to that of calves from CON dams. Increased AMPK activity has been shown to increase glucose uptake, fatty acid

oxidation, and mitochondrial biogenesis by increasing the expression of genes responsible for these metabolic pathways (Jager et al., 2007). The ability for AMPK to increase glucose uptake is very important as skeletal muscle is responsible for 65% of fetal glucose disposal (Hay, 2003). In an AMPK knockout study using mice, researchers found that AMPK modulates several metabolic genes within muscle tissue and could be a candidate for transmitting exercise signals to the nucleus (Jorgensen et al., 2006). Therefore, the increased AMPK expression could potentially lead to increased glucose uptake and cell recovery in skeletal muscle in cattle and decrease triglycerides within skeletal muscle resulting in leaner beef.

In addition to investigating the effects of MEL on skeletal muscle, we also looked at blood plasma and PR adipose tissue. The effects of MEL on decreasing adiposity is well documented in rodents (Elliott et al., 1989; Puchalski et al., 2003; Raskind et al., 2007; Korhonen et al., 2008). Maternal supplementation of MEL during late gestation resulted in no difference in fetal PR weight of calves between treatment groups. This is surprising as studies with sheep (Seron-Ferre et al., 2015) and hamsters (Heldmaier and Hoffmann, 1974) have shown MEL to increase BAT growth. The absence of BAT accretion in the calves may potentially be due to MEL decreasing relative gene expression of adipogenic genes: ADIPOQ, CEBPA, PPARg, and SCD.

Studies on the effects of ADIPOQ have shown increased ADIPOQ expression to reduce plasma glucose, reverse insulin resistance, and decrease triglyceride content of adipose tissue (Yamauchi et al., 2001; Nishizawa et al., 2002; Diez and Iglesias, 2003). Yamauchi et al. (2001) suggested that ADIPOQ may be partially regulated by PPARg due to their findings of no detectable ADIPOQ expression in adipose depleted mice which was

achieved by a severe reduction in PPARg activity. Stimulation of PPARg not only mediates adipose accretion, but adipogenesis during fetal development. Permanent differentiation of mesenchymal stem cells into adipocytes requires self-reinforcing regulation of transcription factors CEBPA and PPARg (Clarke et al., 1997; Wu et al., 1999). When CEBPA is induced and binds to the promoter of PPARg, it activates the expression of PPARg which further stimulates the expression of CEBPA (Clarke et al., 1997; Wu et al., 1999). With the activation and expression of PPARg, terminal adipogenic differentiation is achieved through the induction of many genes that are important for triglyceride uptake and storage (Frohnert et al., 1999; Rosen and MacDougald, 2006). Decreased expression of CEBPA and PPARg causes decrease fat deposition (Tontonoz et al., 1994; Forman et al., 1995; Barak et al., 1999; Lan et al., 2013), with CEBPA also being attributed as a regulator for BAT differentiation (Armengol et al., 2012). The stimulation of SCD plays an important role in adipose development through mediating MUFA synthesis, as it is the rate-limiting enzyme for biosynthesis (Ntambi et al., 2002). Mice with SCD knocked out have shown to exhibit reduced triglyceride synthesis and storage, resulting in decreased adiposity and mice had increased insulin sensitivity (Ntambi et al., 2002).

After observing decreases in genes responsible for adipogenic gene express in PR adipose tissue and the increase of metabolic gene AMPK in LM muscle tissue, we decided to look at metabolic genes in PR adipose tissue as well. Maternal supplementation of MEL during late gestation resulted in decreased IGF1 relative gene expression and tended to decrease IGF2 in PR adipose tissue. The effects of IGF2 is mainly responsible for fetal growth and IGF1 is mainly responsible for postnatal growth

and development (Florini et al., 1991; Haig and Graham, 1991; Braxton et al., 1993; Bass et al., 1999; Le Roith et al., 2001; Gluckman and Pinal, 2003; Gonzalez et al., 2013). The stimulation of IGF1 has shown to play an important role in adipogenesis by increasing the recruitment of cells thereby increasing adipose cell numbers (Hu et al., 2015), while IGF2 has been suggested to play a role in preventing terminal adipocyte differentiation (Gardan et al., 2008; Kleiman et al., 2013).

In Summary, maternal supplementation of MEL during late gestation does impact LM muscle and PR adipose tissue development of fetal calves by d 240 of gestation. The increase in metabolic associated genes within the LM promoting lipid oxidation and energy uptake paired with the decreased adipogenic gene expression could lead to calves with less adiposity and improved muscle accretion. Future analysis of fetal PR adipose morphology via IHC will be needed to determine the extent of physical changes to size and/or number of adipocytes. Also, further research into the effects of maternal supplementation of MEL during late gestation on postnatal calves will be needed to determine long term implications.

Table 3.1 Accession, sequences, amplicon length, and efficiency of primers used for QuantiNova™ SYBR® Green real-time PCR quantification of Longissimus dorsi gene expression.

Gene[1]	Accession	Forward Primer	Reverse Primer	Amplicon Size	Efficiency
IGF1	NM_001077828.1	TTGGTGGATGCTCTCCAGTTC	AGCAGCACTCATCCACGATTC	117	1.02
IGF1R	NM_001244612.1	AAGAACCATGCCTGCAGAAGG	GGATTCTCAGGTTCTGGCCATT	104	1.05
IGF2	HQ703509.1	GACCGCGGCTTCTACTTCAG	AAGAACTTGCCCACGGGGTAT	202	0.97
IGF2R	NM_174352.2	GATGAAGGAGGCTGCAAGGAT	CCTGATGCCTGTAGTCCAGCTT	99	0.95
BMP	XM_001788198.2	CAGAGGAAGGGCTTCCAGGCA	GGAACACCAGCTCCACACCAT	177	0.96
CYS	NM_174029.1	GTGGAGCTTGGCCGGACTACAT	CACCAGGTTGATGGTGTTCATCC	143	1.04
LOX	NM_173932.4	GGCTTGAGTCCTGGCTGCTATGA	GTGCAGCCCGAGGCATATGCG	202	0.99
AMPK	NM_001109802	ACCATTCTTGGTTGCTGAAACTC	CACCTTGGTGTTTGGATTTCTG	80	0.99
Beta Actin	NM_173979	GTCGACACCGCAACCAGTT	AAGCCGGCCTTGCACAT	85	0.94

[1] IGF1 = insulin-like growth factor 1, IGF1R = IGF1 receptor, IGF2 = insulin-like growth factor 2, IGF2R = IGF2 receptor, BMP = bone morphogenetic protein, CYS = cystatin, LOX = lysyl oxidase, AMPK = adenosine monophosphate-activated protein kinase-α

Table 3.2 Assays, accession, amplicon length, and efficiency of primers used for TaqMan® real-time PCR quantification of Longissimus dorsi gene expression.

Gene[1]	Assay ID	Accession	Amplicon Size	Efficiency
Beta Actin	Bt03279174_g1	NP_776404	141	0.96
Myf5	Bt03223134_m1	NP_776541	98	0.95
MyoG	Bt03258928_m1	NP_001104795.1	96	0.96
MyoD	Bt03244740_m1	NP_001035568.2	84	0.95
CEBPA	Bt03224529_s1	NP_789741	124	0.99
SCD	Bt04307478_m1	NP_776384.3	89	0.97
PPARg	Bt03217547_m1	NP_851367.1	85	0.93
PNPLA2	Bt03234128_m1	NP_001039470.1	77	0.98

[1] Myf5 = myogenic factor 5, MyoG = myogenin, MyoD = myogenic differentiation 1, CEBPA = CCAAT enhancer binding protein alpha, SCD = stearoyl-CoA desaturase, PPARg = peroxisome proliferator activated receptor gamma, PNPLA2 = patatin-like phospholipase domain containing 2.

Table 3.3 Assays, accession, amplicon length, and efficiency of primers used for TaqMan® real-time PCR quantification of perirenal adipose tissue gene expression.

Gene[1]	Assay ID	Accession	Amplicon Size	Efficiency
Beta Actin	Bt03279174_g1	NP_776404	141	0.97
UCP1	Bt04301238_m1	NM_001166528.1	74	0.92
ADIPOQ	Bt03292341_s1	NM_174742.2	121	0.94
CEBPA	Bt03224529_s1	NP_789741	124	0.92
PPARG	Bt03272016_m1	NM_001101152.2	65	0.94
SCD	Bt04307478_m1	NP_776384.3	89	0.95
PNPLA2	Bt03234128_m1	NP_001039470.1	77	0.99
IGF2	Bt03259225_m1	NP_776512.2	54	0.95
IGF1	Bt03252282_m1	NM_001077828.1	65	0.99
IGF1R	Bt03649217_m1	NP_001231541.1	70	0.93

[1] UCP1 = uncoupling protein 1, ADIPOQ = adiponectin, CEBPA = CCAAT enhancer binding protein alpha, PPARg = peroxisome proliferator activated receptor gamma, SCD = stearoyl-CoA desaturase, PNPLA2 = patatin-like phospholipase domain containing 2, IGF2 = insulin-like growth factor 2, IGF1 = insulin-like growth factor 1, IGF1R = IGF1 receptor.

Table 3.4 Fetal umbilical artery composition of saturated (SFA), monounsaturated (MUFA), and polyunsaturated fatty acids (PUFA) of calves CON (*n*=6), MEL (*n*=6).

	Fetal Umbilical Artery (mg/ml)			
	Treatment			
Fatty Acid	**CON**	**MEL**	**SEM**	***P* Value**
SFA	0.2812	0.2665	0.0221	0.52
15:0	0.0096	0.0077	0.0017	0.30
16:0	0.1696	0.1628	0.0133	0.62
17:0	0.0118	0.0082	0.0035	0.32
18:0	0.0900	0.0883	0.0065	0.80
MUFA	0.1818	0.1727	0.0153	0.57
14:1n-5	0.0062	0.0035	0.0037	0.48
16:1n-7	0.0306	0.0285	0.0026	0.44
17:1n-8	0.0096	0.0078	0.0021	0.43
18:1n-trans	0.0010	0.0000	0.0009	0.30
18:1n-9 cis	0.1342	0.1330	0.0121	0.92
PUFA	0.1044	0.0940	0.0131	0.45
18:2n-6	0.0474	0.0467	0.0033	0.83
18:3n-3	0.0142	0.0143	0.0051	0.98
20:3n-6	0.0106	0.0070	0.0020	0.11
20:4n-6	0.0248	0.0217	0.0049	0.54
20:5n-3	0.0062	0.0047	0.0019	0.44
22:6	0.0012	0.0000	0.0011	0.30
TOTAL	0.5676	0.5333	0.0462	0.48
SI*	0.9860	1.0067	0.0434	0.65
DI**	0.3880	0.3933	0.0058	0.38

*SI = saturation index (total SFA/total MUFA + total PUFA)

**DI = desaturation index (16:1n-7 + 18:1n-9 cis/16:0 + 16:1n-7 + 18:0 + 18:1n-9 cis)

Table 3.5 Fetal umbilical artery composition in percent of saturated (SFA), monounsaturated (MUFA), and polyunsaturated fatty acids (PUFA) of calves CON (*n*=6), MEL (*n*=6).

	Fetal Umbilical Artery[1] (%)			
	Treatment			
Fatty Acid	**CON**	**MEL**	**SEM**	***P* Value**
SFA	49.5600	50.1083	1.0867	0.63
15:0	1.6380	1.4100	0.2492	0.38
16:0	29.9420	30.5733	0.5802	0.30
17:0	2.0180	1.5550	0.5655	0.43
18:0	15.9660	16.5717	0.7104	0.42
MUFA	32.0600	32.3733	0.7948	0.70
14:1n-5	1.0880	0.5900	0.6531	0.47
16:1n-7	5.3740	5.3750	0.1825	1.00
17:1n-8	1.6580	1.4683	0.2987	0.54
18:1n-trans	0.2220	0.0000	0.2004	0.30
18:1n-9 cis	23.7140	24.9383	1.0539	0.28
PUFA	18.3780	17.5183	1.6326	0.61
18:2n-6	8.3640	8.7633	0.4156	0.36
18:3n-3	2.4280	2.5850	0.8981	0.87
20:3n-6	1.8860	1.2967	0.3636	0.14
20:4n-6	4.3240	3.9933	0.7190	0.66
20:5n-3	1.1780	0.8767	0.3998	0.47
22:6	0.2000	0.0000	0.1805	0.30

[1] Fatty acid normalized percentages to total fatty acids

Table 3.6 Fetal umbilical vein composition of saturated (SFA), monounsaturated (MUFA), and polyunsaturated fatty acids (PUFA) of calves CON (*n*=6), MEL (*n*=6).

	Fetal Umbilical Vein (mg/ml)			
	Treatment			
Fatty Acid	**CON**	**MEL**	**SEM**	***P* Value**
SFA	0.2783	0.2872	0.0207	0.68
15:0	0.0070	0.0127	0.0036	0.16
16:0	0.1680	0.1698	0.0112	0.87
17:0	0.0070	0.0113	0.0037	0.28
18:0	0.0963	0.0935	0.0087	0.75
MUFA	0.1990	0.1933	0.0214	0.80
14:1n-5	0.0020	0.0020	0.0013	1.00
16:1n-7	0.0283	0.0282	0.0023	0.94
17:1n-8	0.0090	0.0110	0.0036	0.59
18:1n-trans	0.0260	0.0303	0.0265	0.87
18:1n-9 cis	0.1340	0.1217	0.0237	0.62
PUFA	0.0967	0.1357	0.0235	0.14
18:2n-6	0.0453	0.0480	0.0022	0.26
18:3n-3	0.0157	0.0165	0.0007	0.25
20:3n-6	0.0077	0.0080	0.0018	0.86
20:4n-6	0.0237	0.0232	0.0050	0.92
20:5n-3	0.0040	0.0042	0.0015	0.91
22:6	0.0000^{x}	0.0362^{y}	0.0176	0.08
TOTAL	0.5743	0.6165	0.0548	0.47
SI*	0.9500	0.8850	0.0696	0.38
DI**	0.3767	0.3617	0.0307	0.64

$^{x–y}$ Means within a row without common superscript represent tendencies *(*$P \geq 0.05$ and $P \leq 0.10$)

*SI = saturation index (total SFA/total MUFA + total PUFA)

**DI = desaturation index (16:1n-7 + 18:1n-9 cis/16:0 + 16:1n-7 + 18:0 + 18:1n-9 cis)

Table 3.7 Fetal umbilical vein composition in percent of saturated (SFA), monounsaturated (MUFA), and polyunsaturated fatty acids (PUFA) of calves CON (*n*=6), MEL (*n*=6).

	Fetal Umbilical Vein[1] (%)			
	Treatment			
Fatty Acid	**CON**	**MEL**	**SEM**	***P* Value**
SFA	48.6700	46.7883	1.8450	0.34
15:0	1.2367	2.0233	0.5595	0.20
16:0	29.4500	27.6833	1.4001	0.25
17:0	1.2067	1.8033	0.5462	0.31
18:0	16.7700	15.2817	0.9339	0.16
MUFA	34.4033[x]	31.4650[y]	1.5222	0.09
14:1n-5	0.2833	0.3417	0.2025	0.78
16:1n-7	4.9800	4.6067	0.3386	0.31
17:1n-8	1.5133	1.7700	0.5536	0.66
18:1n-trans	4.1933	4.7467	4.1065	0.90
18:1n-9 cis	23.4300	19.9983	3.8784	0.41
PUFA	16.9233	21.7467	2.8208	0.13
18:2n-6	8.0867	7.8067	0.6111	0.66
18:3n-3	2.8300	2.6983	0.2931	0.67
20:3n-6	1.3467	1.2933	0.2404	0.83
20:4n-6	3.9433	3.7133	0.5807	0.70
20:5n-3	0.7167	0.6700	0.2422	0.85
22:6	0.0000[x]	5.5667[y]	2.6797	0.08

[x–y] Means within a row without common superscript represent tendencies *($P \geq 0.05$ and $P \leq 0.10$)*

[1] Fatty acid normalized percentages to total fatty acids

Table 3.8 Fetal perirenal fat composition of saturated (SFA), monounsaturated (MUFA), and polyunsaturated fatty acids (PUFA) of calves CON (*n*=6), MEL (*n*=6).

	Fetal Perirenal fat (mg/ml)			
	Treatment			
Fatty Acid	**CON**	**MEL**	**SEM**	***P* Value**
SFA	285.4800	278.6900	22.1971	0.77
8:0	0.1760	0.1464	0.0301	0.35
10:0	0.4026	0.3177	0.0615	0.20
12:0	0.4292	0.3540	0.0835	0.39
14:0	16.6552	15.1861	3.1679	0.65
15:0	0.2430	0.2334	0.0211	0.66
16:0	203.4000	201.9400	14.8767	0.92
18:0	64.1806	60.5114	5.9566	0.55
MUFA	265.8800	280.2300	12.1603	0.27
14:1n-5	5.1440	5.4031	0.7405	0.73
16:1n-7	40.2998	39.5599	3.3678	0.83
17:1n-8	1.4928	1.5276	0.1284	0.79
18:1n-trans	1.0998	1.1584	0.0493	0.26
18:1n-9 cis	215.5100	230.1100	12.3752	0.27
20:1n-9	2.0660	2.2594	0.3186	0.56
24:1n-9	0.2640	0.2110	0.0456	0.27
PUFA	4.7594	4.4243	0.5140	0.53
18:2n-6	1.8620	1.7579	0.1472	0.50
18:3n-6	0.0852	0.0720	0.0128	0.33
18:3n-3	0.8818	0.9223	0.0651	0.55
20:2	0.1144	0.1237	0.0292	0.76
20:3n-6	0.3958	0.3194	0.0899	0.42
20:4n-6	0.9070	0.7610	0.1433	0.33
20:5n-3	0.0876	0.1176	0.0233	0.23
22:6	0.4256	0.3507	0.0991	0.47
TOTAL	556.1200	563.3500	23.2497	0.76
SI*	1.0588	0.9879	0.1031	0.51
DI**	0.4902	0.5074	0.0235	0.48

*SI = saturation index (total SFA/total MUFA + total PUFA)

**DI = desaturation index (16:1n-7 + 18:1n-9 cis/16:0 + 16:1n-7 + 18:0 + 18:1n-9 cis)

Table 3.9 Fetal perirenal fat composition in percent of saturated (SFA), monounsaturated (MUFA), and polyunsaturated fatty acids (PUFA) of calves CON (*n*=6), MEL (*n*=6).

	Fetal Perirenal fat[1] (%)			
	Treatment			
Fatty Acid	**CON**	**MEL**	**SEM**	***P* Value**
SFA	51.1814	49.3514	2.4252	0.47
8:0	0.0314	0.0260	0.0055	0.35
10:0	0.0716	0.0566	0.0101	0.17
12:0	0.0764	0.0627	0.0137	0.34
14:0	2.9674	2.6827	0.4982	0.58
15:0	0.0432	0.0417	0.0034	0.67
16:0	36.4966	35.7701	1.5633	0.65
18:0	11.4946	10.7116	0.7826	0.34
MUFA	47.9658	49.8613	2.4136	0.45
14:1n-5	0.9236	0.9616	0.1248	0.77
16:1n-7	7.2716	7.0387	0.6347	0.72
17:1n-8	0.2674	0.2726	0.0220	0.82
18:1n-trans	0.1978	0.2064	0.0092	0.37
18:1n-9 cis	38.8826	40.9404	2.3259	0.40
20:1n-9	0.3744	0.4039	0.0628	0.65
24:1n-9	0.0480	0.0374	0.0087	0.25
PUFA	0.8528	0.7873	0.0850	0.46
18:2n-6	0.3338	0.3134	0.0241	0.42
18:3n-6	0.0154	0.0127	0.0022	0.25
18:3n-3	0.1588	0.1641	0.0123	0.67
20:2	0.0204	0.0219	0.0048	0.77
20:3n-6	0.0704	0.0566	0.0152	0.38
20:4n-6	0.1622	0.1351	0.0244	0.29
20:5n-3	0.0158	0.0211	0.0044	0.25
22:6	0.0760	0.0621	0.0170	0.44

[1] Fatty acid normalized percentages to total fatty acids

Table 3.10 Fetal trunk plasma composition of saturated (SFA), monounsaturated (MUFA), and polyunsaturated fatty acids (PUFA) of calves CON (*n*=6), MEL (*n*=6).

	Fetal Plasma (mg/ml)			
	Treatment			
Fatty Acid	**CON**	**MEL**	**SEM**	***P* Value**
SFA	0.3564	0.2479	0.0920	0.27
15:0	0.0090	0.0074	0.0039	0.70
16:0	0.1892	0.1497	0.0308	0.23
17:0	0.0088	0.0044	0.0038	0.28
18:0	0.1498	0.0863	0.0543	0.27
MUFA	0.2170	0.1573	0.0452	0.22
14:1n-5	0.0006	0.0000	0.0005	0.26
16:1n-7	0.0294[x]	0.0241[y]	0.0026	0.07
17:1n-8	0.0084	0.0063	0.0022	0.36
18:1n-trans	0.0120	0.0001	0.0099	0.26
18:1n-9 cis	0.1662	0.1264	0.0303	0.22
PUFA	0.1818	0.0840	0.0816	0.26
18:2n-6	0.1216	0.0447	0.0641	0.26
18:3n-3	0.0014	0.0000	0.0012	0.26
20:3n-6	0.0116	0.0067	0.0044	0.29
20:4n-6	0.0294	0.0184	0.0080	0.20
20:5n-3	0.0096	0.0039	0.0057	0.34
22:6	0.0084	0.0106	0.0018	0.27
TOTAL	0.7554	0.4894	0.2184	0.25
SI[*]	0.9600	1.0286	0.0430	0.14
DI[**]	0.3800	0.3871	0.0130	0.60

[x–y] Means within a row without common superscript represent tendencies ($P \geq 0.05$ and $P \leq 0.10$)

[*]SI = saturation index (total SFA/total MUFA + total PUFA)

[**]DI = desaturation index (16:1n-7 + 18:1n-9 cis/16:0 + 16:1n-7 + 18:0 + 18:1n-9 cis)

Table 3.11 Fetal trunk plasma composition in percent of saturated (SFA), monounsaturated (MUFA), and polyunsaturated fatty acids (PUFA) of calves CON (*n*=6), MEL (*n*=6).

	Fetal Plasma[1] (%)			
	Treatment			
Fatty Acid	**CON**	**MEL**	**SEM**	***P* Value**
SFA	48.8320	50.6714	1.1309	0.13
15:0	1.0620	1.4929	0.3533	0.25
16:0	28.5280	30.5771	2.1035	0.35
17:0	0.9900	0.9314	0.1355	0.67
18:0	18.2540	17.6700	1.0046	0.57
MUFA	31.2480	32.1543	1.5655	0.58
14:1n-5	0.0480	0.0071	0.0279	0.17
16:1n-7	4.7780	4.9614	0.5412	0.74
17:1n-8	1.2060	1.2829	0.1597	0.64
18:1n-trans	0.6680	0.0343	0.5543	0.28
18:1n-9 cis	24.5440	25.8657	1.5711	0.42
PUFA	19.9180	17.1771	2.5486	0.31
18:2n-6	11.9920	9.1643	2.4893	0.28
18:3n-3	0.2560	0.0000	0.2120	0.26
20:3n-6	1.4100	1.3271	0.1756	0.65
20:4n-6	3.9900	3.7629	0.4484	0.62
20:5n-3	0.8860	0.7786	0.2673	0.70
22:6	1.3820^{x}	2.1400^{y}	0.3517	0.06

$^{x–y}$ Means within a row without common superscript represent tendencies *(*$P \geq 0.05$ and $P \leq 0.10$)

[1] Fatty acid normalized percentages to total fatty acids

Table 3.12 Maternal plasma composition of saturated (SFA), monounsaturated (MUFA), and polyunsaturated fatty acids (PUFA) of calves CON (*n*=6), MEL (*n*=6).

	Maternal Plasma (mg/ml)			
	Treatment			
Fatty Acid	**CON**	**MEL**	**SEM**	***P* Value**
SFA	0.5550	0.5570	0.0581	0.97
15:0	0.0196	0.0179	0.0019	0.38
16:0	0.2514	0.2473	0.0188	0.83
17:0	0.0182	0.0174	0.0023	0.74
18:0	0.2664	0.2746	0.0361	0.83
MUFA	0.3140	0.3093	0.0273	0.87
14:1n-5	0.0186	0.0181	0.0021	0.83
16:1n-7	0.0314	0.0300	0.0025	0.59
17:1n-8	0.0110	0.0107	0.0016	0.86
18:1n-trans	0.0372	0.0386	0.0077	0.86
18:1n-9 cis	0.2160	0.2123	0.0186	0.85
PUFA	0.5496	0.5140	0.0500	0.49
18:2n-6	0.3038	0.2840	0.0313	0.54
18:3n-3	0.1486	0.1429	0.0148	0.71
20:3n-6	0.0246	0.0206	0.0027	0.16
20:4n-6	0.0468	0.0389	0.0061	0.22
20:5n-3	0.0242	0.0239	0.0018	0.86
22:6	0.0016	0.0040	0.0016	0.16
TOTAL	1.4186	1.3803	0.1278	0.77
SI*	0.6420	0.6743	0.0345	0.37
DI**	0.3280	0.3186	0.0133	0.49

*SI = saturation index (total SFA/total MUFA + total PUFA)

**DI = desaturation index (16:1n-7 + 18:1n-9 cis/16:0 + 16:1n-7 + 18:0 + 18:1n-9 cis)

Table 3.13 Maternal plasma composition in percent of saturated (SFA), monounsaturated (MUFA), and polyunsaturated fatty acids (PUFA) of calves CON (*n*=6), MEL (*n*=6).

	Maternal Plasma[1] (%)			
	Treatment			
Fatty Acid	**CON**	**MEL**	**SEM**	***P* Value**
SFA	39.0940	40.2229	1.1765	0.36
15:0	1.3820	1.2843	0.0933	0.32
16:0	17.8360	17.9429	0.4434	0.81
17:0	1.2640	1.2600	0.0868	0.96
18:0	18.6100	19.7329	1.0756	0.32
MUFA	22.2260	22.4186	0.7255	0.80
14:1n-5	1.3320	1.3014	0.1170	0.80
16:1n-7	2.2240	2.1986	0.1545	0.87
17:1n-8	0.7720	0.7643	0.0962	0.94
18:1n-trans	2.5680	2.7400	0.4035	0.68
18:1n-9 cis	15.3300	15.4186	0.7042	0.90
PUFA	38.6820	37.3600	1.2863	0.33
18:2n-6	21.3200	20.5829	0.8042	0.38
18:3n-3	10.4720	10.4300	0.7707	0.96
20:3n-6	1.7560	1.4914	0.1574	0.12
20:4n-6	3.3240	2.8043	0.3413	0.16
20:5n-3	1.7020	1.7600	0.1520	0.71
22:6	0.1080	0.2900	0.1134	0.14

[1] Fatty acid normalized percentages to total fatty acids

Table 3.14 Fetal morphometrics with body weight (**BW**; kg) and Longissimus dorsi (**LM**) weight (kg), circumference (cm), and length (cm) of muscle and perirenal (**PR**) adipose tissue weight (kg) for calves CON (*n*=6), MEL (*n*=6).

	Morphometric Measurements			
	Treatment			
Measurements	**CON**	**MEL**	**SEM**	***P* Value**
BW (kg)	24.0000	22.9000	1.9000	0.56
LM Weight (kg)	0.2218[x]	0.2633[y]	0.0227	0.10
LM Circumference (cm)	32.8833	38.5667	4.1250	0.21
LM Length (cm)	10.0667[x]	11.4500[y]	0.6564	0.07
PR Weight (kg)	0.0623	0.1667	0.0984	0.32

[x–y] Means within a row without common superscript represent tendencies *(*$P \geq 0.05$ and $P \leq 0.10$)

Table 3.15 QuantiNova™ SYBR® Green real-time PCR quantification of Fetal Longissimus dorsi (**LM**) PCR relative expression of IGF1, IGF1R, IGF2, IGF2R, BMP, CYS, LOX, and AMPK of calves CON (*n*=6), MEL (*n*=6).

	Longissimus dorsi PCR Relative Expression			
	Treatment			
Gene[1]	**CON**	**MEL**	**SEM**	***P* Value**
IGF1	5.3333	7.6667	1.7847	0.23
IGF1R	5.5000	7.5000	1.8359	0.31
IGF2	5.5000	7.5000	1.5753	0.24
IGF2R	5.6667	7.3333	1.6777	0.35
BMP	5.6667	7.3333	1.8053	0.38
CYS	4.3333[a]	8.6667[b]	1.4985	0.02
LOX	5.5000	7.5000	1.7213	0.28
AMPK	4.5000[a]	8.5000[b]	1.5516	0.03

[a–b] Means within a row without common superscript differ *(P* < 0.05)

[1] IGF1 = insulin-like growth factor 1, IGF1R = IGF1 receptor, IGF2 = insulin-like growth factor 2, IGF2R = IGF2 receptor, CYS = cystatin, AMPK = adenosine monophosphate-activated protein kinase-α, LOX = lysyl oxidase, BMP = bone morphogenetic protein

Table 3.16 TaqMan® real-time PCR quantification of Fetal Longissimus dorsi (**LM**) PCR relative expression of IGF1, IGF1R, IGF2, IGF2R, BMP, CYS, LOX, and AMPK of calves CON (*n*=6), MEL (*n*=6).

	LM PCR Relative Expression			
	Treatment			
Gene[1]	**CON**	**MEL**	**SEM**	***P* Value**
Myf5	6.4167	6.5833	1.9003	0.93
MyoG	5.2500	7.7500	1.6429	0.17
MyoD	6.0000	7.0000	1.7717	0.59
CEBPA	5.2500	7.7500	1.8130	0.21
SCD	5.8333	7.1667	1.9245	0.51
PPARg	6.1667	6.8333	1.5986	0.69
PNPLA2	5.4167	7.5833	1.6073	0.21

[1]Myf5 = myogenic factor 5, MyoG = myogenin, MyoD = myogenic differentiation 1, CEBPA = CCAAT enhancer binding protein alpha, SCD = stearoyl-CoA desaturase, PPARg = peroxisome proliferator activated receptor gamma, PNPLA2 = patatin-like phospholipase domain containing 2.

Table 3.17 Fetal perirenal adipose tissue (**PR**) PCR relative expression of ADIPOQ, IGF1, and UCP1 of calves CON (*n*=6), MEL (*n*=6).

	PR PCR Relative Expression			
	Treatment			
Gene[1]	**CON**	**MEL**	**SEM**	***P* Value**
UCP1	7.0000	6.0000	1.9484	0.62
ADIPOQ	8.8333[a]	4.1667[b]	1.3878	0.01
CEBPA	8.1667[a]	4.8333[b]	1.2172	0.03
PPARG	8.3333[a]	4.6667[b]	1.4530	0.04
SCD	8.3333[a]	4.6667[b]	1.2247	0.02
PNPLA2	7.8333	5.1667	1.7105	0.16
IGF2	8.0000[x]	5.0000[y]	1.5694	0.09
IGF1	8.6667[a]	4.3333[b]	1.2910	0.01
IGF1R	7.3333	5.6667	1.6833	0.35

[a–b] Means within a row without common superscript differ *(P* < 0.05)

[x–y] Means within a row without common superscript represent tendencies *(P* ≥ 0.05 and *P* ≤ 0.10)

[1] UCP1 = uncoupling protein 1, ADIPOQ = adiponectin, CEBPA = CCAAT enhancer binding protein alpha, PPARg = peroxisome proliferator activated receptor gamma, SCD = stearoyl-CoA desaturase, PNPLA2 = patatin-like phospholipase domain containing 2, IGF2 = insulin-like growth factor 2, IGF1 = insulin-like growth factor 1, IGF1R = IGF1 receptor .

Table 3.18 Fetal immunohistochemistry of Longissimus dorsi (**LM**) with number of primary to secondary fibers (Prime:Sec), number of PAX7 activated nuclei to total nuclei (PAX7:Nuclei), total number of nuclei to number of myofibers (Nuclei:Fiber), and cross-sectional areas of primary and secondary fibers (Prime CSA; Sec CSA) of calves CON (*n*=6), MEL (*n*=6).

	Longissimus dorsi Immunohistochemistry			
	Treatment			
Gene	**CON**	**MEL**	**SEM**	***P* Value**
Prime:Sec[1]	5.3645	6.1296	0.5060	0.17
PAX7:Nuclei[2]	0.1285[x]	0.2042[y]	0.0356	0.07
Nuclei:Fiber[3]	0.6716	0.5922	0.0592	0.22
Prime CSA[4]	517.7500	535.4900	181.1200	0.92
Sec CSA[5]	635.4700	469.1600	281.0800	0.57

[x–y] Means within a row without common superscript represent tendencies *(*$P \geq 0.05$ and $P \leq 0.10$)

[1] Ratio of primary to secondary myofibers (Primary fiber total/Secondary fiber total)

[2] Ratio of PAX7 activated nuclei to total nuclei (PAX7 total/Nuclei total)

[3] Ratio of nuclei total to number of total myofibers (Nuclei total/Myofiber total)

[4-5] Cross-sections area of primary and secondary myofibers (μm)

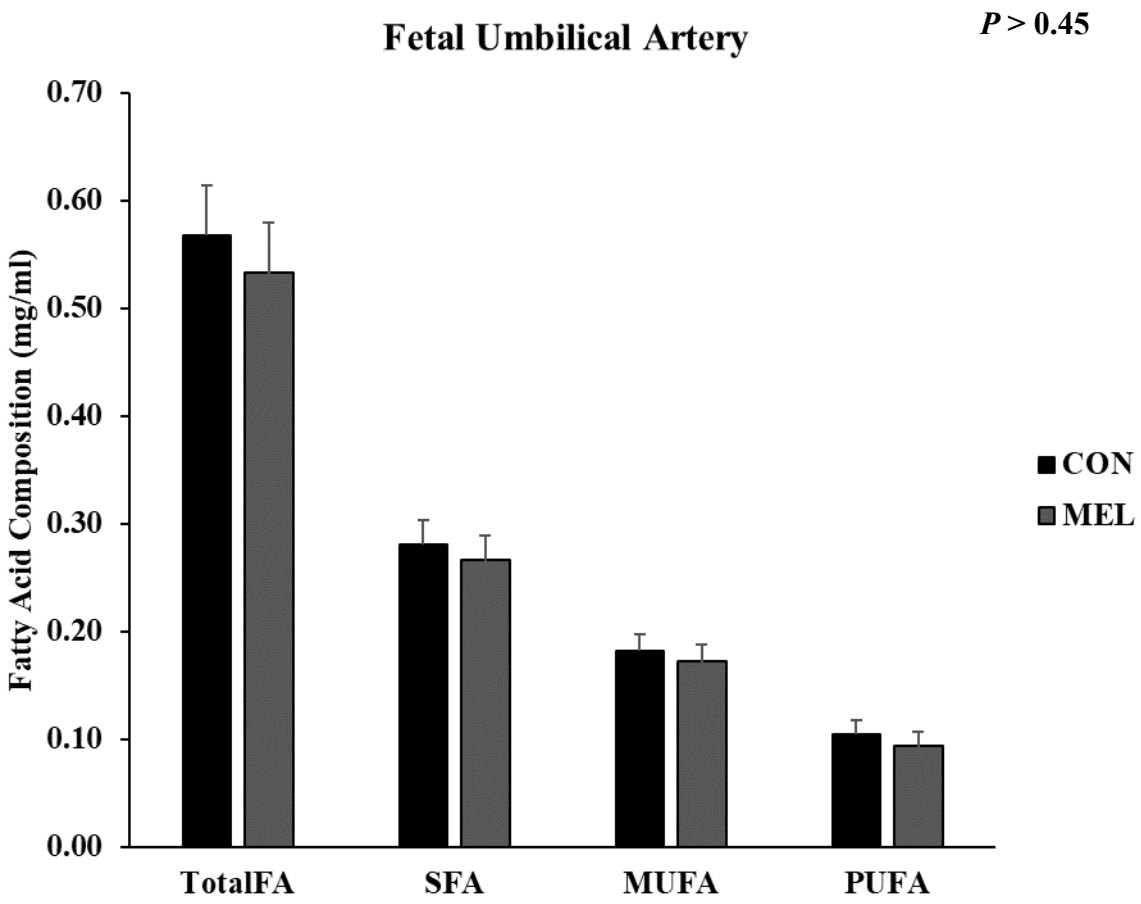

Figure 3.1 Fetal umbilical artery composition of saturated (SFA), monounsaturated (MUFA), and polyunsaturated fatty acids (PUFA), in milligrams per kilogram, from fetuses harvested from CON (n=6) vs. MEL (n=6) treated dams.

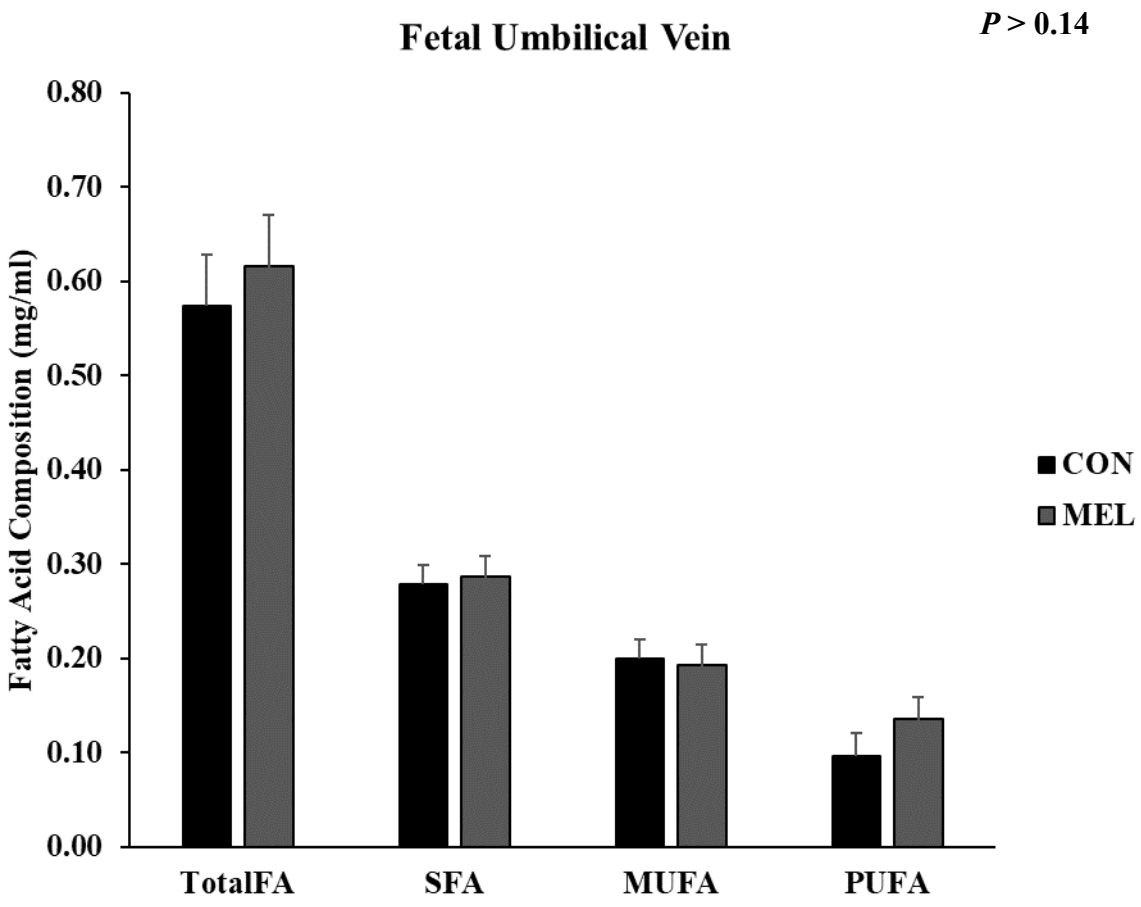

Figure 3.2 Fetal umbilical vein composition of saturated (SFA), monounsaturated (MUFA), and polyunsaturated fatty acids (PUFA), in milligrams per kilogram, from fetuses harvested from CON (n=6) vs. MEL (n=6) treated dams.

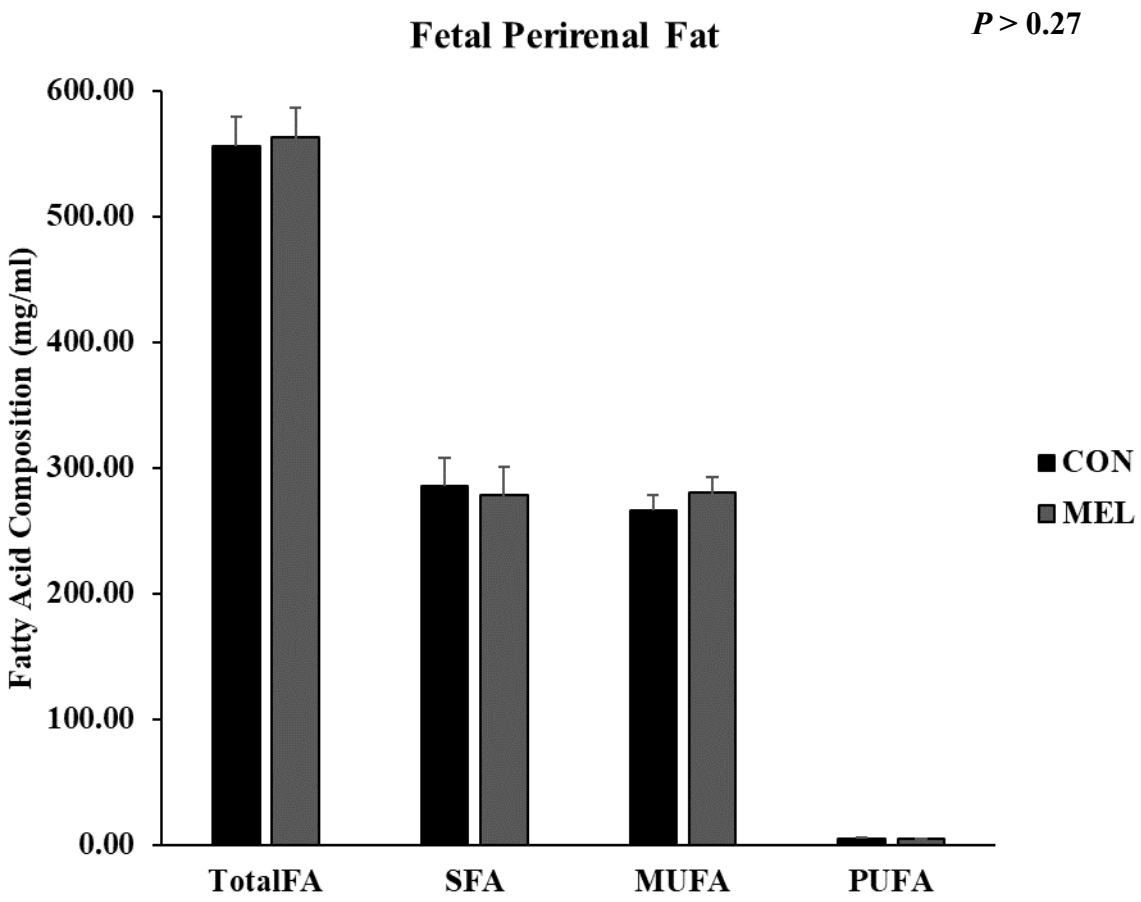

Figure 3.3 Fetal perirenal fat composition of saturated (SFA), monounsaturated (MUFA), and polyunsaturated fatty acids (PUFA), in milligrams per kilogram, from fetuses harvested from CON (n=6) vs. MEL (n=6) treated dams.

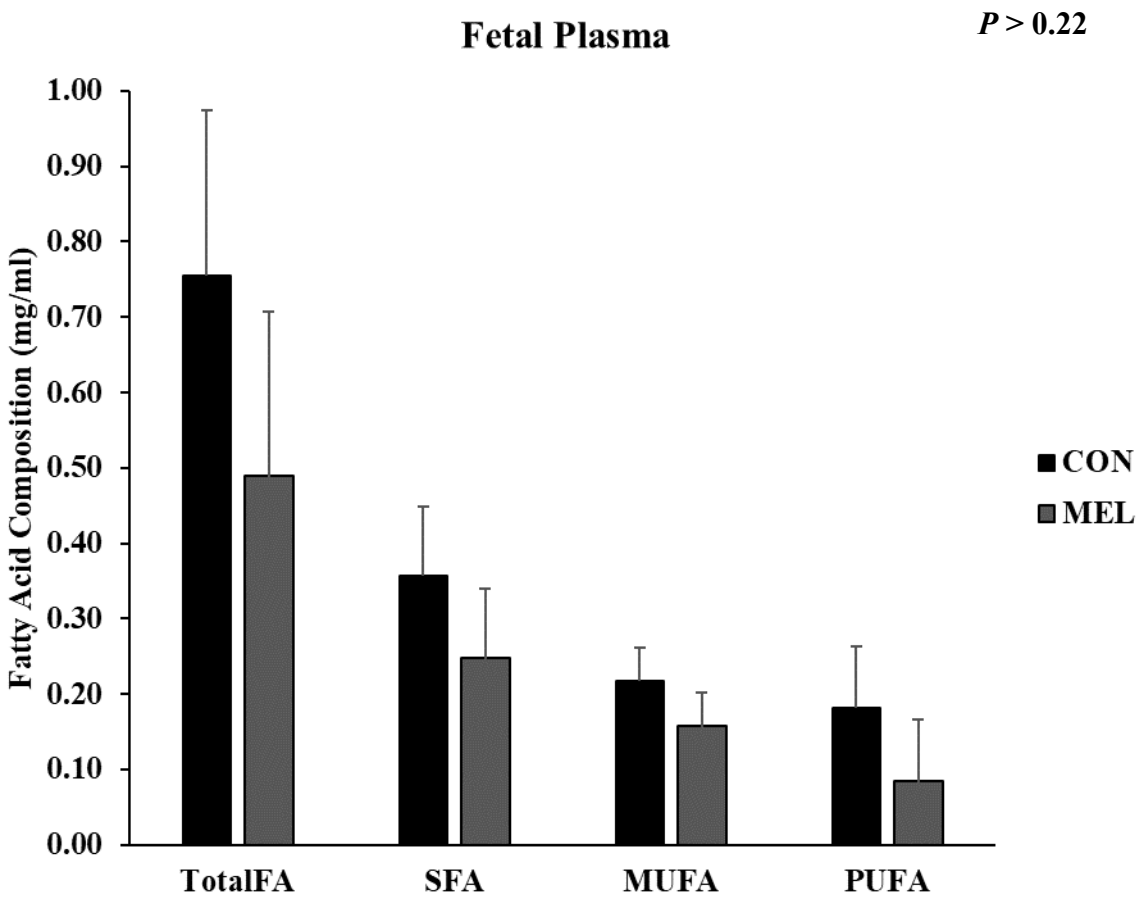

Figure 3.4 Fetal trunk plasma composition of saturated (SFA), monounsaturated (MUFA), and polyunsaturated fatty acids (PUFA), in milligrams per kilogram, from fetuses harvested from CON (n=6) vs. MEL (n=6) treated dams.

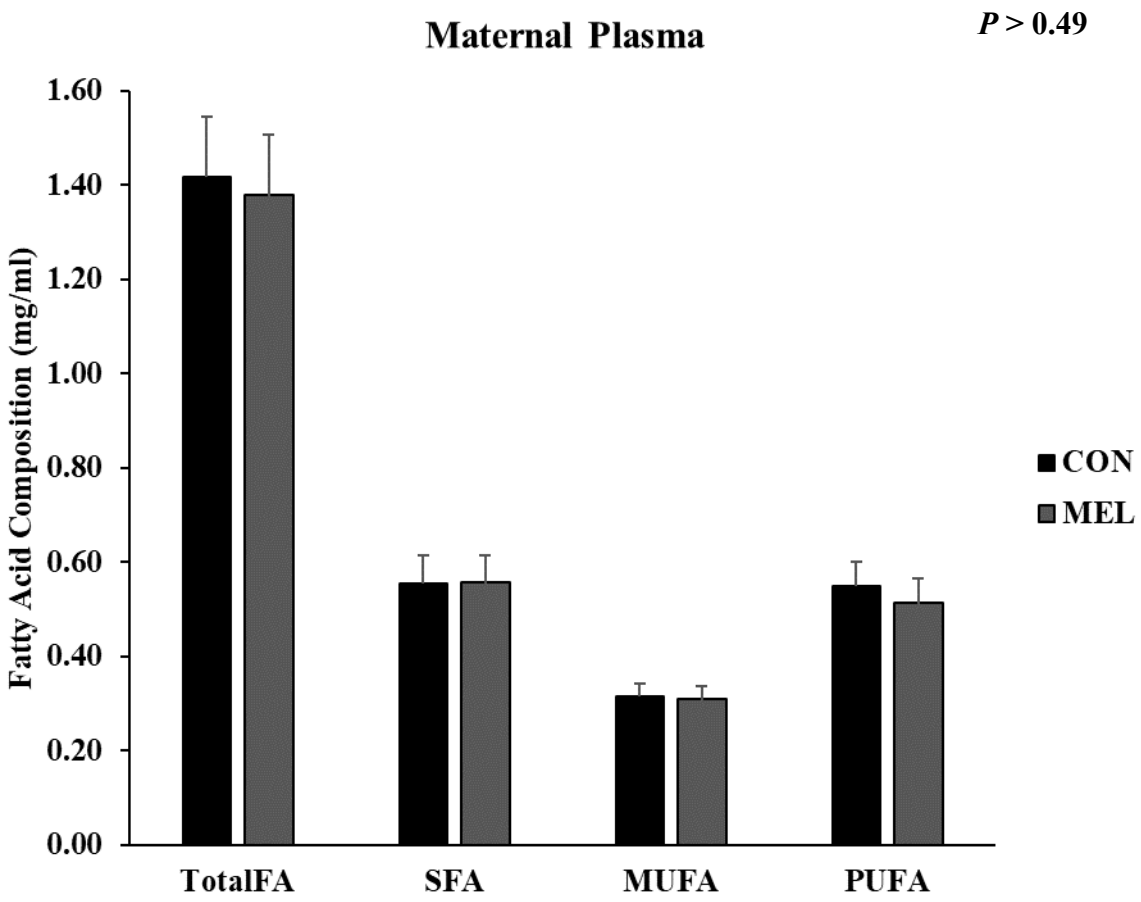

Figure 3.5 Maternal plasma composition of saturated (SFA), monounsaturated (MUFA), and polyunsaturated fatty acids (PUFA), in milligrams per kilogram, from fetuses harvested from CON (n=6) vs. MEL (n=6) treated dams.

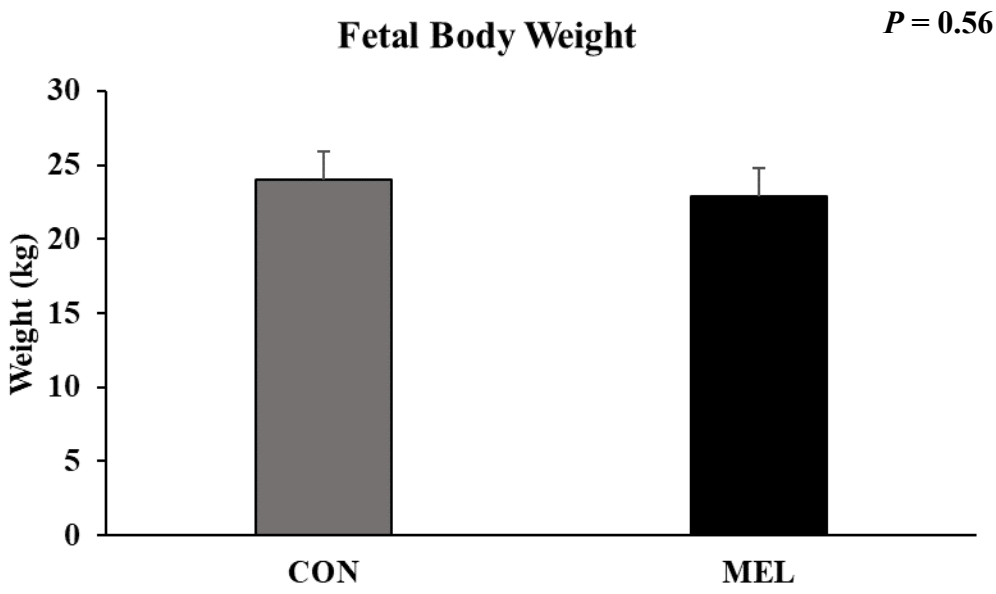

Figure 3.6 Body weight average from fetuses harvested from CON (n=6) vs. MEL (n=6) treated dams.

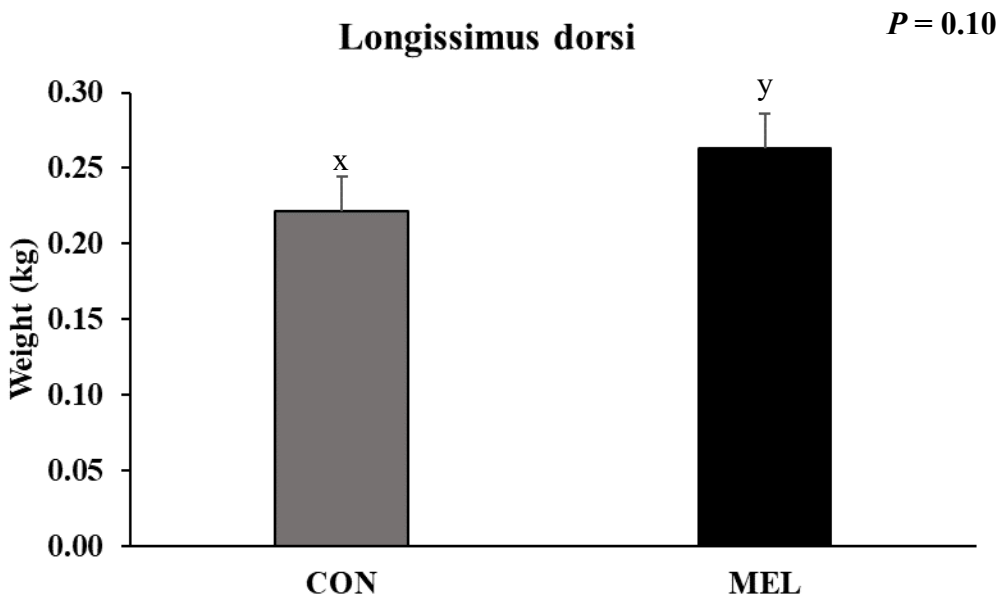

Figure 3.7 Fetal Longissimus dorsi average weight (kg) from fetuses harvested from CON (n=6) vs. MEL (n=6) treated dams. $^{x–y}$ Means within a row without common superscript represent tendencies *(*$P \geq 0.05$ and $P \leq 0.10$)

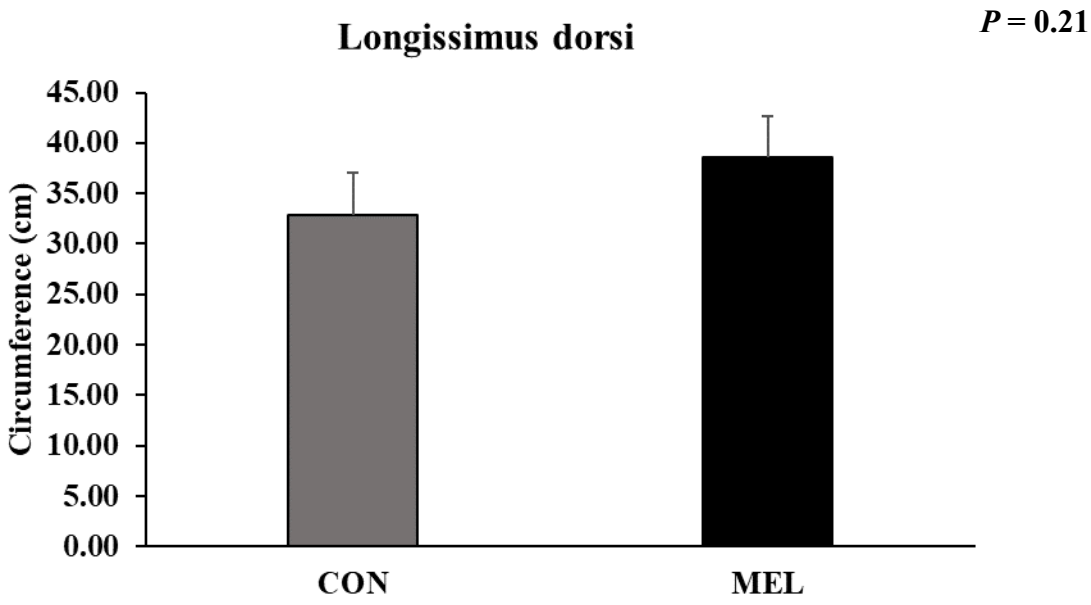

Figure 3.8 Fetal Longissimus dorsi average circumference (cm) from fetuses harvested from CON (n=6) vs. MEL (n=6) treated dams. $^{x–y}$ Means within a row without common superscript represent tendencies *(*$P \geq 0.05$ and $P \leq 0.10$)

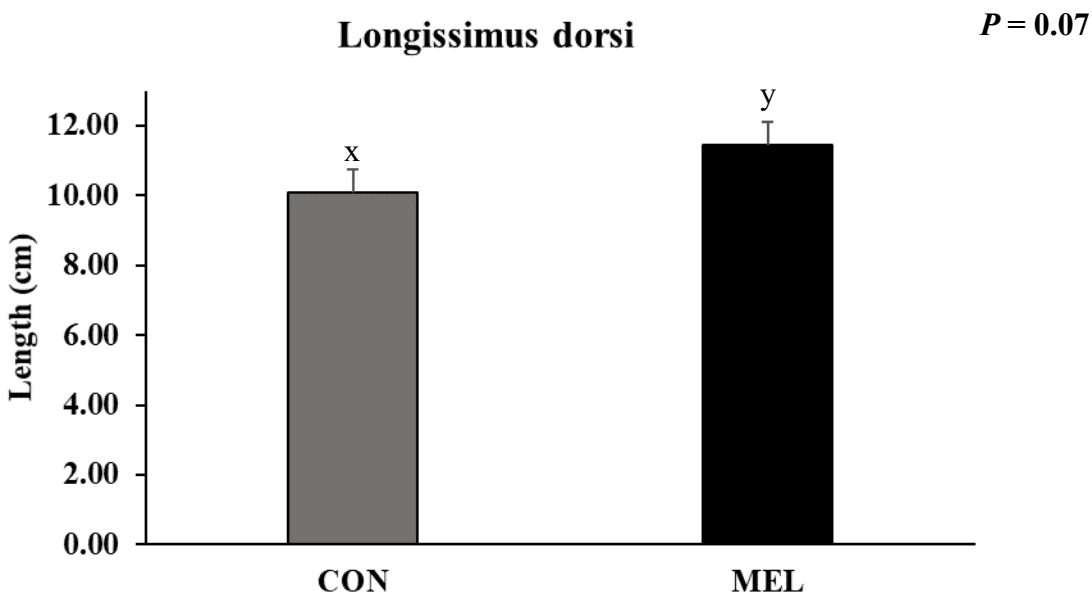

Figure 3.9 Fetal Longissimus dorsi average length (cm) from fetuses harvested from CON (n=6) vs. MEL (n=6) treated dams. $^{x–y}$ Means within a row without common superscript represent tendencies *(*$P \geq 0.05$ and $P \leq 0.10$)

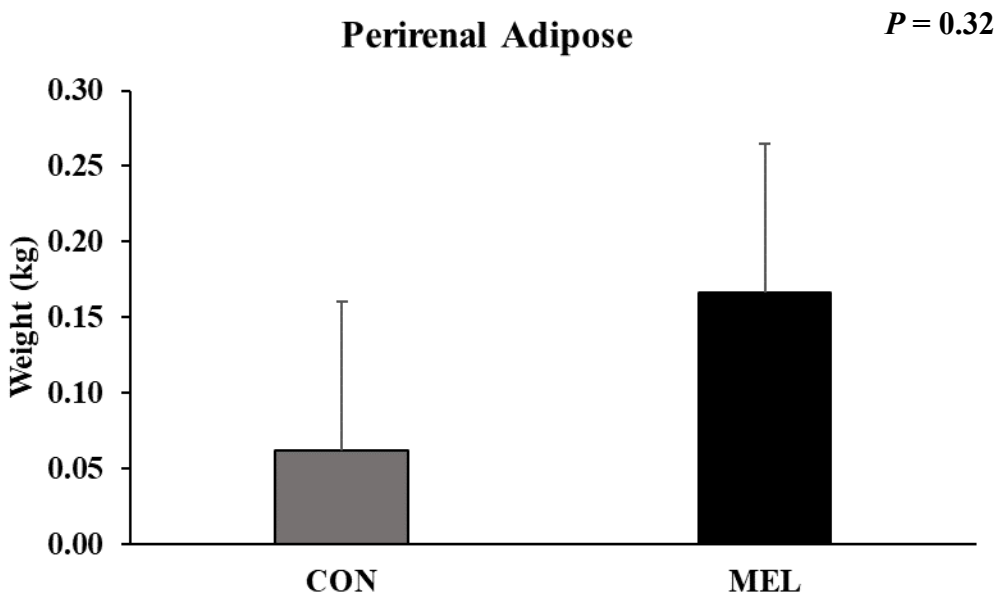

Figure 3.10 Fetal perirenal adipose tissue average weight (kg) from fetuses harvested from CON (n=6) vs. MEL (n=6) treated dams.

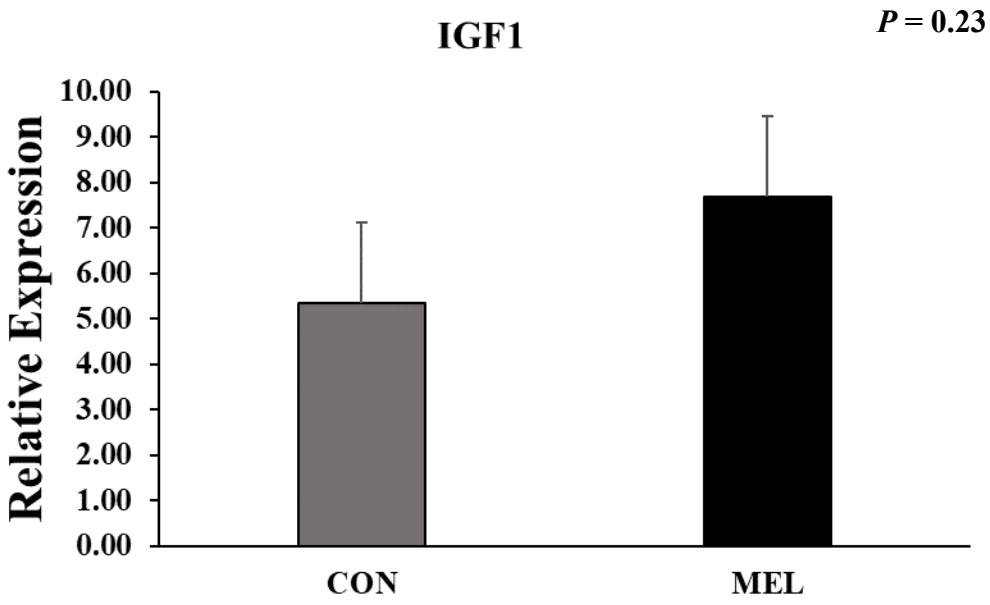

Figure 3.11 Relative expression (mRNA abundance) of Insulin-Like Growth factor 1 in Longissimus dorsi, from fetuses harvested from CON (n=6) vs. MEL (n=6) treated dams.

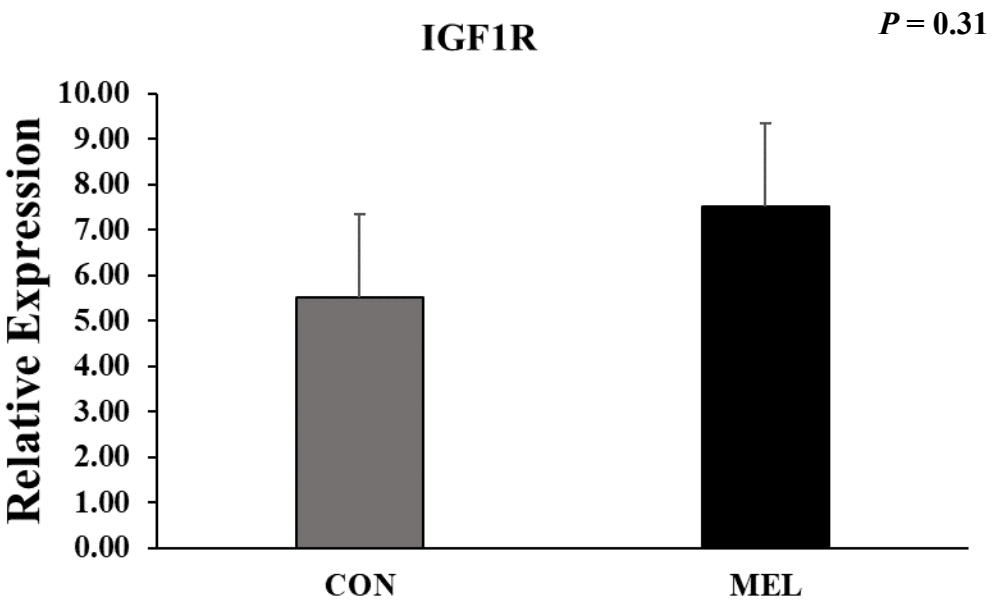

Figure 3.12 Relative expression (mRNA abundance) of Insulin-Like Growth factor 1 receptor in Longissimus dorsi, from fetuses harvested from CON (n=6) vs. MEL (n=6) treated dams.

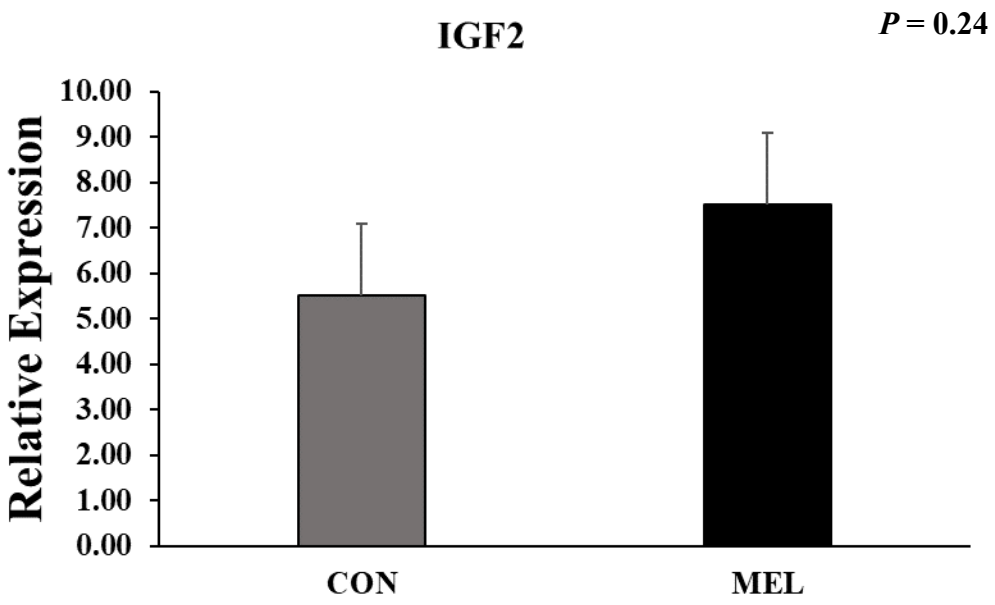

Figure 3.13 Relative expression (mRNA abundance) of Insulin-Like Growth factor 2 in Longissimus dorsi, from fetuses harvested from CON (n=6) vs. MEL (n=6) treated dams.

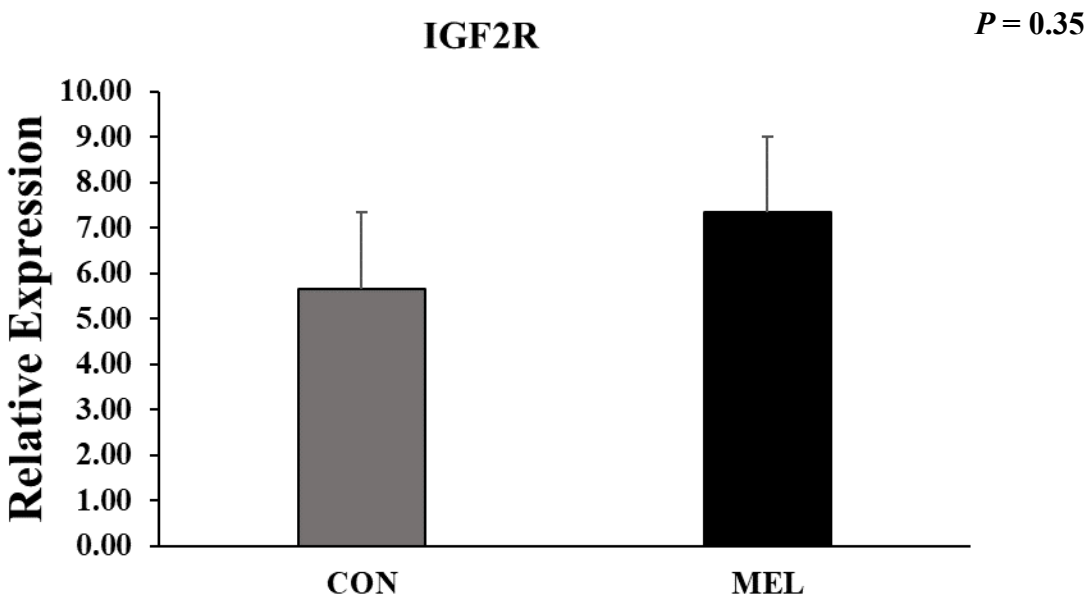

Figure 3.14 Relative expression (mRNA abundance) of Insulin-Like Growth factor 2 receptor in Longissimus dorsi, from fetuses harvested from CON (n=6) vs. MEL (n=6) treated dams.

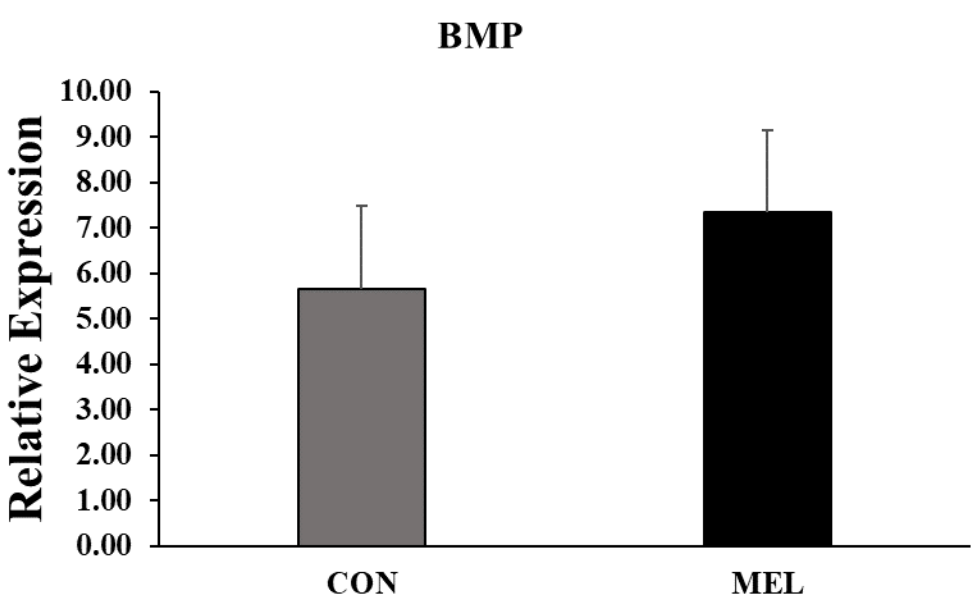

Figure 3.15 Relative expression (mRNA abundance) of bone morphogenetic protein in Longissimus dorsi, from fetuses harvested from CON (n=6) vs. MEL (n=6) treated dams.

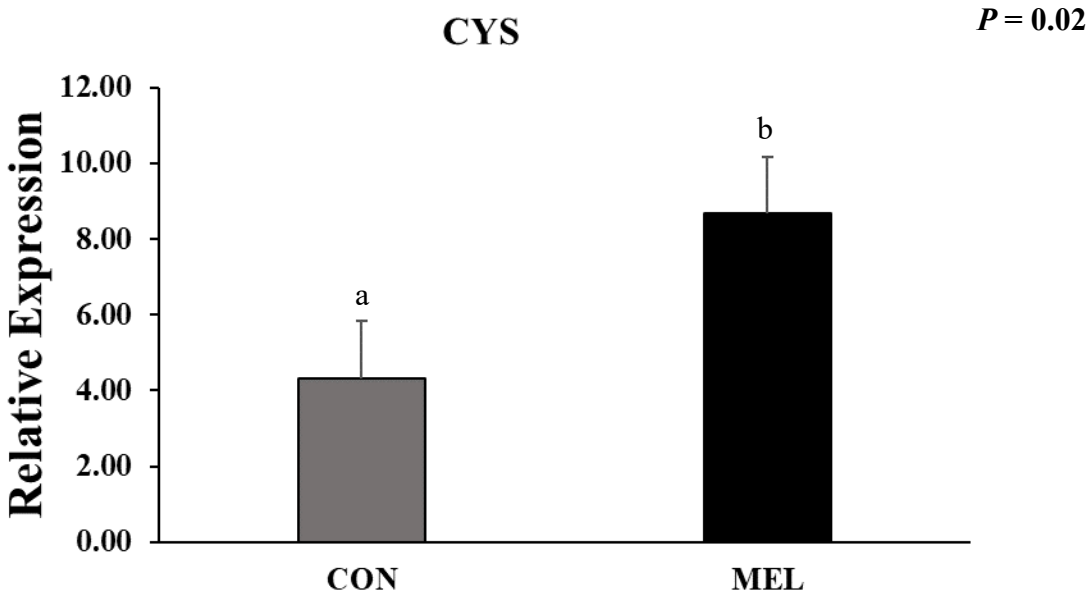

Figure 3.16 Relative expression (mRNA abundance) of cystatin in Longissimus dorsi, from fetuses harvested from CON (n=6) vs. MEL (n=6) treated dams. [a–b] Means within a row without common superscript differ *(P* < 0.05)

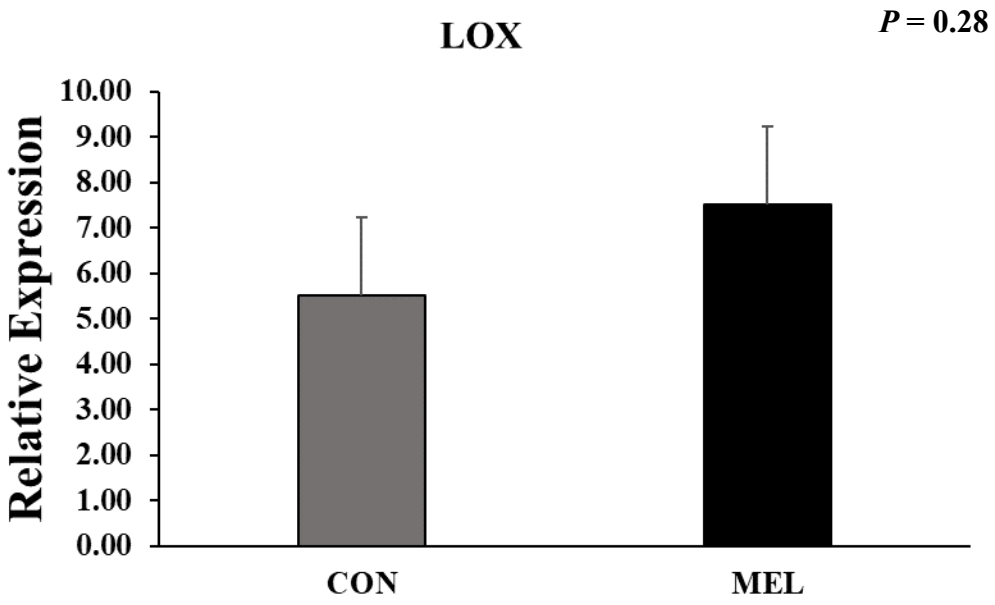

Figure 3.17 Relative expression (mRNA abundance) of lysyl oxidase in Longissimus dorsi, from fetuses harvested from CON (n=6) vs. MEL (n=6) treated dams.

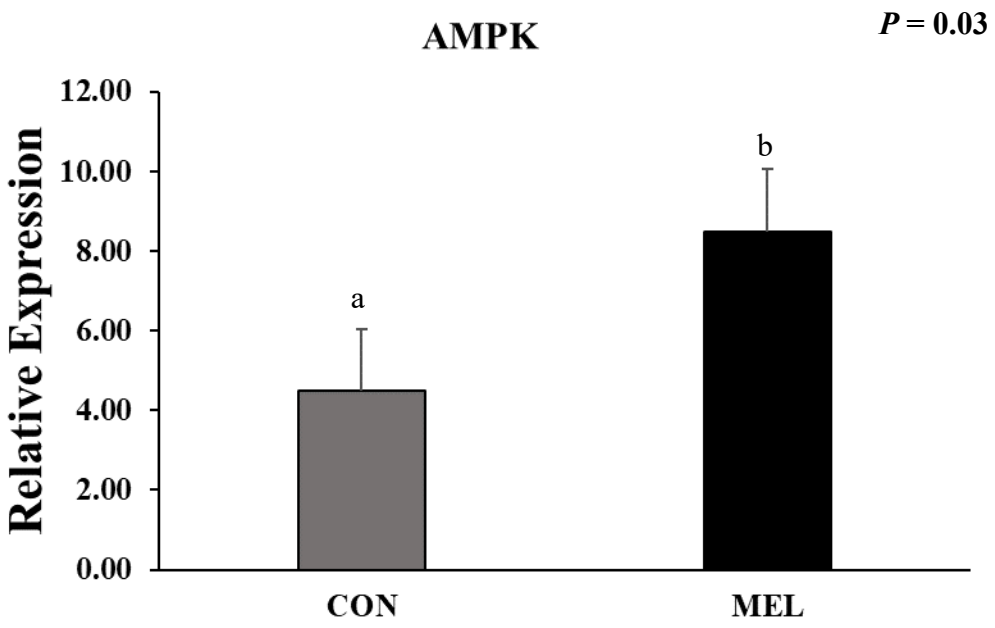

Figure 3.18 Fetal Relative expression (mRNA abundance) of adenosine monophosphate-activated protein kinase-α in Longissimus dorsi, from fetuses harvested from CON (n=6) vs. MEL (n=6) treated dams. [a–b] Means within a row without common superscript differ *(P* < 0.05)

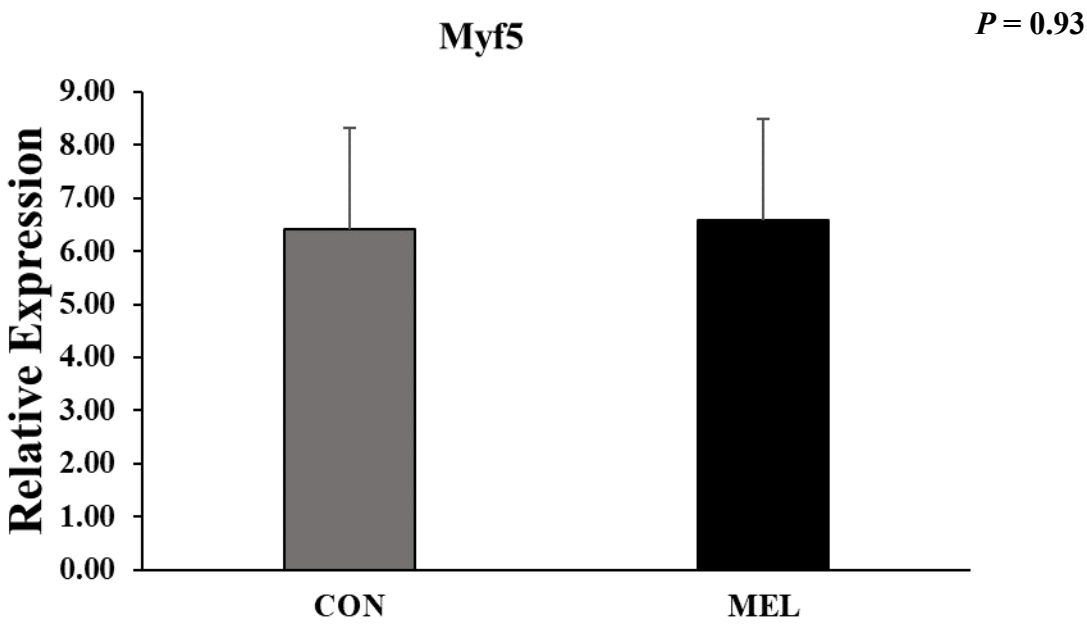

Figure 3.19 Fetal Relative expression (mRNA abundance) of myogenic factor 5 in Longissimus dorsi, from fetuses harvested from CON (n=6) vs. MEL (n=6) treated dams.

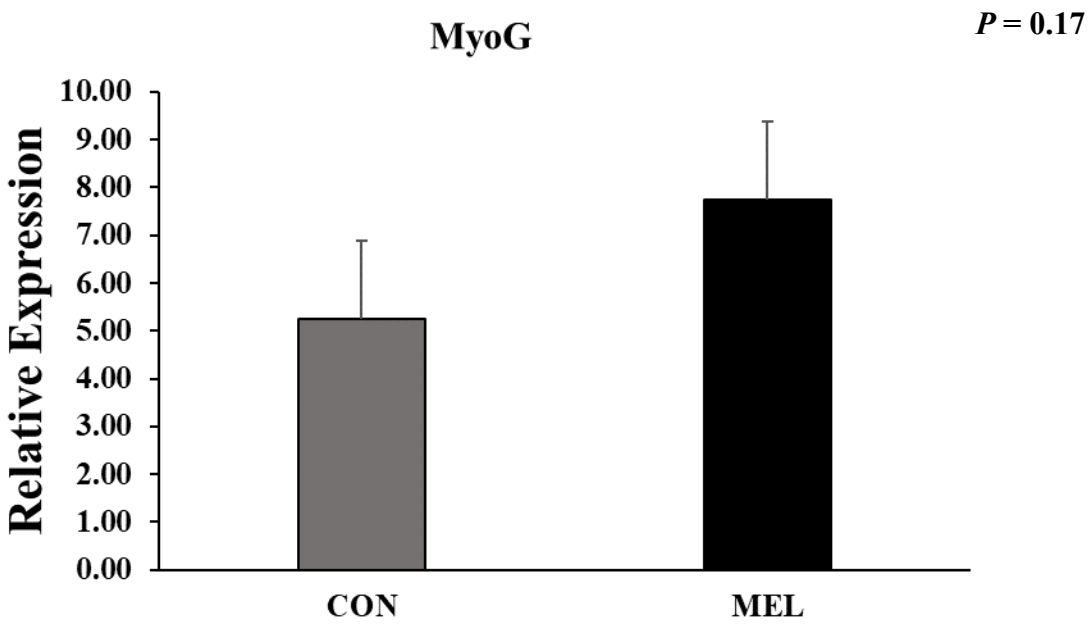

Figure 3.20 Fetal Relative expression (mRNA abundance) of myogenin in Longissimus dorsi, from fetuses harvested from CON (n=6) vs. MEL (n=6) treated dams.

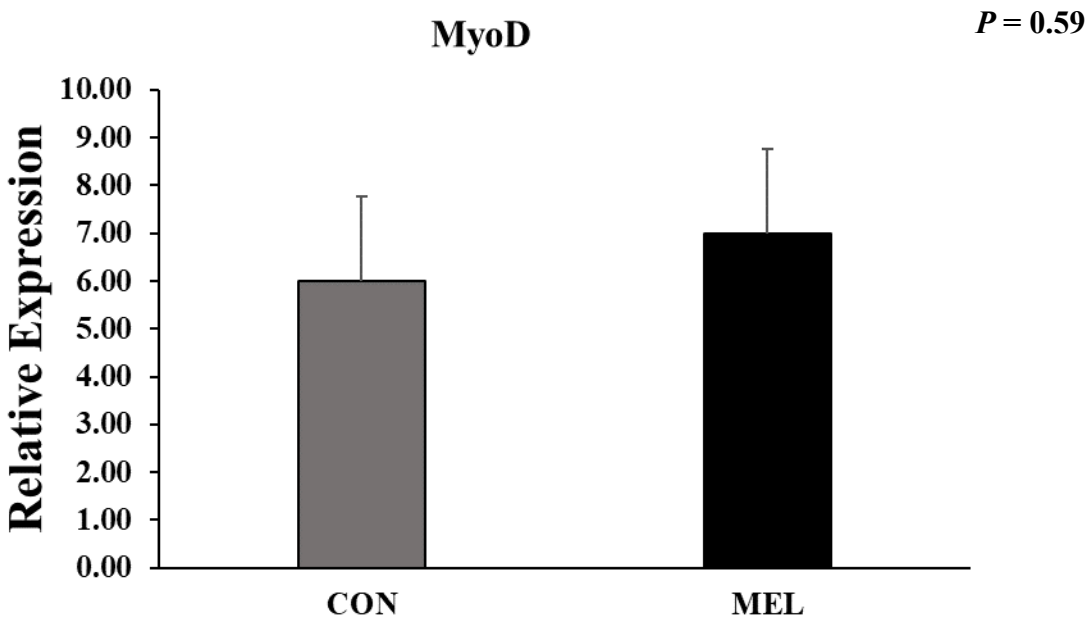

Figure 3.21 Fetal Relative expression (mRNA abundance) of myogenic differentiation 1 in Longissimus dorsi, from fetuses harvested from CON (n=6) vs. MEL (n=6) treated dams.

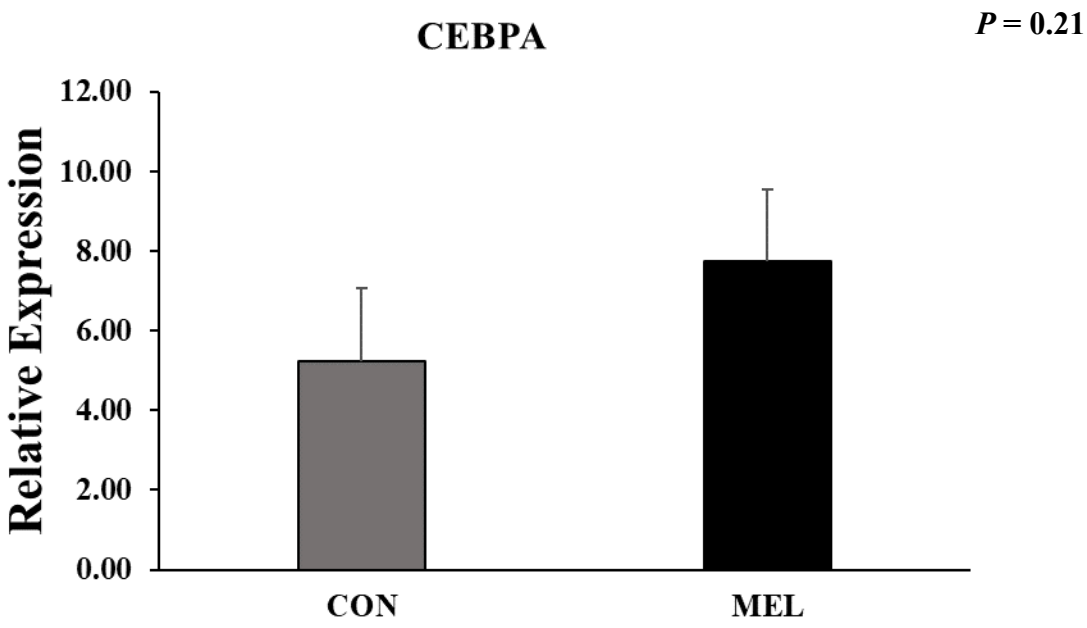

Figure 3.22 Fetal Relative expression (mRNA abundance) of CCAAT enhancer binding protein alpha in Longissimus dorsi, from fetuses harvested from CON (n=6) vs. MEL (n=6) treated dams.

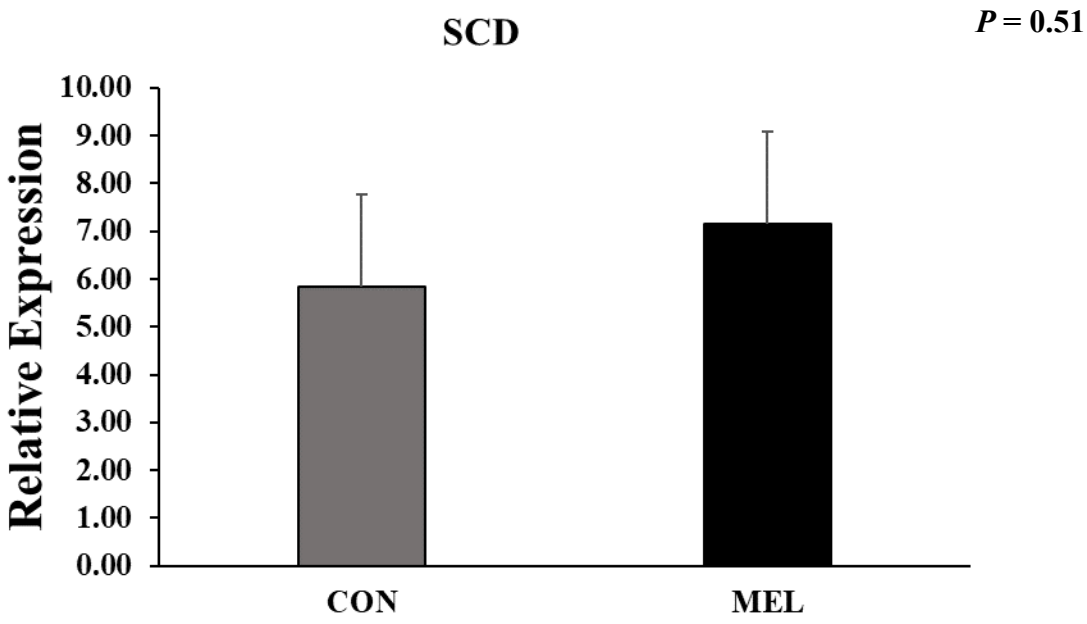

Figure 3.23 Fetal Relative expression (mRNA abundance) of stearoyl-CoA desaturase in Longissimus dorsi, from fetuses harvested from CON (n=6) vs. MEL (n=6) treated dams.

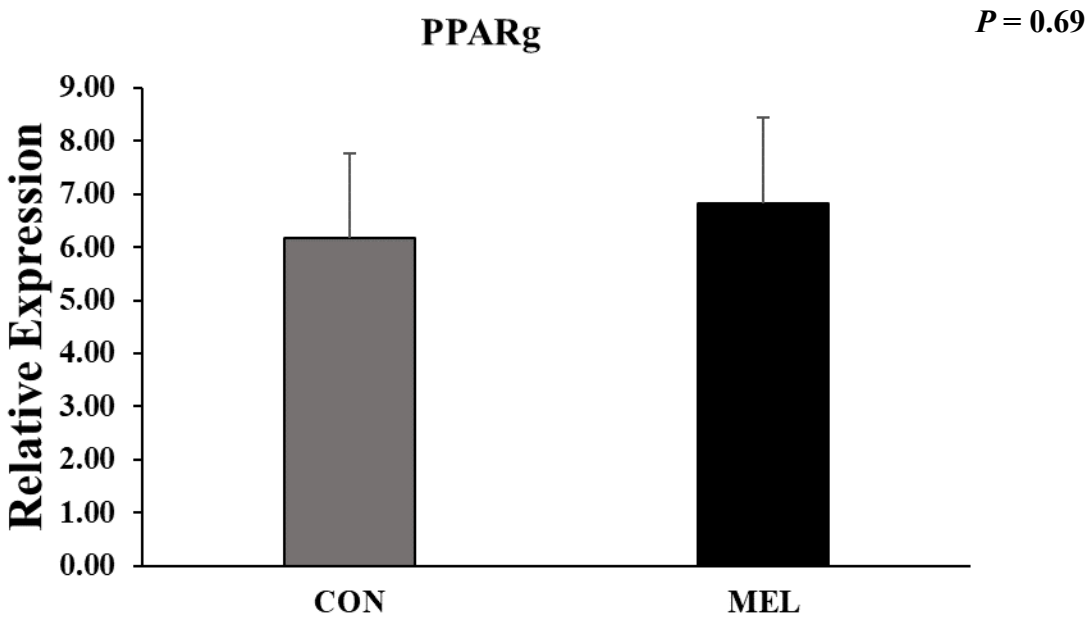

Figure 3.24 Fetal Relative expression (mRNA abundance) of peroxisome proliferator activated receptor gamma in Longissimus dorsi, from fetuses harvested from CON (n=6) vs. MEL (n=6) treated dams.

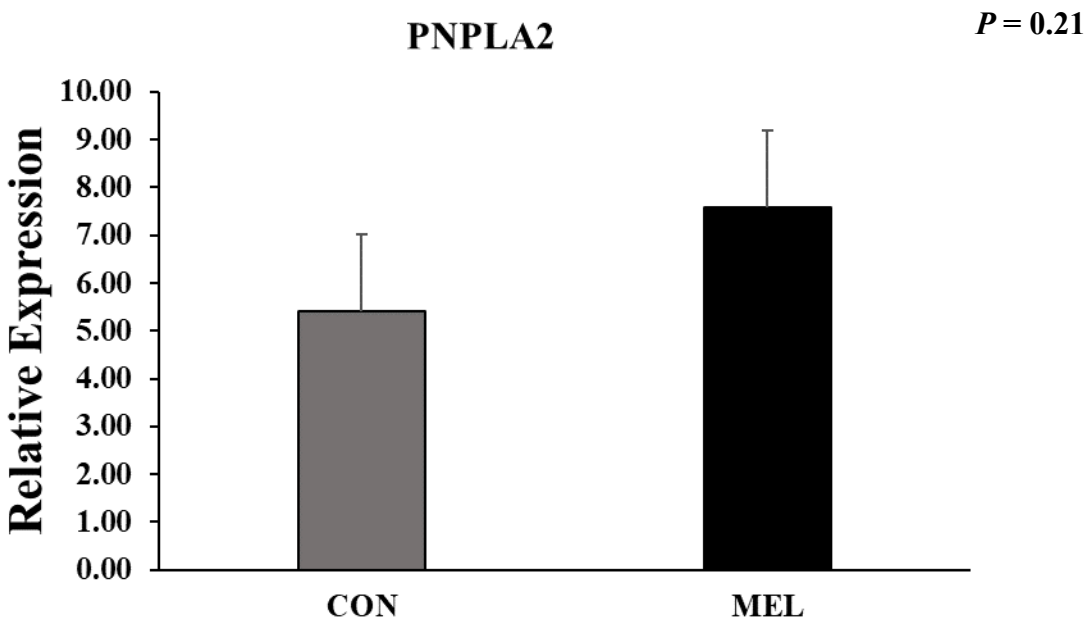

Figure 3.25 Fetal Relative expression (mRNA abundance) of patatin-like phospholipase domain containing 2 in Longissimus dorsi, from fetuses harvested from CON (n=6) vs. MEL (n=6) treated dams.

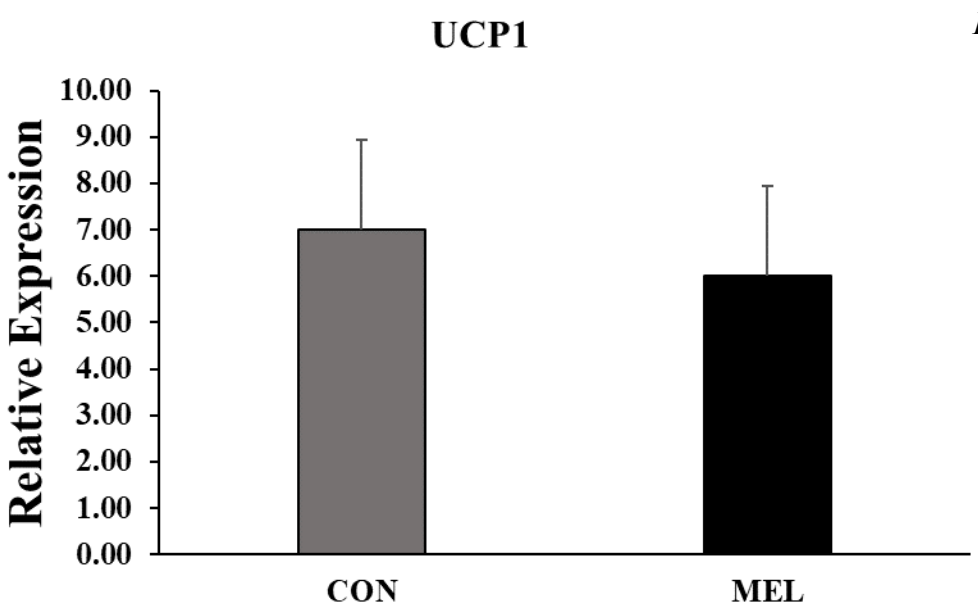

Figure 3.26 Fetal Relative expression (mRNA abundance) of uncoupling protein 1 in perirenal adipose tissue, from fetuses harvested from CON (n=6) vs. MEL (n=6) treated dams.

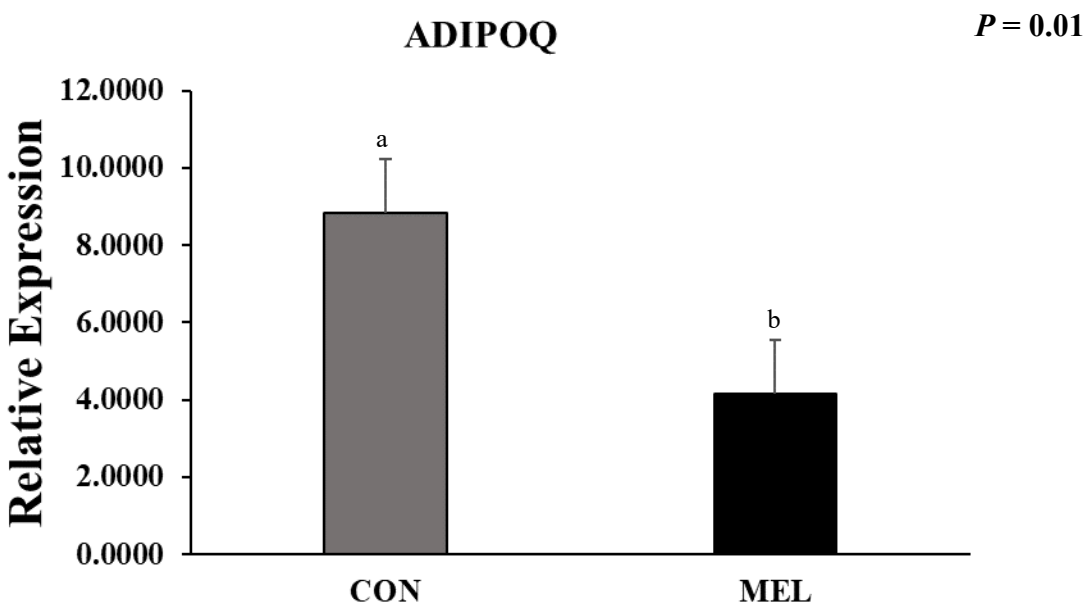

Figure 3.27 Fetal Relative expression (mRNA abundance) of adiponectin in perirenal adipose tissue, from fetuses harvested from CON (n=6) vs. MEL (n=6) treated dams. [a-b] Significance of means without common letters ($P \leq 0.05$).

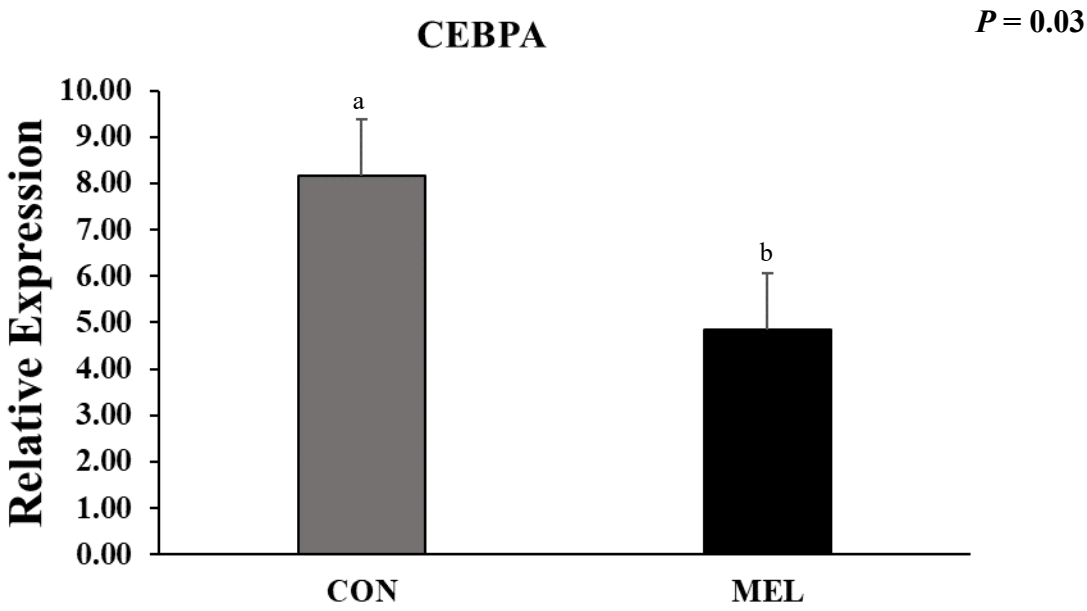

Figure 3.28 Fetal Relative expression (mRNA abundance) of CCAAT enhancer binding protein alpha in perirenal adipose tissue, from fetuses harvested from CON (n=6) vs. MEL (n=6) treated dams. [a-b] Significance of means without common letters *(P* ≤ 0.05)

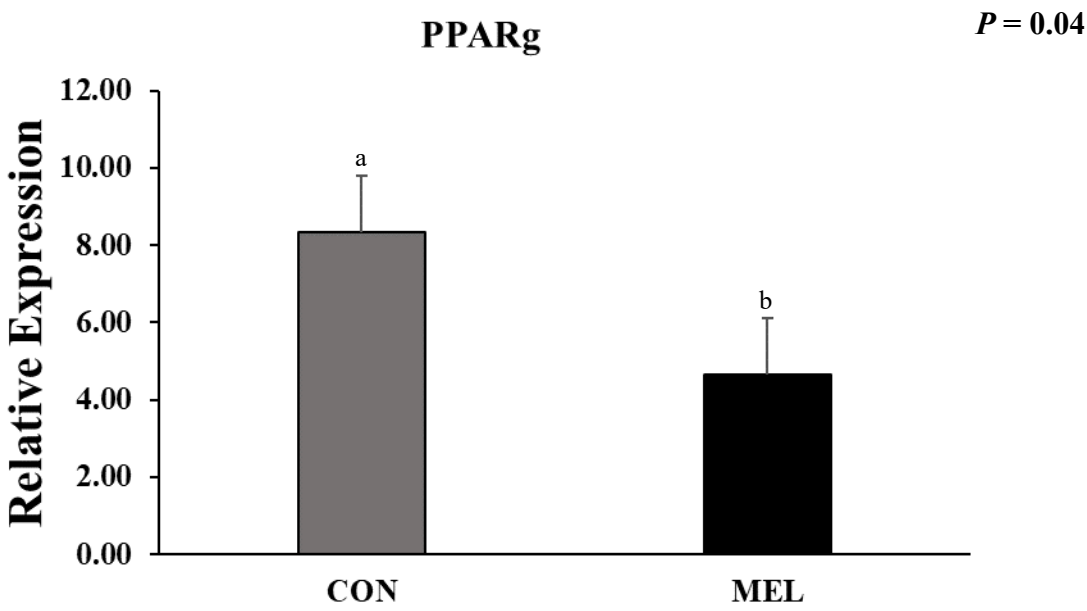

Figure 3.29 Fetal Relative expression (mRNA abundance) of peroxisome proliferator activated receptor gamma in perirenal adipose tissue, from fetuses harvested from CON (n=6) vs. MEL (n=6) treated dams. [a-b] Significance of means without common letters *(P* ≤ 0.05)

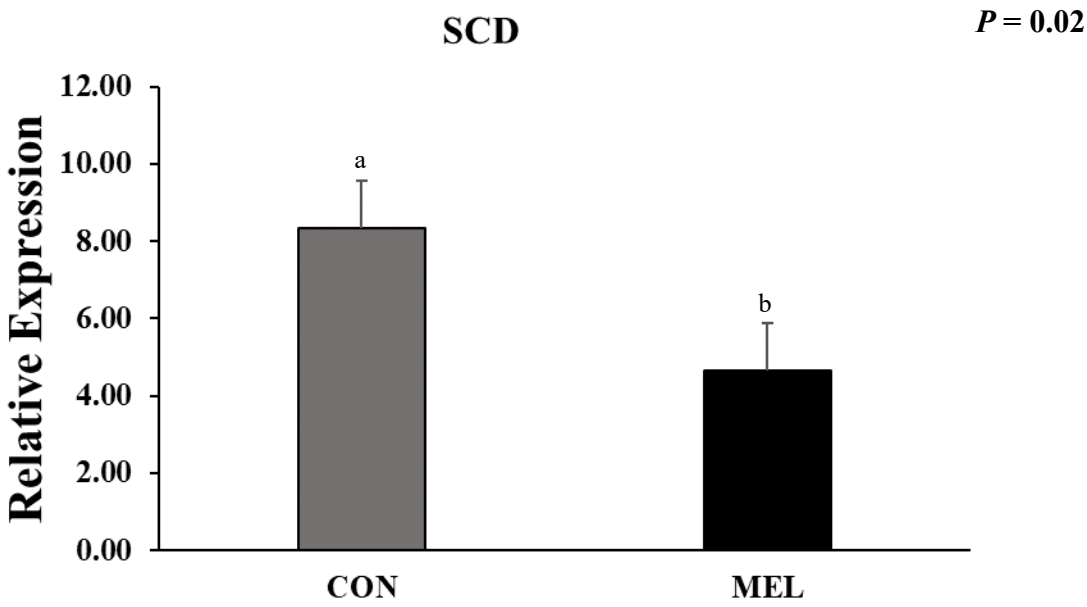

Figure 3.30 Fetal Relative expression (mRNA abundance) of stearoyl-CoA desaturase in perirenal adipose tissue, from fetuses harvested from CON (n=6) vs. MEL (n=6) treated dams. [a-b] Significance of means without common letters ($P \leq 0.05$).

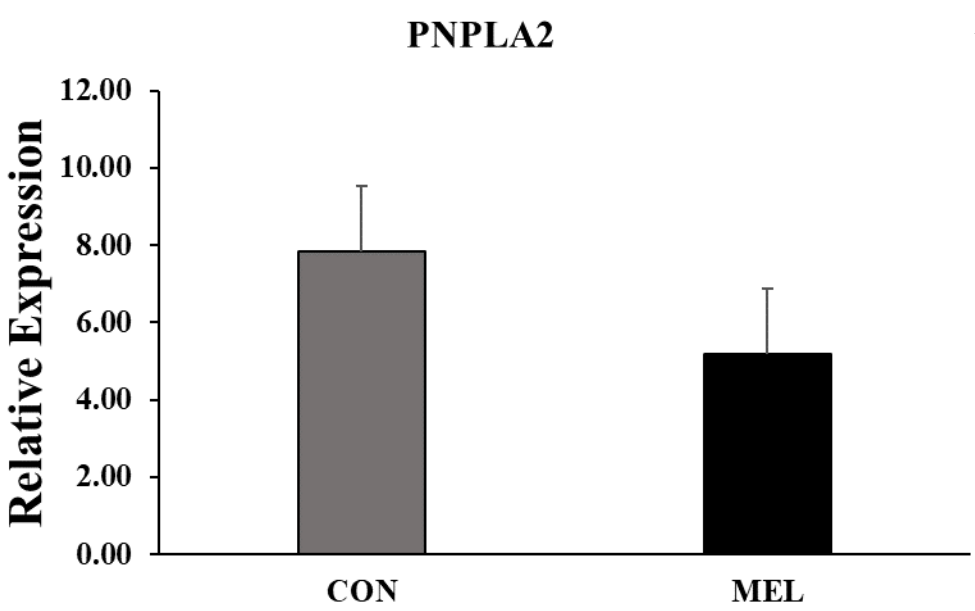

Figure 3.31 Fetal Relative expression (mRNA abundance) of patatin-like phospholipase domain containing 2 in perirenal adipose tissue, from fetuses harvested from CON (n=6) vs. MEL (n=6) treated dams.

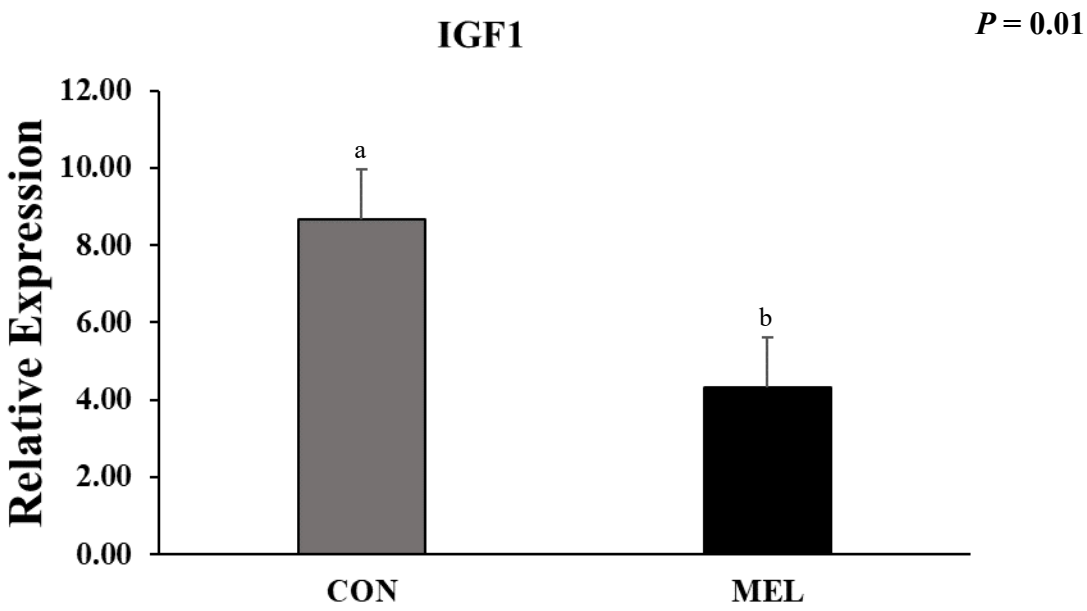

Figure 3.32 Fetal Relative expression (mRNA abundance) of insulin-like growth factor 1 in perirenal adipose tissue, from fetuses harvested from CON (n=6) vs. MEL (n=6) treated dams. [a-b] Significance of means without common letters ($P \leq 0.05$).

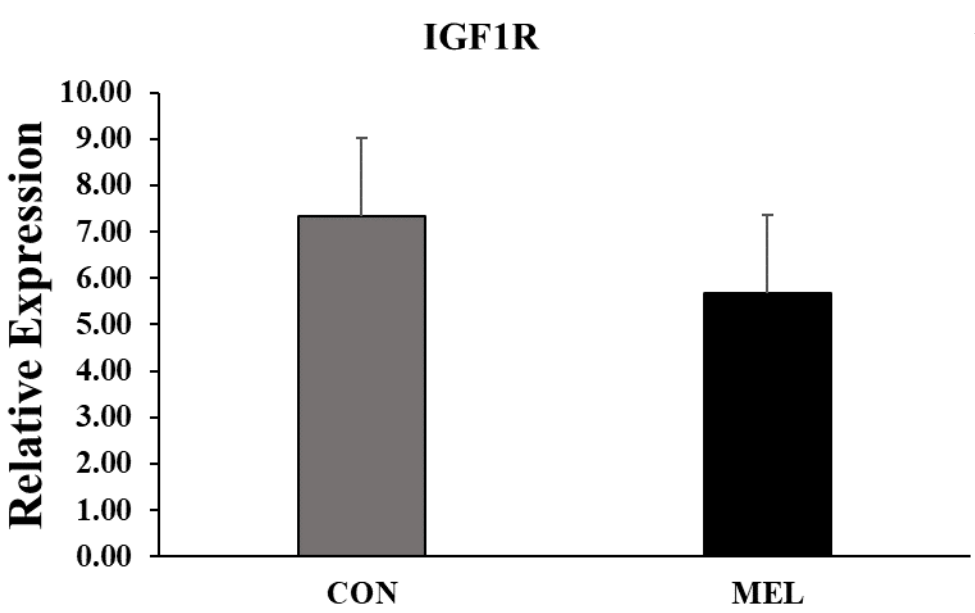

Figure 3.33 Fetal Relative expression (mRNA abundance) of insulin-like growth factor 1 receptor in perirenal adipose tissue, from fetuses harvested from CON (n=6) vs. MEL (n=6) treated dams.

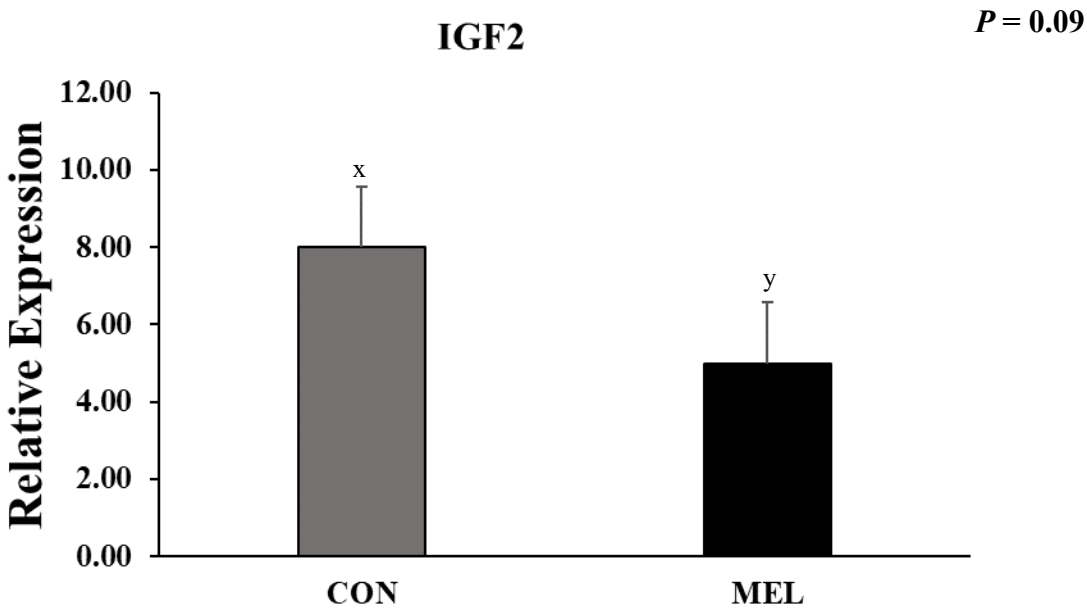

Figure 3.34 Fetal Relative expression (mRNA abundance) of insulin-like growth factor 2 in perirenal adipose tissue, from fetuses harvested from CON (n=6) vs. MEL (n=6) treated dams. $^{x\text{-}y}$ Significance of means without common letters ($P \leq 0.05$)

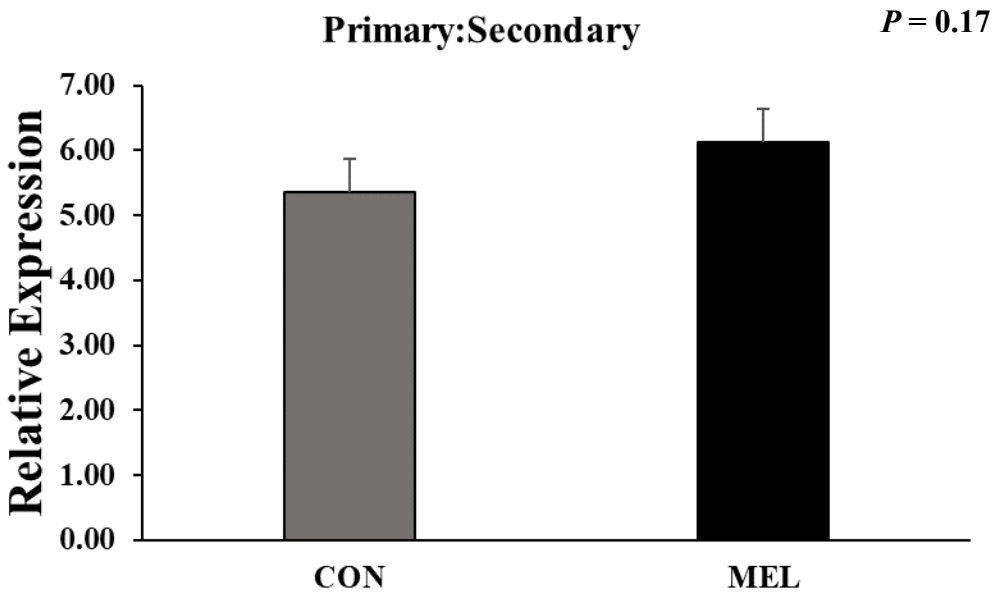

Figure 3.35 Fetal Longissimus dorsi primary to secondary muscle fibers from fetuses harvested from CON (n=6) vs. MEL (n=6) treated dams.

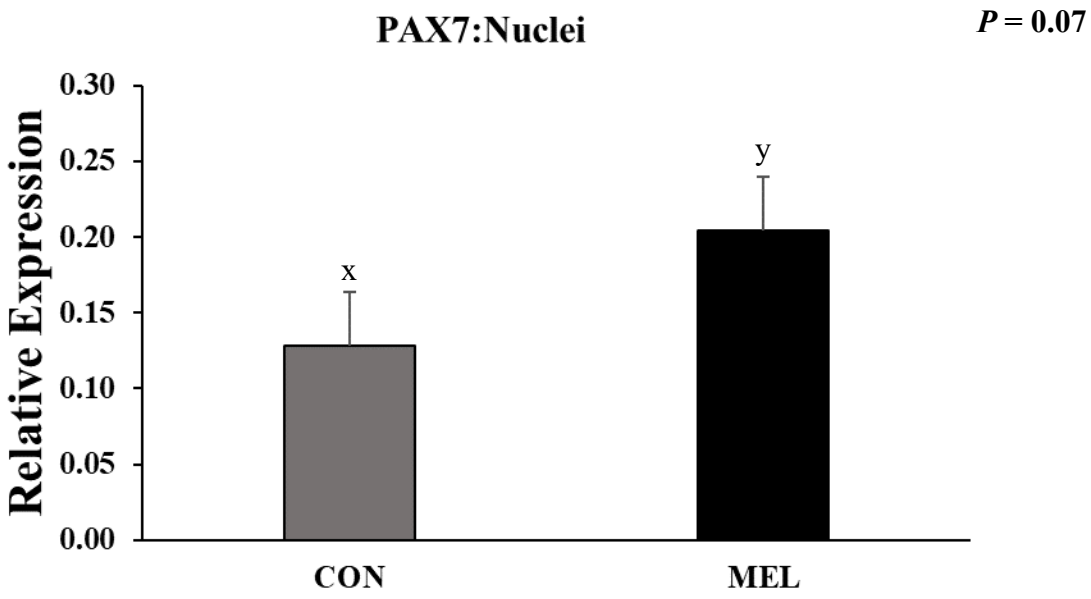

Figure 3.36 Fetal Longissimus dorsi PAX7 activated nuclei to total nuclei from fetuses harvested from CON (n=6) vs. MEL (n=6) treated dams. [x-y] Tendencies of means without common letters ($P > 0.05$ and $P \leq 0.10$).

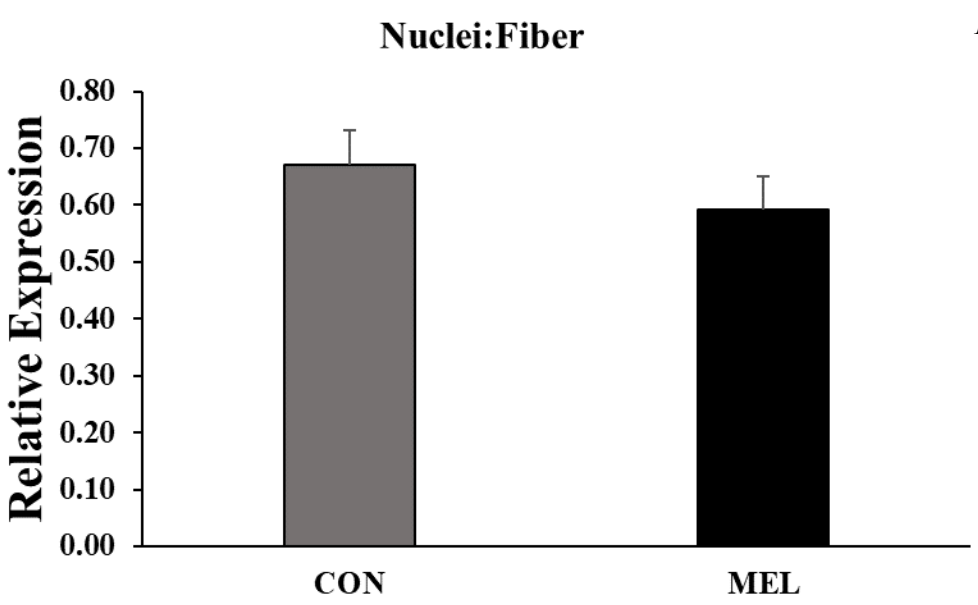

Figure 3.37 Fetal Longissimus dorsi total nuclei to total muscle fibers from fetuses harvested from CON (n=6) vs. MEL (n=6) treated dams.

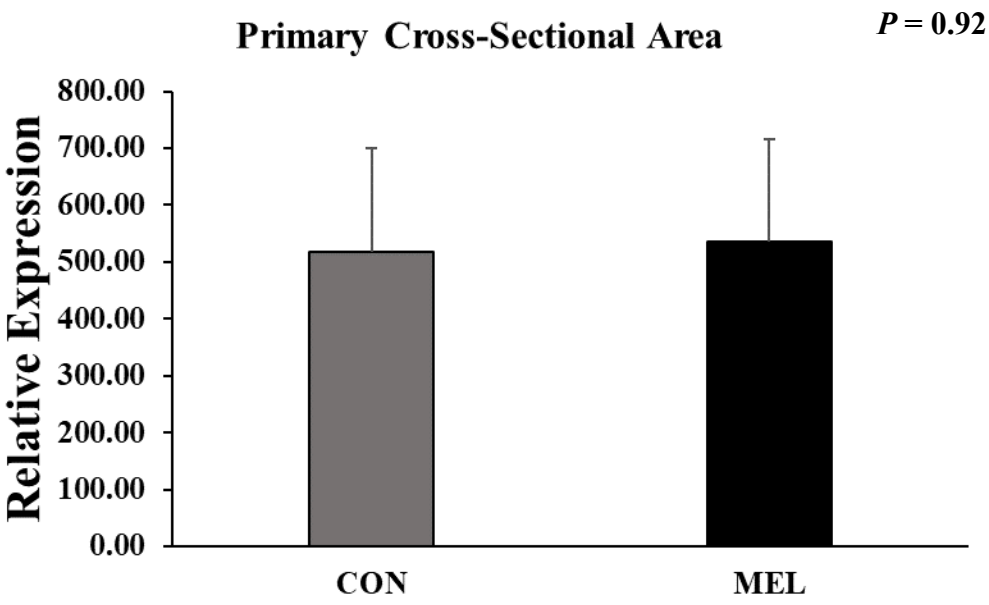

Figure 3.38 Fetal Longissimus dorsi average primary muscle fiber cross-sectional area from fetuses harvested from CON (n=6) vs. MEL (n=6) treated dams.

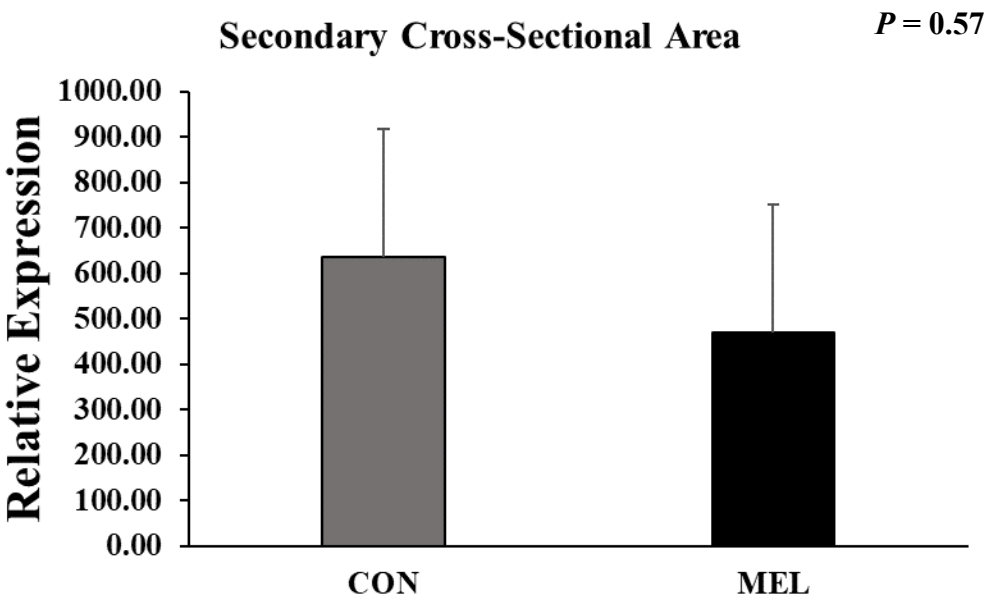

Figure 3.39 Fetal Longissimus dorsi average secondary muscle fiber cross-sectional area from fetuses harvested from CON (n=6) vs. MEL (n=6) treated dams.

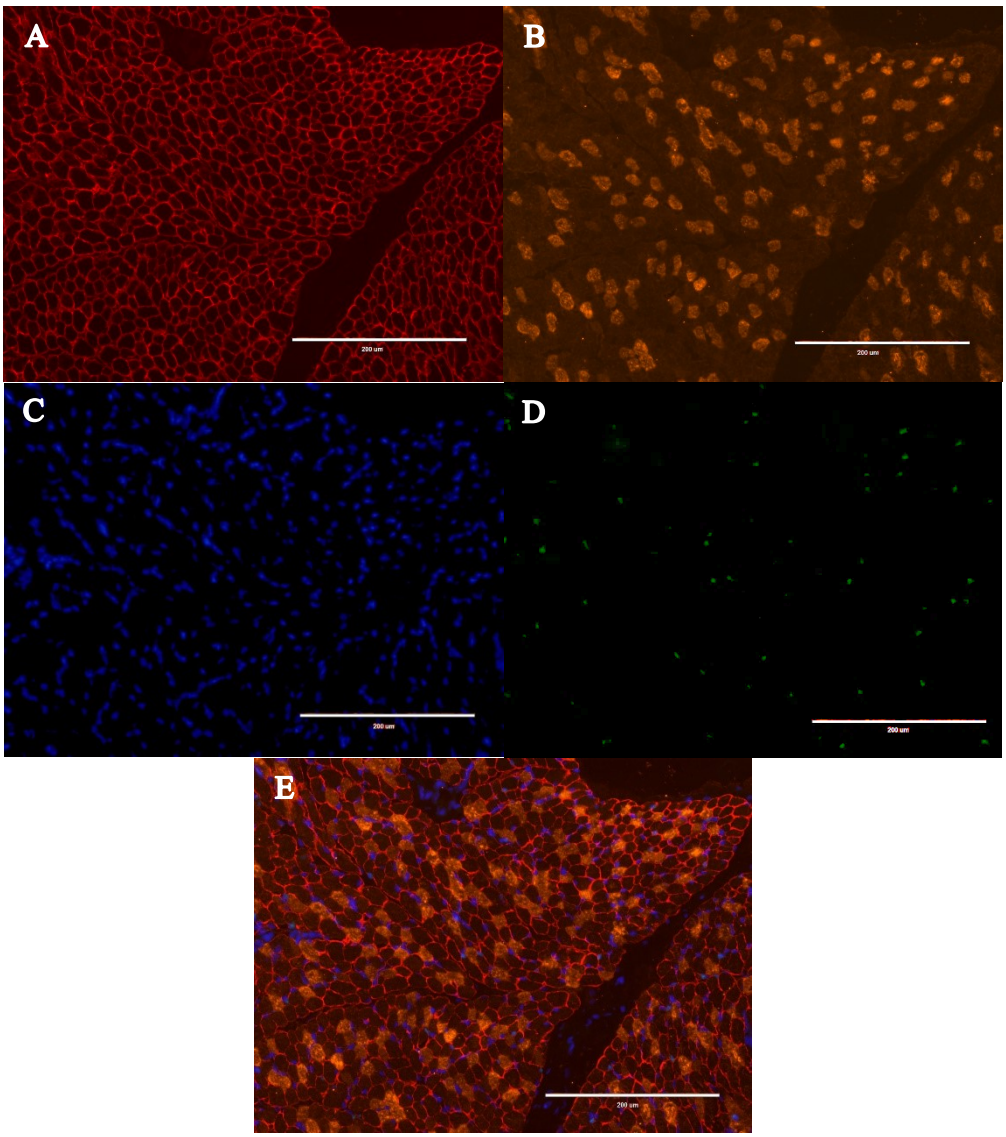

Figure 3.40 Fetal Longissimus dorsi immunohistochemistry in calves CON (n=6), MEL (n=6). Scale bar is 200 µm in length. Image A. immunofluorescent staining of dystrophin, C-terminal antibody (Red; PA1-37587, Thermo Scientific, Waltham, MA). Image B. immunofluorescent staining of BA-D5, myosin heavy chain IgG2b, (Yellow; Developmental Studies Hybridoma Bank, University of Iowa, Iowa City, IA). Image C. immunofluorescent staining of nuclei, Hoescht (Blue; CAT # 33342, Thermo Scientific, Waltham, MA). Image D. immunofluorescent staining of PAX7, hybridoma cell supernatant (Green; Developmental Studies Hybridoma Bank). Image E. overlays images 1 A-D.

3.6 References

Anderson, C. M., F. Lopez, H. Y. Zhang, K. Pavlish, and J. N. Benoit. 2005. Reduced uteroplacental perfusion alters uterine arcuate artery function in the pregnant Sprague-Dawley rat. Biol. Reprod. 72:762–766

Armengol J, Villena JA, Hondares E, Carmona MC, Sul HS, Iglesias R, et al. Pref-1 in brown adipose tissue: specific involvement in brown adipocyte differentiation and regulatory role of C/EBPδ. Biochem J (2012) 443:799–810. doi:10.1042/BJ20111714

Barak, Y., M.C. Nelson, E.S. Ong, Y.Z. Jones, P. Ruiz-Lozano, K.R. Chien, A. Koder, R.M. Evans PPARγ is required for placental, cardiac, and adipose tissue development Mol. Cell, 4 (1999), pp. 585-595

Bass, J., J. Oldham, M. Sharma, and R. Kambadur. 1999. Growth factors controlling muscle development. Dom. Ani. Endo. 17: 191-197

Braxton, L., Hollingshead P, Warburton C, Dowd M, Pitts-Meek S, Dalton D, Gillett N, Stewart T A. 1993. IGF-I is required for normal embryonic growth in mice. Genes Dev 7:2609–2617, pmid:8276243

Brett, K. E., Z. M. Ferraro, J. Yockell-Lelievre, A. Gruslin, and K. B. Adamo. 2014. Maternal–Fetal Nutrient Transport in Pregnancy Pathologies. Int. J. Mol. Sci. 15:16153-16185

Brockus, K. E., C. G. Hart, B. O. Fleming, T. Smith, S. H. Ward, C. O. Lemley. 2016a. Effects of Supplementing Holstein Heifers with Dietary Melatonin during Late Gestation on Growth and Cardiovascular Measurements of their Offspring. Reprod. Dom. Anim. 51: 240-247; doi: 10.1111/rda.12672

Brockus, K. E., C. G. Hart, C. L. Gilfeather, B. O. Fleming, and C. O. Lemley. 2016b. Dietary melatonin alters uterine artery hemodynamics in pregnant Holstein heifers. Dom. Ani. Endo. 55:1-10Department of Health (1994) Report on health and social subjects No. 46. Nutritional aspects of cardiovascular disease. London: HMSO.

Carstens, G. E., P. C. Mostyn, M. A. Lammoglia, R. C. Vann, R. C. Apter, and R. D. Randel. 1997. Genotypic effects on norepinephrine- induced changes in thermogenesis, metabolic hormones, and metabolites in newborn calves. J. Anim. Sci. 75:1746–1755.

Clarke, S. L., C. E. Robinson, and J. M. Gimble. 1997. CAAT/ enhancer binding proteins directly modulate transcription from the peroxisome

proliferator-activated receptor γ 2 promoter. Biochem. Biophys. Res. Commun. 240:99–103

Diez JJ, Iglesias P: The role of the novel adipocyte-derived hormone adiponectin in human disease. Eur J Endocrinol148 :293– 300,2003

Du., M., J. Tong, J. Zhao, K. R. Underwood. M. Zhu, S. P. Ford, and P. W. Nathanielsz. 2010. Fetal programming of skeletal muscle development in ruminant animals. J. Anim. Sci. 88:E51–E60. doi:10.2527/jas.2009-2311

Duarte, M. S., M. P. Gionbelli, P. V. R. Paulino, N. V. L. Serão, C. S. Nascimento, M. E. Botelho, T. S. Martins, S. C. V. Filho, M. V. Dodson, S. E. F. Guimarães, and M. Du. 2014. Maternal overnutrition enhances mRNA expression of adipogenic markers and collagen deposition in skeletal muscle of beef cattle fetuses. J. Anim. Sci. 92:3846–3854. https://doi.org/10.2527/jas.2014-7568

Dubocovich, M.L., Yun, K., Al-Ghoul, W.M., Benloucif, S., Masana, M.I., 1998. Selective MT2 melatonin receptor antagonists block melatonin-mediated phase advances of circadian rhythms. FASEB J. 12, 1211–1220.

Dubocovich, M.L., Delagrange, P., Krause, D.N., Sugden, D., Cardinali, D.P., Olcese, J. 2010. International Union of Basic and Clinical Pharmacology. LXXV. Nomenclature, classification, and pharmacology of G protein-coupled melatonin receptors. Pharmacol. Rev. 62, 343–380.

Eifert, A. W., Matthew E. Wilson, Kimberly A. Vonnahme, Leticia E. Camacho, Pawel P. Borowicz, Dale A. Redmer, Sinibaldo Romero, Sheri Dorsam, Jodie Haring, Caleb O. Lemley, Effect of melatonin or maternal nutrient restriction on vascularity and cell proliferation in the ovine placenta, Animal Reproduction Science, Volume 153, 2015, Pages 13-21

Elliott JA, Bartness TJ, Goldman BD. Effect of melatonin infusion duration and frequency on gonad, lipid, and body mass in pinealectomized male Siberian hamsters. J Biol Rhythms 1989; 4: 439–455.

Ferrazzi E, Rigano S, Bozzo M, Bellotti M, Giovannini N, GalanH&Battaglia FC (2000). Umbilical vein blood flow ingrowth-restricted fetuses. Ultrasound Obstet Gynecol 16,432–438.

Florini, J. R., K. A. Magri, D. Z. Ewton, P. L. James, K. Grindstaff, and P. S. Rotwein. 1991. “Spontaneous” differentiation of skeletal myoblasts is dependent upon autocrine secretion of insulin-like growth factor-II. J. Biol. Chem. 266:15917–15923

Forman, B. M., P Tontonoz, J Chen, R.M Evans 15-Deoxy-Δ-12,14-prostaglandin J2 is a ligand for the adipocyte determination factor PPARγ Cell, 83 (1995), pp. 803-812

Frohnert, B. I., T. Y. Hui, and D. A. Bernlohr. 1999. Identification of a functional peroxisome proliferator-responsive element in the murine fatty acid transport protein gene. J. Biol. Chem. 274:3970–3977.

Funston, R. N., D. M. Larson, and K. A. Vonnahme. 2010. Effects of maternal nutrition on conceptus growth and offspring performance: Implications for beef cattle production. J. Anim. Sci. 88:E205-E215. doi:10.2527/jas.2009-2351

Gardan, D., Mourot, J., Louveau, I. Decreased expression of the IGF-II gene during porcine adipose cell differentiation. Mol Cell Endocrinol. 2008;292:63–68

Gluckman, P. D., Catherine S. Pinal; Regulation of Fetal Growth by the Somatotrophic Axis, The Journal of Nutrition, Volume 133, Issue 5, 1 May 2003, Pages 1741S–1746

Gonzalez, J. M., L. E. Camacho, S. M. Ebarb, K. C. Swanson, K. A. Vonnahme, AA. M. Stelzleni, and S. E. Johnson. 2013. Realimentation of nutrient restricted pregnant beef cows supports compensatory fetal muscle growth. J Anim. Sci. 91:4797–4806

Ha E, Yim SV, Chung JH et al. Melatonin stimulates glucose transport via insulin receptor substrate-1/phosphatidylinositol 3-kinase pathway in C2C12 murine skeletal muscle cells. J Pineal Res 2006; 41:67–72.

Haig, D., and C. Graham. 1991. Genomic imprinting and the strange case of the insulin-like growth factor II receptor. Cell. 64:1045–1046

Hay Jr, W. W. 2003. Nutrition and development of the fetus: carbohydrate and lipid metabolism, in Nutrition in Pediatrics (Basic Science and Clinical Applications), W. Walker, J. Watkins, and C. Duggan, Eds., pp. 449–470, BC Decker, Ontario, Canada

Heldmaier G, Hoffmann K (1974) Melatonin stimulates growth of brown adipose tissue. Nature 247:224–225

Hu, L., G. Yang, D. Hagg, G. Sun, J.M. Ahn, N. Jiang, C.L. Ricupero, J. Wu, C.H. Rodhe, J.A. Ascherman, L. Chen, J.J. Mao IGF1 promotes adipogenesis by a lineage bias of endogenous adipose stem/progenitor cells Stem Cells, 33 (2015), pp. 2483-2495

Huang Y. Yan X. Zhu M. J. McCormick R. J. Ford S. P. Nathanielsz P. W. Du M. 2010. Enhanced transforming growth factor-β signaling and fibrogenesis in ovine fetal skeletal muscle of obese dams at late gestation. Am. J. Physiol. Endocrinol. Metab. 298:E1254–E1260.

Hutcheson, D. A., J. Zhao, A. Merrell, M. Haldar, and G. Kardon. 2009. Embryonic and fetal limb myogenic cells are derived from developmentally distinct progenitors and have different requirements for beta-catenin. Genes Dev. 23:997–1013.

Jager, S., C. Handschin, J. S. Pierre, and B. M. Spiegelman. 2007. AMP-activated protein kinase (AMPK) action in skeletal muscle via direct phosphorylation of PGC-1α. Bio. Sci. 104:12017-12022

Jorgensen SB, Richter EA, Wojtaszewski JFP. Role of AMPK in skeletal muscle metabolic regulation and adaptation in relation to exercise. J Physiol (Lond) 2006; 574 (1): 17–31

Jimenez-Aranda, A., G. Fernandez-Vazquez, D. Campos, M. Tassi, L. Velasco-Perez, D. X. Tan, R. J. Reiter, and A. Agil. 2013. Melatonin induces browning of inguinal white adipose tissue in Zucker diabetic fatty rats. J. Pineal. Res. 55:416-423. Doi:10.1111/jpi.12089

Juaniaux E, Poston L, Burton GJ. Placental-related diseases of pregnancy: involvement of oxidative stress and implications in human evolution. Hum Reprod Update 12: 747–755, 2006.

Karunaratne, J. F., C. J. Ashton, and N. C. Stickland. 2005. Fetal programming of fat and collagen in porcine skeletal muscles. J Anat. 207: 763-768

Kleiman, A., E.C. Keats, N.G. Chan, Z.A. Khan Elevated IGF2 prevents leptin induction and terminal adipocyte differentiation in hemangioma stem cells Exp. Mol. Pathol., 94 (2013), pp. 126-136

Konje JC, Howarth ES, Kaufmann P & Taylor DJ (2003). Longitudinal quantification of uterine artery blood volumeflow changes during gestation in pregnancies complicated byintrauterine growth restriction. Br J Obstet Gynecol 110,301–305.

Korhonen T, Mustonen AM, Nieminen P, Saarela S. Effects of cold exposure, exogenous melatonin and short-day treatment on the weight-regulation

and body temperature of the Siberian hamster (Phodopus sungorus). Regul Pept 2008; 149: 60–66

Krauchi K., Cajochen C., Mori D., Graw A.T., Wirz-Justice A. (1997) Early evening melotonin and S20098 advance circadian phase and nocturnal regulation of core body temperature. Am J Physiol 272:R1178–R1188

Kwon H, Ford SP, Bazer FW, Spencer TE, Nathanielsz PW, Nijland MJ, Hess BW, Wu G. Maternal nutrient restriction reduces concentrations of amino acids and polyamines in ovine maternal and fetal plasma and fetal fluids. Biol Reprod 71: 901–908, 2004.

Lan X, Cretney EC, Kropp J, Khateeb K, Berg MA, Penagaricano F, Magness R, Radunz AE, Khatib H (2013) Maternal diet during pregnancy induces gene expression and DNA methylation changes in fetal tissues in sheep. Front Genet 4:49

Le Gouic S, Atgie C, Viguerie-Bascands N, Hanoun N, Larrouy D, Ambid L, Raimbault S, Ricquier D, Delagrange P, Guardiola-Lemaitre B, Pénicaud L, Casteilla L. Characterization of a melatonin binding site in Siberian hamster brown adipose tissue. Eur J Pharmacol 1997; 339: 271–278.

Le Roith, D., C. Bondy, S. Yakar, J. L. Liu, and A. Butler. 2001. The somatomedin hypothesis: 2001. Endocr. Rev. 22:53-57

Lemley, C. O., A. M. Meyers, L. E. Camacho, T. L. Neville, D. J. Newman, J. S. Caton, K. A. Vonnahme. 2012. Melatonin supplementation alters uteroplacental hemodynamics and fetal development in an ovine model of intrauterine growth restriction. Am. J. Physiol. Regul. Integr. Comp. Physiol. 302: 454–467; doi:10.1152/ajpregu.00407.2011

Lemley, C. O., L. E. Camacho, and K. A. Vonnahme. 2013. Uterine Infusion of Melatonin or Melatonin Receptor Antagonist Alters Ovine Feto-Placental Hemodynamics During Midgestation. Bio. of Repro. 89:41-49

Livak, K. J. and T. D. Schmittgen. 2001. Analysis of Relative Gene Expression Data Using Real-Time Quantitative PCR and the 2−ΔΔCT Method. Methods. 25:402-408

Nathanielsz, P. W., L. Poston, and P. D. Taylor. 2007. In utero exposure to maternal obesity and diabetes: Animal models that identify and characterize implications for future health. Clin. Perinatol. 34:515–526.18063102

Nishizawa H, Shimomura I, Kishida K et al. (2002) Androgens decrease plasma adiponectin, an insulin-sensitizing adipocyte-derived protein. Diabetes 51:2734–2741

Nixon, A. J., Choy, V. J., Parry, A. L., Pearson, A. J. (1993) Fiber growth initiation in hair follicles of goats treated with melatonin. J. Exp. Zool. 267,47-56

Ntambi, J. M., M Miyazaki, J.P Stoehr, H Lan, C.M Kendziorski, B.S Yandell, et al. Loss of stearoyl-CoA desaturase-1 function protects mice against adiposity Proc Natl Acad Sci., 99 (2002), pp. 11482-11486

O'Fallon, J. V., J. R. Busboom, M. L. Nelson, and C. T. Gaskins. 2007. A direct method for fatty acid methyl ester synthesis: Application to wet meat tissues, oils, and feedstuffs. J. Anim. Sci. 85:1511–1521. doi:10.2527/jas.2006-491.

Paulis L, Simko F. Blood pressure modulation and cardiovascular protection by melatonin: potential mechanisms behind. Physiol Res 56: 671–684, 2007.

Pechanova O, Paulis L, Simko F. Peripheral and central effects of melatonin on blood pressure regulation. Int J Mol Sci 2014; 15:17920–17937

Puchalski SS, Green JN, Rasmussen DD. Melatonin effect on rat body weight regulation in response to high-fat diet at middle age. Endocrine 2003; 21: 163–167

Raskind MA, Burke BL, Crites NJ, Tapp AM, Rasmussen DD. Olanzapine-induced weight gain and increased visceral adiposity is blocked by melatonin replacement therapy in rats. Neuropsychopharmacology 2007; 32: 284–288

Regnault TR, de Vrijer B, Galan HL, Davidsen ML, Trembler KA, Battaglia FC, Wilkening RB, Anthony RV. The relationship between transplacental oxygen diffusion and placental expression of PlGF, VEGF and their receptors in a placental insufficiency model of fetal growth restriction. J Physiol 550: 641–656, 2003.

Rehfeldt, C. and Kuhn, G. Consequences of birth weight for postnatal growth performance and carcass quality in pigs as related to myogenesis. J. Anim. Sci. 2006; 84: 113–123

Reynolds, L. P., and D. A. Redmer. 1995. Utero-placental vascular development and placental function. J. Anim. Sci. 73:1839–1851.7545661

Reynolds, L. P., Borowicz, P. P., Vonnahme, K. A., Johnson, M. L., Grazul-Bilska, A. T., Redmer, D. A. and Caton, J. S. (2005), Placental angiogenesis in sheep models of compromised pregnancy. The Journal of Physiology, 565: 43–58. doi:10.1113/jphysiol.2004.081745

Richter, H. G., J. A. Hansell, S. Raut, and D. A. Giussani. 2009. Melatonin improves placental efficiency and birth weight and increases the placental expression of antioxidant enzymes in undernourished pregnancy. J. Pineal. Res. 46:357–364.

Rigano S, Bozzo M, Ferrazzi E, Belloti M, Battaglia FC, Galan HL. Early and persistent reduction in umbilical vain blood flow in the growthrestricted fetus: a longitudinal study. Am J Obstet Gynecol 185: 834–838,2001.

Rosen, E. D., and O. A. MacDougald. 2006. Adipocyte differentiation from the inside out. Nat. Rev. Mol. Cell Biol. 7:885–896

Seron-Ferre, M., H. Reynolds. N. A. Mendez, M. Mondaca, F. Valenzuela, R. Ebensperger, G. J. Valenzuela, E. A. Herrera, A. J. Llanos, and C. Torres-Farfan. 2015. Impact of maternal melatonin suppression on amount and functionality of brown adipose tissue (BAT) in newborn sheep. Fendo. 5:1-11; doi: 10.3389/fendo.2014.00232

Stratos I, Richter N, Rotter R et al. Melatonin restores muscle regeneration and enhances muscle function after crush injury in rats. J Pineal Res 2012; 52:62–70.

Thureen PJ, Trembler KA, Meschia G, Makowski EL, Wilkening RB. Placental glucose transport in heat-induced fetal growth retardation. Am J Physiol Regul Integr Comp Physiol 263: R578–R585, 1992.

Tontonoz, P., E Hu, B.M Spiegelman Stimulation of adipogenesis in fibroblasts by PPARγ2, a lipid-activated transcription factor Cell, 79 (1994), pp. 1147-1156

Vonnahme, K. A., C. O. Lemley, P. Shukla, S. T. O'Rourke. 2013.Placental programming: How the maternal environment can impact placental function,, Journal of Animal Science 91: 2467–2480, https://doi.org/10.2527/jas.2012-5929

Wallace JM, Bourke DA, Aitken RP, Leitch N, Hay WW Jr. Blood flows and nutrient uptakes in growth-restricted pregnancies induced by overnourishing adolescent sheep. Am J Physiol Regul Integr Comp Physiol 282: R1027–R1036, 2002.

Wang, B., X. Fu, X. Liang, Z. Wang, Q. Yang, W. Nie, J. Zhao, P. Gao, M.J. Zhu, J.M. De Avila, J.W. Maricelli, B.D. Rodger, and M. Du. 2017. Maternal retinoids increase PDGFRα progenitor population and beige adipogenesis in progeny by stimulating vascular development. E. Bio. Medicine. 18:288–299. doi:10.1016/j.ebiom.2017.03.041

Wolden-Hanson, T., D. R. Mitton, R. L. McCants, S. M. Yellon, C. W. Wilkinson, A. M. Matsumoto, D. D Rasmussen; Daily Melatonin Administration to Middle-Aged Male Rats Suppresses Body Weight, Intraabdominal Adiposity, and Plasma Leptin and Insulin Independent of Food Intake and Total Body Fat, Endocrinology, Volume 141, Issue 2, 1 February 2000, Pages 487–497

Wu, Z., E. D. Rosen, R. Brun, S. Hauser, G. Adelmant, A. E. Troy, C. McKeon, G. J. Darlington, and B. M. Spiegelman. 1999. Cross-regulation of C/EBPα and PPARγ controls the transcriptional pathway of adipogenesis and insulin sensitivity. Mol. Cell 3:151–158.

Yamauchi, T, et al. The fat-derived hormone adiponectin reverses insulin resistance associated with both lipoatrophy and obesity. Nat. Med. 2001. 7:941-946.

Zhu, M. J., S. P. Ford, W. J. Means, B. W. Hess, P. W. Nathanielsz, and M. Du. 2006. Maternal nutrient restriction affects properties of skeletal muscle in offspring. J. Physiol. 575:241–250.16763001

CHAPTER IV

EFFECT OF MATERNAL MELATONIN SUPPLEMENTATION DURING LATE GESTATION ON NEONATAL LOIN MUSCLE GENE EXPRESSION DURING EARLY POSTNATAL LIFE

4.1 Abstract

Melatonin is a natural hormone that is secreted by the pineal gland and has effects on economically important reproductive and carcass tissues including muscle and adipose tissue. Supplemental melatonin during gestation increased postnatal weight of calves starting at 8 weeks of age (Brockus et al., 2016). The objectives of the study were to determine the effects of maternal melatonin supplementation during late gestation on relative gene expression in the Longissimus dorsi (**LM**) of bovine offspring. Beef heifers (n = 32) and cows (n = 25) consisting of purebred Angus, purebred Hereford, or crossbred genetics, were bred via timed-artificial insemination and assigned to one of two treatment groups. The treatment groups consisted of melatonin supplementation (**MEL**) or without supplementation (**CON**). Supplementation of MEL was delivered via two- 24 mg implants with the CON receiving two placebo implants at days 180, 210, and 240 of gestation. After day 240 of gestation, dams received no further treatments. At the time of parturition (**d 0**), Longissimus dorsi biopsies of the calves were collected to undergo gene

expression via qPCR analysis. Maternal supplementation of MEL during late gestation resulted in no difference ($P > 0.05$) in calf birth weights between treatments, however, calves from MEL treated dams averaged 20 kg body weight increase ($P = 0.03$) at d 195 compared to calves from CON dams. There were no differences ($P > 0.05$) between treatment groups for observed LM adipogenic and fibrogenic relative gene expressions. Though calves from MEL treated dams have a tendency for increased ($P = 0.09$) AMPK relative expression at birth, with increased MyoD ($P = 0.04$), IGF2 ($P = 0.01$), and a tendency for increased IGF1 ($P = 0.05$), by d 195 of age. At birth and d195, specific genes that are responsible for muscle metabolism and accretion have shown to be increased that can aid in superior muscle growth compared to calves from CON dams. Further testing of important time periods such as weaning, yearling, and harvesting could provide important data into the long-term changes as the animal continues to grow and develop until reaching market.

4.2 Introduction

With the rapidly increasing global population, the need for improving the efficiency of livestock in terms of meat production is vital. Prenatal myogenic and adipogenic development are a large determinant of the animal's future postnatal production potential. Economically important tissues such as muscle and adipose are of a lower developmental priority compared to vital organs and nervous tissues (Zhu et al., 2006; Du et al., 2010). This leaves muscle and adipose tissue development particularly susceptible to the prevailing nutritional environment in utero (Zhu et al., 2006; Du et al., 2010). Stimuli and insults during the development of these tissues can set the stage for increased production efficiency, maximal growth, and superior carcasses, or lead to

impaired growth, inferior carcass composition, and increased risk of morbidity and mortality. Fetal programming is a change in the growth trajectory due to a stimulus or insult during a critical time in development for the fetus resulting in persisting effects into the postnatal phases of life or production (Nathanielsz et al., 2007). The first of these critical time points in growth for livestock is during prenatal development, at which point the fetus is completely dependent on the dam for nutrients. Nutrients for the fetus are in maternal circulation and must cross over to the fetus through the placenta. The nutritional status of the dam can have long lasting effects on fetal development by permanently altering the development of adipogenesis, fibrogenesis, and myogenesis (Karunaratne et al., 2005; Rehfeldt and Kuhn, 2006; Zhu et al., 2006; Funston et al., 2010; Huang et al., 2010; Duarte et al., 2014; Wang et al., 2017).

Approaches to prevent or rescue compromised pregnancies include identifying agents and mechanisms to improve uteroplacental nutrient exchange and in turn augment the in utero nutritional environment experienced by the fetus. Among these, supplementation of melatonin has been investigated as a novel therapeutic approach to increase uteroplacental blood flow (Lemley et al., 2012 and 2013; Brockus et al., 2016). Melatonin is a natural hormone produced from the pineal gland and derived from tryptophan. Melatonin has been described as having pleiotropic properties acting as a vasodilator, strong antioxidant, and signaling molecule for regulating natural circadian rhythm (Richter et al., 2009). The known melatonin receptors include MT1 and MT2 (Dubocovich et al., 1998, 2010) and their presence has been detected on peripheral tissues including muscle (Stratos et al., 2012) and adipose tissue (Le Gouic et al., 1997). In skeletal muscle, binding of melatonin to these receptors stimulates glucose transport

into muscle cells (Ha et al., 2006), increases the number of satellite cells, reduces inflammation, and inhibits apoptosis by modulating associated signaling pathways (Stratos et al., 2012). Melatonin increased insulin receptor substrate-1 is phosphorylated and the activity of phosphatidylinositol 3-kinase is increased, resulting in increased glucose uptake (Ha et al., 2006). Studies have found melatonin to cause increased hair follicle growth in goats (Nixon et al.,1993), cardiovascular influence (Pechanova et al.,2014), and decreased core body temperature in humans (Krauchi et al.,1997). However, studies looking at similar effects in cattle was lacking. A study conducted by Brockus et al. (2016) supplemented Holstein heifers with melatonin to look at effects on offspring blood pressure, heart rate, liver blood flow, skin temperature, and hair growth. They found that calves from dams supplemented with melatonin during their last trimester of gestation, had significantly higher body weights at weeks 8 and 9 of age (Brockus et al., 2016). They hypothesized that melatonin supplementation could have altered skeletal muscle development of the calves, providing impetus for the current study (Brockus et al., 2016).

This lead us to investigate the effects of MEL supplementation on skeletal muscle by collecting the entire fetal LM muscle to look at different morphometric measurements consisting of weight, circumference, and length, as outline in Section 3.3. Maternal supplementation of MEL during late gestation resulted in fetal LM tending to weigh more and be longer than that of calves from CON treated dams (Section 3.4). Also, analysis with immunohistochemistry showed calves from dams treated with MEL having a tendency for increased PAX7 activated nuclei to total nuclei ratio. This is important as the activation of PAX7 is required for fetal myoblast formation, and $PAX7^{+}$ progenitor

cells act as a foundation and give rise to myogenic cells necessary for fetal skeletal muscle accretion (Hutcheson et al., 2009). Skeletal muscle being a heterogenous tissue, and MEL known effects on adipose metabolism (Elliott et al., 1989; Puchalski et al., 2003; Raskind et al., 2007; Korhonen et al., 2008), lead us to collect plasma samples consisting of: fetal umbilical artery and vein plasma, fetal trunk plasma, and maternal plasma a long with fetal perirenal (**PR**) adipose tissue, as outlined in Section 3.3. To summarize the findings, calves from MEL supplemented dams had decreased adipogenic relative gene expression in PR adipose tissue (Table 3.17). To investigate the effects on calves from MEL treated dams, we decided to use a longitudinal approach looking at the postnatal development of their offspring at birth and d 195 of age.

Therefore, our hypothesis was that increased maternal melatonin concentration during late gestation will lead to calves with altered metabolic programing of postnatal skeletal muscle. Additionally, the increased uterine blood flow will improve postnatal growth by programming increased myogenic mRNA gene expression in postnatal skeletal muscle. The specific objectives of the study were to determine the effects of maternal melatonin supplementation during late gestation on gene expression in the Longissimus dorsi (**LM**) of bovine offspring.

4.3 Materials and Methods

4.3.1 Animal Care and Treatment

The current study was conducted under an approved Mississippi State University Institutional Animal Care and Use Committee protocol (#16-036).

A total of 87 heifers and 65 cows that consisted of purebred Angus, purebred Hereford, or crossbred genetics, were bred via timed-artificial insemination (**AI**) at the H.

H. Leveck Animal Research Center. Heifers were bred on December 10, 2015, and cows were bred on December 21, 2015. At 120 days post-AI, heifers and cows were examined via ultrasonography to confirm pregnancy. This resulted in 32 heifers and 25 cows with confirmed conception. Then dams were blocked by bodyweight and randomly assigned to one of 2 maternal treatment groups. The 2 maternal treatment groups consist of a melatonin treatment (**MEL**; n = 29) and a no melatonin treatment (**CON**; n = 28). The MEL group was administered two ear impants (MelatoninImplants.com) containing 24mg MEL each, every 30 days starting at d 180 of gestation (baseline) and ending on d 240 of gestation. The MEL implant on d 240 of gestation was expected to provide increased maternal MEL concentration approximately till d 270 of gestation. After d 270 of gestation, all dams received no further treatments throughout the study. Both maternal treatment groups were managed the same throughout the study and had access to similar dietary regimes with ad libitum water access. Within 24 hours of parturition (**d 0**), calves were weighed, tattooed, ear tagged, serum and plasma collected, and live muscle biopsies of the LM taken with subsequent samples collected at 195 d of age (**d 195**).

4.3.2 Longissimus dorsi biopsy collection

Muscle biopsy samples were collected from 35 calves on day 0 of age (CON = 17, MEL = 18) to serve as a biological baseline for the study. At day 195 of age, 31 calves (CON = 15, MEL = 16) had a second LM biopsy collected to analyze for changes in mRNA gene expression. Four of the calves were removed from this study because they required special management and their day 0 data will not be included. The landmark for the biopsies was located behind the 13^{th} rib, in the middle of the muscle relative to the lumbar vertebra, on the left side of each calf. After cleaning the biopsy site, 1 cc of

Lidocaine (Aspen, Liberty, MO) was injected to provide local analgesia. After allowing sufficient time for the anesthetic, a 14-gauge piercing needle was used to penetrate fully through the skin. Then three biopsies of approximatly1g each of LM tissue were extracted using a 14-gauge x 9 cm Quick-Core® Biopsy Needle (COOK, Bloomington, IN) behind the 13th rib. The biopsy needle was inserted through the punctured skin at a 45-degree angle relative to the LM fibers. Tissue samples were stored in cryotubes at -80°C until further analysis.

4.3.3 Longissimus dorsi Analysis of Relative Gene Expression

4.3.3.1 QuantiNova™ SYBR® Green PCR Kit

Nucleic acids were isolated from the LM biopsy samples using 700 µl of QIAzol® Lysis Reagent (QIAGEN, Hilden, Germany), followed by purification with the use of RNA using a miRNeasy® Mini Kit (QIAGEN, Hilden, Germany). Extracted total RNA was quantified using a NanoDrop One spectrophotometer (Thermo scientific, Waltham, MA). Samples exhibiting 260 nm/280 nm ratios between 1.9 and 2.1 were deemed acceptable for downstream procedures and stored at -80°C. For each sample, duplicate cDNA synthesis reactions were conducted using 100 ng of total RNA using QuantiNova™ Reverse Transcription Kits (QIAGEN, Hilden, Germany) according to the manufacturers protocol. The genes of interest for LM tissue cystatin (**CYS**), adenosine monophosphate-activated protein kinase-α (**AMPK**). Beta actin was used as a housekeeping gene. Gene specific primers for the genes of interest (Table 4.1) were designed and validated for quantitative PCR (**qPCR**). Primer efficiencies were determined by plotting the threshold cycle versus the log of the input concentrations for 8, 10-fold serial dilutions of pooled LM muscle cDNA. Primer sets and assays with

efficiencies between 0.9 and 1.1 were considered acceptable for real time PCR analysis. Each of the duplicate cDNA samples were subjected to duplicate qPCR reactions using QuantiNova™ SYBR® Green PCR Kit (QIAGEN, Hilden, Germany). A master mix containing SYBR® Green, forward and reverse primers (diluted 1:20), and ROX reference dye along with 112.5 ng of cDNA was pipetted into a 96-well MicroAmp® Fast Optical Reaction Plate (Applied Biosystems, Foster City, CA). The plate was then covered with Masterclear real-time PCR Film (Eppendorf, Hamburg, Germany), briefly vortexed and centrifuged, then placed in QuantiStudio™ 3 (Applied Biosystems, Foster City, CA) for real-time qPCR analysis. Thermal cycling parameters used consisted of: a hold stage at 95°C for 2 minutes; PCR stage with step 1 at 95°C for 5 seconds followed by step 2 at 60°C for 10 seconds for 50 cycles; with a melting curve stage have step 1 at 95°C for 1 second then step 2 60°C for 20 seconds and step 3 (dissociation) at 95°C for 1 second (capturing every 0.1°C/s). Replicate threshold cycle (**CT**) values were averaged and used for relative quantification using the $2^{-\Delta\Delta C}{}_{\mathrm{T}}$ method (Livak and Schmittgen, 2001).

4.3.3.2 TaqMan™ fast advanced master mix

Nucleic acids were isolated from the LM biopsy samples using 700 µl of QIAzol® Lysis Reagent (QIAGEN, Hilden, Germany), followed by purification with the use of RNA using a miRNeasy® Mini Kit (QIAGEN, Hilden, Germany). Extracted total RNA was quantified using a NanoDrop One spectrophotometer (Thermo scientific, Waltham, MA). Samples exhibiting 260 nm/280 nm ratios between 1.9 and 2.1 were deemed acceptable for downstream procedures and stored at -80°C. For each sample, duplicate cDNA synthesis reactions were conducted using 100 ng of total RNA using QuantiNova™ Reverse Transcription Kits (QIAGEN, Hilden, Germany) according to the

manufacturer protocol. The genes of interest for LM were insulin-like growth factor 1 (**IGF1**), IGF1 receptor (**IGF1R**), insulin-like growth factor 2 (**IGF2**), IGF2 receptor (**IGF2R**), myogenic factor 5 (**Myf5**), myogenin (**MyoG**), myogenic differentiation 1 (**MyoD**), stearoyl-CoA desaturase (**SCD**), peroxisome proliferator activated receptor gamma (**PPARg**), and patatin-like phospholipase domain containing 2 (**PNPLA2**). Beta actin was used as a housekeeping gene. Assays for the genes of interest (Table 4.2) were validated for efficiency and specificity prior to qPCR. Primer efficiencies were determined by plotting the threshold cycle versus the log of the input concentrations for 8, 10-fold serial dilutions of pooled PR adipose tissue cDNA. Primer sets and assays with efficiencies between 0.9 and 1.1 were considered acceptable for real time PCR analysis. Complementary DNA was amplified in duplicate using TaqMan™ fast advanced master mix (Thermo scientific, Waltham, MA). A master mix containing TaqMan™ fast advanced master mix and gene assay was pipetted along with 37.5 ng of cDNA into a 96-well MicroAmp® Fast Optical Reaction Plate (Applied Biosystems, Foster City, CA). The plate was then covered with Masterclear real-time PCR Film (Eppendorf, Hamburg, Germany), briefly vortexed and centrifuged, then placed in QuantiStudio™ 3 (Applied Biosystems, Foster City, CA) for real-time qPCR analysis. Thermal cycling parameters used consisted of: a hold stage at 50°C for 2 minutes; polymerase activation hold at 95°C for 20 seconds; PCR stage with step 1 at 95°C for 1 second followed by step 2 at 60°C for 20 seconds for 40 cycles. Replicate CT values were averaged and used for relative quantification using the $2^{-\Delta\Delta CT}$ method (Livak and Schmittgen, 2001).

4.3.4 Statistical Analysis

Gene expressions and morphometrics were analyzed using MIXED procedure of the Statistical Analysis System (SAS software version 9.4, SAS Institute, Cary, NC, USA). Where the model statement included: treatment, calf sex, treatment x calf sex interaction, parity, treatment x parity interaction, and breed of dam, treatment x breed, calf day of age, and treatment x day interaction. Data found to be nonnormally distributed were tested using the Wilcoxon rank sum test. Gestation length served as covariate for d 0 with d 195 having age of calf as covariate. Least square means and standard error of the means were reported. Pairwise comparisons between the least squares means of the factor levels were computed using the PDIFF option of the LSMEANS statement. Statistical significance was determined at $P \leq 0.05$, and P-values falling within $P > 0.05$ and $P \leq 0.10$ were considered a trend.

4.4 Results

4.4.1 D 0 Morphometric Analysis

Birth weight was not different *(*$P > 0.05$) in calves from MEL treated dams compared to calves from CON treated dams (Table 4.3; Figure 4.1).

4.4.2 D 0 Longissimus dorsi Relative Gene Expression Analysis

At d 0, LM relative gene expression did not differ ($P > 0.05$) for the following: CYS, IGF1, IGF1R, IGF2, IGF2R, MyoG, MyoD, Myf5, PPARg, PNPLA2, or SCD between calves from MEL compared to CON dams (Table 4.4, 4.5; Figures 4.3, 4.5-4.14). At d 0, LM relative gene expression of AMPK tended to be increased ($P = 0.09$) in calves from MEL compared to CON dams (Table 4.4; Figure 4.4).

4.4.3 Day 195 Morphometric Analysis

At d 195, calf body weight was increased ($P = 0.03$) in calves from MEL treated dams compared to calves from CON treated dams (Table 4.3 Figure 4.2).

4.4.4 Day 195 Longissimus dorsi Relative Gene Expression Analysis

At d 195, LM relative gene expression did not differ ($P > 0.05$) for the following: CYS, AMPK, IGF1R, IGF2R, MyoG, Myf5, PPARg, PNPLA2, or SCD between calves from MEL compared to CON dams (Table 4.4, 4.5; Figures 4.3, 4.4, 4.6, 4.8, 4.9, 4.11-4.14). However, LM relative gene expression was increased for IGF2 ($P = 0.01$) and MyoD ($P = 0.04$) with IGF1 tending to be increased ($P = 0.05$) between calves born from MEL treated dams compared to CON dams (Tables 4.5; Figures 4.5, 4.7, 4.10).

4.5 Discussion

Brockus and colleagues, found that Holstein calves from MEL treated dams had no difference in birth weight but had an increased body weight starting at 8 weeks of age compared to calves from CON dams (2016). The authors believed that MEL supplementation to Holstein dams during late gestation may have caused a programmed response leading to a change in fetal skeletal muscle development that potentially caused the increased weight gain (Brockus et al., 2016). To investigate this hypothesis, we conducted twelve fetal necropsies collecting LM muscle, perirenal (**PR**) adipose, umbilical artery and vein plasma, fetal trunk plasma, and maternal plasma samples, as outlined in Section 3.3. The reason for examining fetal muscle and adipose tissue was to observe if MEL supplementation to dams during late gestation had any effects on myogenesis and adipogenesis. The full report of the results from the fetal portion of this

study are shown in Section 3.4. To summarize, maternal supplementation of MEL during late gestation does impact fetal calf LM muscle and PR adipose tissue development by d 240 of gestation. The next step to investigate the claim of increased postnatal calf body weight lead us to conducting a postnatal trial.

In this postnatal study, there was no difference in calf birth weights between treatment groups, which is consistent with the findings of Brockus et al. (2016). However, calves born from MEL treated dams at d 195 weighed an average of 20 kg more than calves from CON dams. This supports the findings of Brockus and colleagues as they observed Holstein calves from MEL treated dams to have increased body weights starting at 8 weeks of age compared to calves from CON dams (2016). Live biopsies of LM muscle tissue were collected at d 0 and d 195 of age to look at postnatal relative gene expression of myogenic, adipogenic, and fibrogenic genes as well as genes responsible for muscle and adipose metabolism (Tables 4.1, 4.2).

Upon qPCR analysis of cDNA from d 0 LM muscle tissue, supplementation of MEL during late gestation caused no change in myogenic or adipogenic relative gene expression compared to that of CON, which is consistent with the fetal results in Section 3.4. However, at the time of birth, LM tissue of calves from MEL treated dams had no difference ($P > 0.05$) in CYS relative gene expression compared to calves from CON dams. This is surprising as MEL supplementation lead to fetal calves at 240 days of gestation with increased ($P = 0.02$) CYS relative gene expression compared to calves from CON dams (Table 3.15). The reason behind the change in expression between 240 days of gestation to birth and the implications are unclear. After analysis of metabolic related genes in LM tissue, we found that IGF1, IGF1R, IGF2, and IGF2R were not

different between treatment groups apart from AMPK, which tended to be increased (P = 0.09). This is identical to fetal results outlined in Section 3.4 except for AMPK which was significantly increased (P = 0.03) in fetal calves from MEL treated dams. Based on these results at the time of birth, calves from MEL supplemented dams had similar myogenic, adipogenic, and fibrogenic relative gene expression to that of calves from CON dams. However, the enhanced LM tissue energy metabolism provided by the elevated AMPK levels could support superior muscle accretion.

To further investigate the observed increase in d 195 body weight, we conducted qPCR analysis of cDNA from d 195 LM muscle tissue. There were no changes in calf LM myogenic, adipogenic, and fibrogenic relative gene expressions; except for MyoD, which was increased in calves born from MEL treated dams. The postnatal expression of MyoD in skeletal muscle is involved with satellite cells differentiation (Grand and Rudnicki, 2007). In the normal, uninjured postnatal animal, MyoD and other myogenic regulatory factor gene expressions are either very low or undetectable in quiescent satellite cells (Beilhartz et al., 1992; Buonanno et al., 1992; Eftimie et al., 1991). However, muscle stress caused by weight bearing or trauma results in the activation of satellite cells from a quiescent state to a proliferative state (Grand and Rudnicki, 2007). The activated satellite cells then begin to express increased levels of MyoD, which ultimately causes them to differentiate into myoblasts and then fuse with myofibers to help with myofiber regeneration (Koishi et al., 1995; Yablonka-Reuveni, 1995; Dhawan and Rando, 2005; Grand and Rudnicki, 2007). The increased LM relative gene expression of MyoD in d 195 calves born from MEL treated dams could aid in muscle hypertrophy and regeneration supporting enhanced muscle accretion compared to calves

from CON dams. Lastly, there were no changes in IGF1R, IGF2R, or AMPK in d 195 calf LM between treatment groups. Although, IGF2 was increased ($P = 0.01$) in d 195 calves born from MEL treated dams and they had a tendency for increased IGF1 ($P = 0.05$) compared to calves from CON dams. In skeletal muscle growth and development, IGF2 is the predominant IGF in fetal development with IGF1 being the primary growth factor responsible for increased postnatal protein synthesis and muscle hypertrophy (Florini et al., 1991; Haig and Graham, 1991; Braxton et al., 1993; Bass et al., 1999; Le Roith et al., 2001; Gluckman and Pinal, 2003; Gonzalez et al., 2013; Wang and Mitch, 2014). In fetal skeletal muscle, IGF2 assists in myoblast cell growth and differentiation and via the mTOR pathway (Erbay et al., 2003; Glass, 2010; Dai et al., 2011; Hornberger, 2011; Ge and Chen, 2012). Current literature on the importance of IGF2 in postnatal animal is currently lacking as levels of IGF2 in postnatal animals is very low (Clark et al., 2015). However, some literature observing the effects of mutations that caused elevated levels of postnatal IGF2 have shown to increase skeletal muscle mass of pigs (Gardan et al., 2008a; Gardan et al., 2008b). The effects of IGF1 on postnatal muscle accretion has been shown to be a combination of satellite cell activation and increasing protein synthesis in myofibers (Barton-Davis et al., 1999; Machida and Booth, 2004).

In Summary, maternal supplementation of MEL during late gestation does impact LM muscle relative gene expression of calves at birth and d 195 of age. At birth and d195, specific genes that are responsible for muscle metabolism and accretion have shown to be increased. With increased muscle energy metabolism and protein synthesis, these calves could support superior muscle growth compared to calves from CON dams. One limitation to this study is the absence of postnatal LM samples for

immunohistochemical (**IHC**) analysis and perirenal adipose for qPCR and IHC analysis. Future research will be needed to provide additional information on the effects of MEL supplementation to dams during late gestation on their offspring's performance from birth up to slaughter.

Table 4.1 Accession, sequences, amplicon length, and efficiency of primers used for QuantiNova™ SYBR® Green real-time PCR quantification of Longissimus dorsi gene expression.

Gene[1]	Accession	Forward Primer	Reverse Primer	Amplicon Size	Efficiency
CYS	NM_174029.1	GTGGAGCTTGGCCGGACTACAT	CACCAGGTTGATGGTGTTCATCC	143	1.04
AMPK	NM_001109802	ACCATTCTTGGTTGCTGAAACTC	CACCTTGGTGTTTGGATTTCTG	80	0.99
Beta Actin	NM_173979	GTCGACACCGCAACCAGTT	AAGCCGGCCTTGCACAT	85	0.94

[1] CYS = cystatin, AMPK = adenosine monophosphate-activated protein kinase-α.

Table 4.2 Assays, accession, amplicon length, and efficiency of primers used for TaqMan® real-time PCR quantification of Longissimus dorsi gene expression.

Gene[1]	Assay ID	Accession	Amplicon Size	Efficiency
Beta Actin	Bt03279174_g1	NP_776404	141	0.96
Myf5	Bt03223134_m1	NP_776541	98	0.95
MyoG	Bt03258928_m1	NP_001104795.1	96	0.96
MyoD	Bt03244740_m1	NP_001035568.2	84	0.95
SCD	Bt04307478_m1	NP_776384.3	89	0.97
PPARg	Bt03217547_m1	NP_851367.1	85	0.93
PNPLA2	Bt03234128_m1	NP_001039470.1	77	0.98
IGF1	Bt03252282_m1	NM_001077828.1	65	0.99
IGF1R	Bt03649217_m1	NP_001231541.1	70	0.93
IGF2	Bt03259225_m1	NP_776512.2	54	0.95
IGF2R	Bt03223452_m1	NP_776777.1	57	0.97

[1] Myf5 = myogenic factor 5, MyoG = myogenin, MyoD = myogenic differentiation 1, SCD = stearoyl-CoA desaturase, PPARg = peroxisome proliferator activated receptor gamma, PNPLA2 = patatin-like phospholipase domain containing 2, IGF1 = insulin-like growth factor 1, IGF1R = IGF1 receptor, IGF2 = insulin-like growth factor 2, IGF2R = IGF2 receptor.

Table 4.3 Morphometric body weight measurements of newborn (**d0**) calves and at 195 days of age (**d195**) from heifers and cows treated with CON (n=17) and MEL (n=18).

	Morphometric Measurements			
	Treatment			
Measurements	**CON**	**MEL**	**SEM**	***P* Value**
d0 BW (kg)	29.2962	30.0535	2.1489	0.73
d195 BW (kg)	203.6800[a]	222.9200[b]	8.4327	0.03

[a–b] Means within a row without common superscript differ *(P* < 0.05)

Table 4.4 QuantiNovaTM SYBR® Green real-time PCR quantification of day 0 and day 195 of age calf Longissimus dorsi (LM) PCR relative expression of IGF1, IGF1R, IGF2, IGF2R, BMP, CYS, LOX, and AMPK of calves CON (n=15) and MEL (n=12).

	Longissimus dorsi PCR Relative Expression				
		Treatment			
Gene[1]	**Day**	**CON**	**MEL**	**SEM**	***P* Value**
CYS	0	13.6312	14.0463	1.8188	0.82
AMPK	0	11.6610[x]	16.0537[y]	2.3984	0.09
CYS	195	12.9846	15.7637	2.1501	0.22
AMPK	195	9.7948	13.4842	2.1658	0.11

[x–y] Means within a row without common superscript represent tendencies *(P* ≥ 0.05 and *P* ≤ 0.10)

[1] CYS = cystatin, AMPK = adenosine monophosphate-activated protein kinase-α.

Table 4.5 TaqMan® real-time PCR quantification of Fetal Longissimus dorsi (LM) PCR relative expression of IGF1, IGF1R, IGF2, IGF2R, BMP, CYS, LOX, and AMPK of calves CON (n=15) and MEL (n=12).

	Longissimus dorsi PCR Relative Expression				
		Treatment			
Gene	**Day**	**CON**	**MEL**	**SEM**	**P Value**
IGF1	0	16.3649	12.6753	2.4820	0.16
IGF1R	0	15.1188	13.8071	2.8333	0.65
IGF2	0	15.3318	11.2373	3.1644	0.21
IGF2R	0	12.2895	15.1951	3.3600	0.40
MyoG	0	10.5495	14.4845	3.3174	0.25
MyoD	0	13.2074	15.2774	3.0557	0.51
Myf5	0	13.4810	13.5475	2.6275	0.98
PPARG	0	14.6599	12.4148	2.8657	0.44
PNPLA2	0	13.5073	15.5713	2.4724	0.42
SCD	0	13.6577	9.9399	3.1103	0.25
IGF1	195	11.3291[x]	16.3203[y]	2.3612	0.05
IGF1R	195	13.8416	15.2951	2.7761	0.61
IGF2	195	10.8386[a]	19.1387[b]	2.6646	0.01
IGF2R	195	15.2453	16.0937	2.7091	0.76
MyoG	195	14.7130	18.1307	2.5274	0.20
MyoD	195	12.5768[a]	18.7497[b]	2.8189	0.04
Myf5	195	13.0385	14.1356	2.9276	0.71
PPARG	195	14.4667	15.5676	3.0531	0.72
PNPLA2	195	13.8538	13.5899	2.6193	0.92
SCD	195	13.7654	15.6272	2.5418	0.47

[a–b] Means within a row without common superscript differ *(P* < 0.05)

[x–y] Means within a row without common superscript represent tendencies *(P* ≥ 0.05 and *P* ≤ 0.10)

[1] Myf5 = myogenic factor 5, MyoG = myogenin, MyoD = myogenic differentiation 1, CEBPA = CCAAT enhancer binding protein alpha, SCD = stearoyl-CoA desaturase, PPARg = peroxisome proliferator activated receptor gamma, PNPLA2 = patatin-like phospholipase domain containing 2, IGF1 = insulin-like growth factor 1, IGF1R = IGF1 receptor, IGF2 = insulin-like growth factor 2, IGF2R = IGF2 receptor.

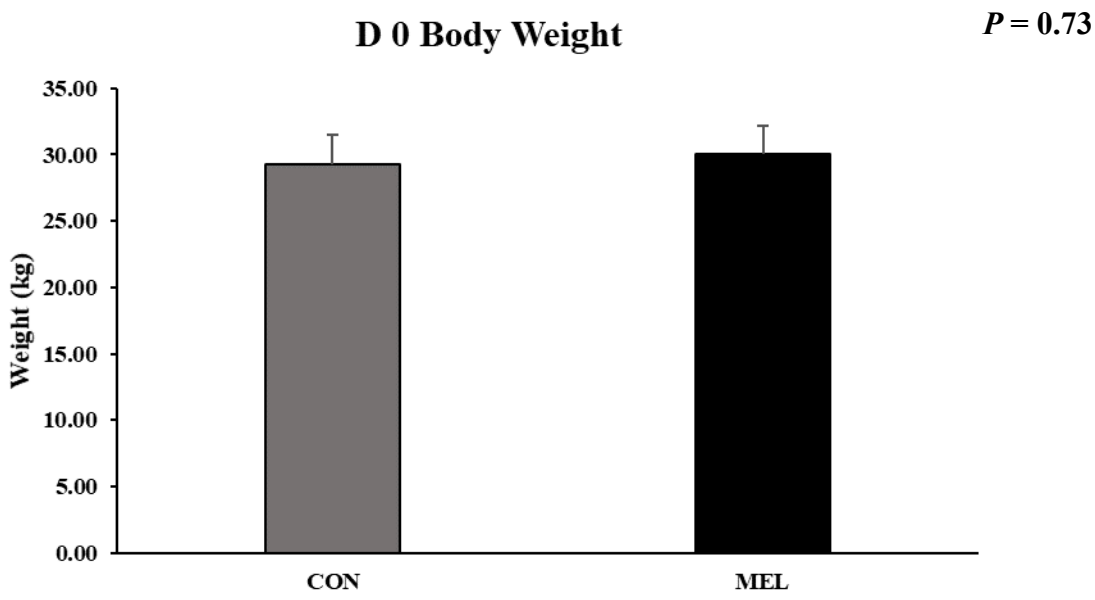

Figure 4.1 Birth weight (d 0) average from offspring born from CON (n=15) or MEL (n=12) treated dams.

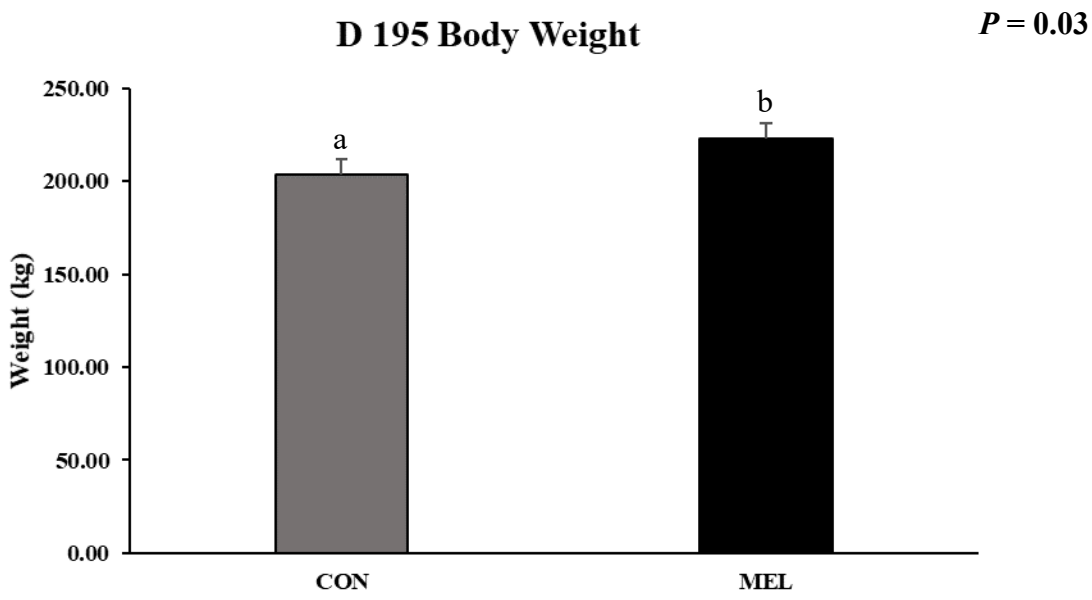

Figure 4.2 Body weight (d 195) average from offspring born from CON (n=15) or MEL (n=12) treated dams. [a–b] Means within a row without common superscript differ *(P* < 0.05)

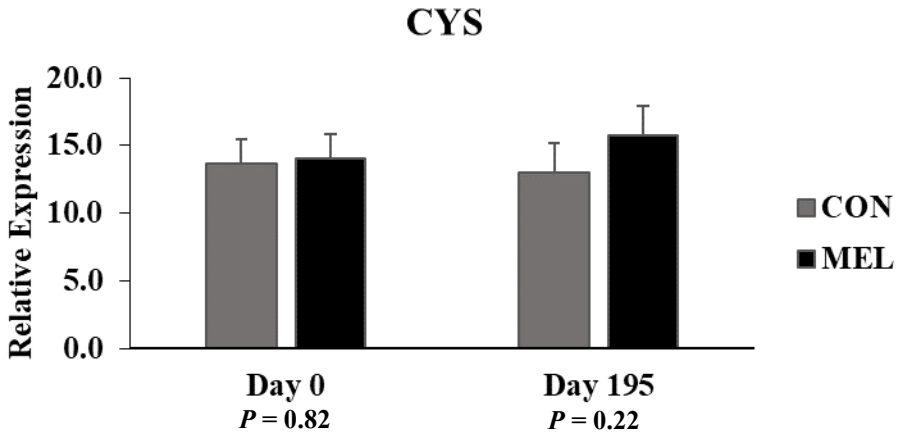

Figure 4.3 Relative expression (mRNA abundance) of cystatin in Longissimus dorsi from day 0 and day 195 offspring born from CON (n=15) or MEL (n=12) treated dams.

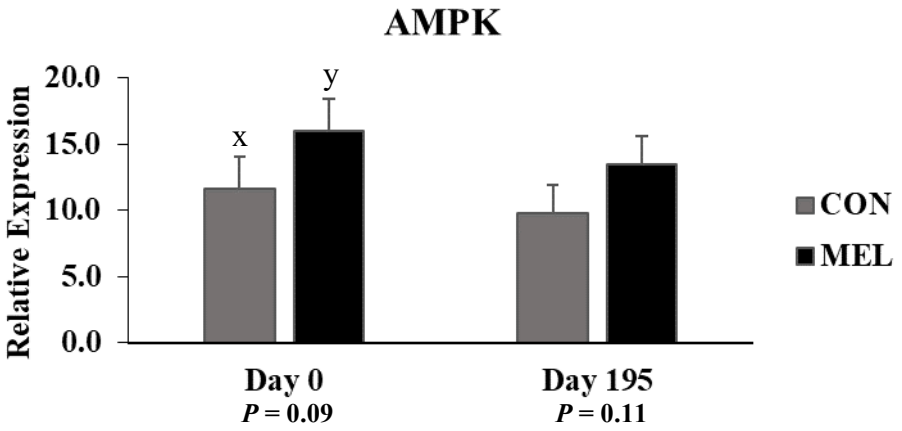

Figure 4.4 Relative expression (mRNA abundance) of adenosine monophosphate-activated protein kinase-α in Longissimus dorsi from day 0 and day 195 offspring born from CON (n=15) or MEL (n=12) treated dams. $^{x–y}$ Means within a row without common superscript represent tendencies *(*$P \geq 0.05$ and $P \leq 0.10$)

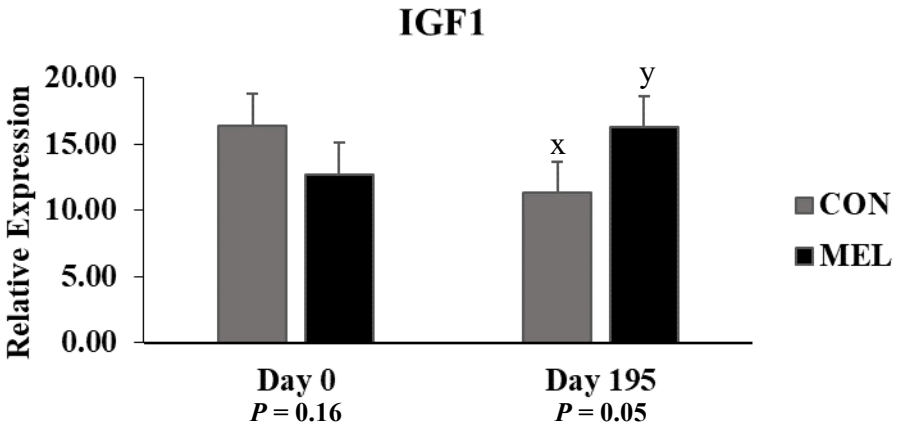

Figure 4.5 Relative expression (mRNA abundance) of Insulin-Like Growth factor 1 in Longissimus dorsi from day 0 and day 195 offspring born from CON (n=15) or MEL (n=12) treated dams. $^{x–y}$ Means within a row without common superscript represent tendencies *(*$P \geq 0.05$ and $P \leq 0.10$)

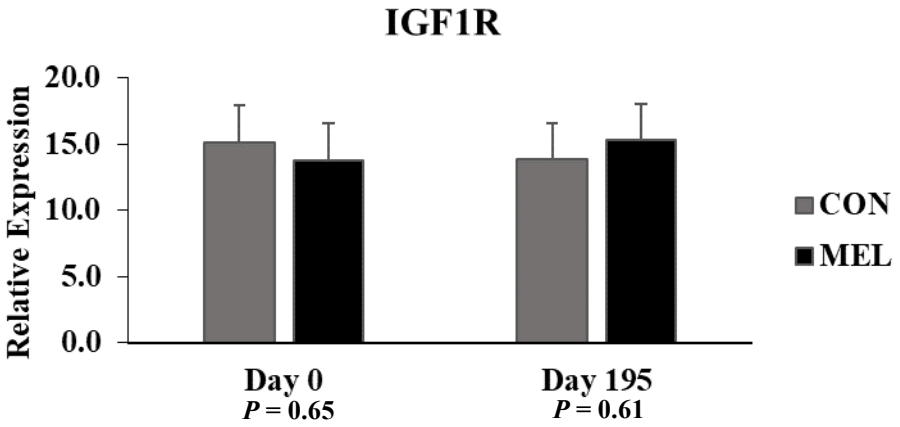

Figure 4.6 Relative expression (mRNA abundance) of Insulin-Like Growth factor 1 receptor in Longissimus dorsi from day 0 and day 195 offspring born from CON (n=15) or MEL (n=12) treated dams.

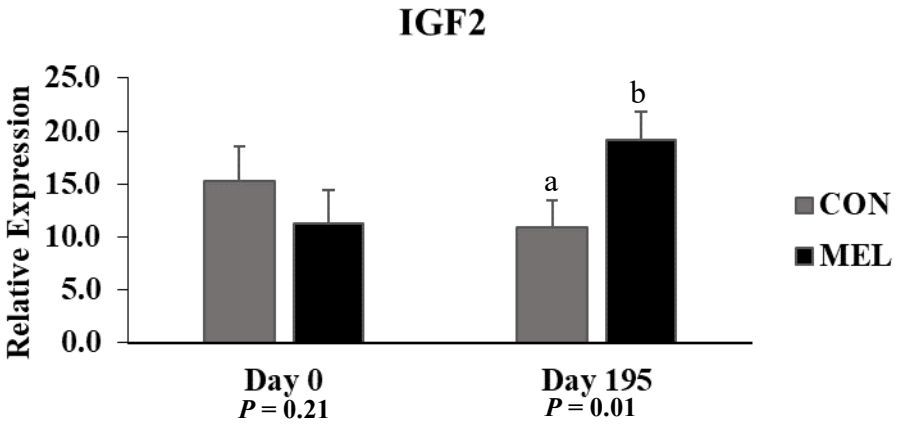

Figure 4.7 Relative expression (mRNA abundance) of Insulin-Like Growth factor 2 in Longissimus dorsi from day 0 and day 195 offspring born from CON (n=15) or MEL (n=12) treated dams. [a–b] Means within a row without common superscript differ *(P* < 0.05)

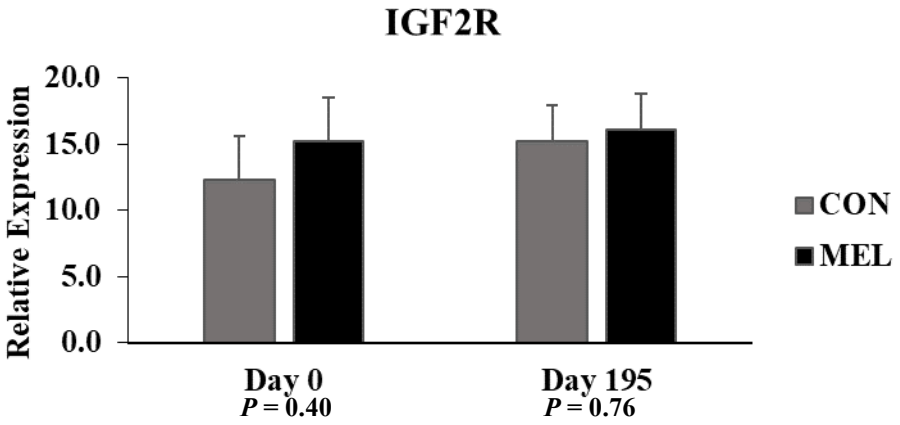

Figure 4.8 Relative expression (mRNA abundance) of Insulin-Like Growth factor 2 receptor in Longissimus dorsi from day 0 and day 195 offspring born from CON (n=15) or MEL (n=12) treated dams.

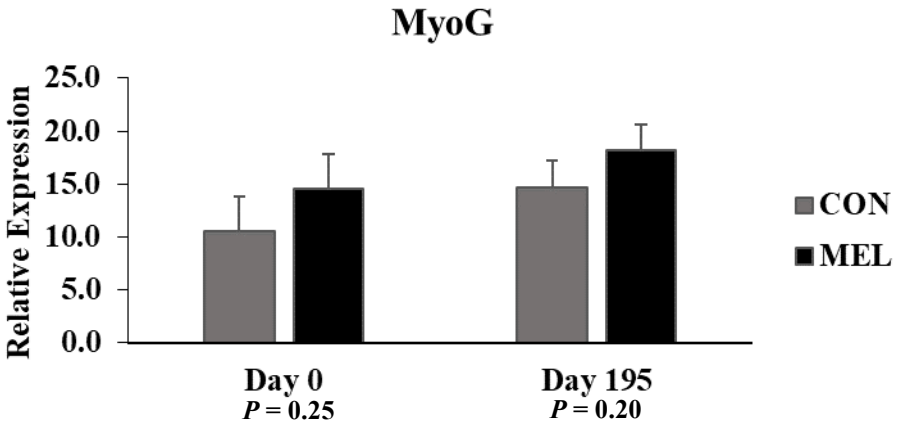

Figure 4.9 Relative expression (mRNA abundance) of myogenin in Longissimus dorsi from day 0 and day 195 offspring born from CON (n=15) or MEL (n=12) treated dams.

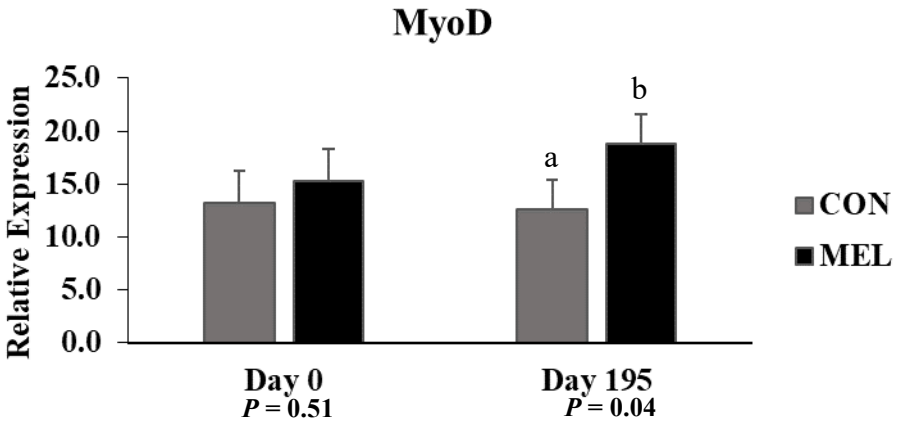

Figure 4.10 Relative expression (mRNA abundance) of myogenic differentiation 1 in Longissimus dorsi from day 0 and day 195 offspring born from CON (n=15) or MEL (n=12) treated dams. [a–b] Means within a row without common superscript differ *(P* < 0.05)

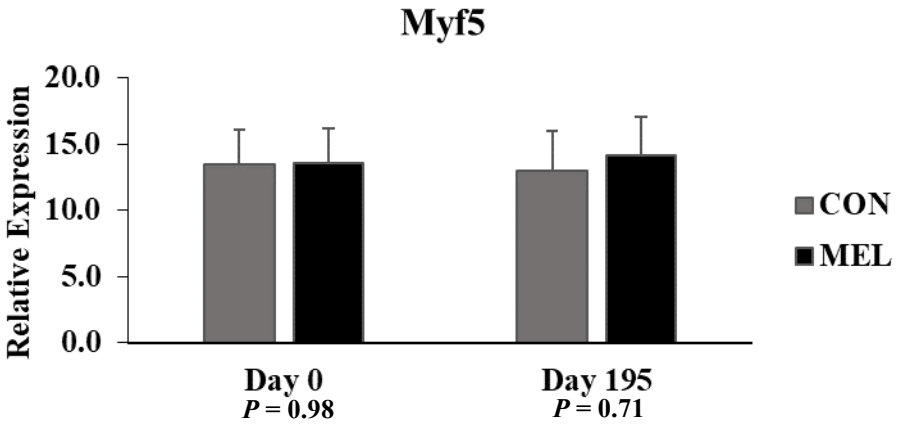

Figure 4.11 Relative expression (mRNA abundance) of myogenic factor 5 in Longissimus dorsi from day 0 and day 195 offspring born from CON (n=15) or MEL (n=12) treated dams.

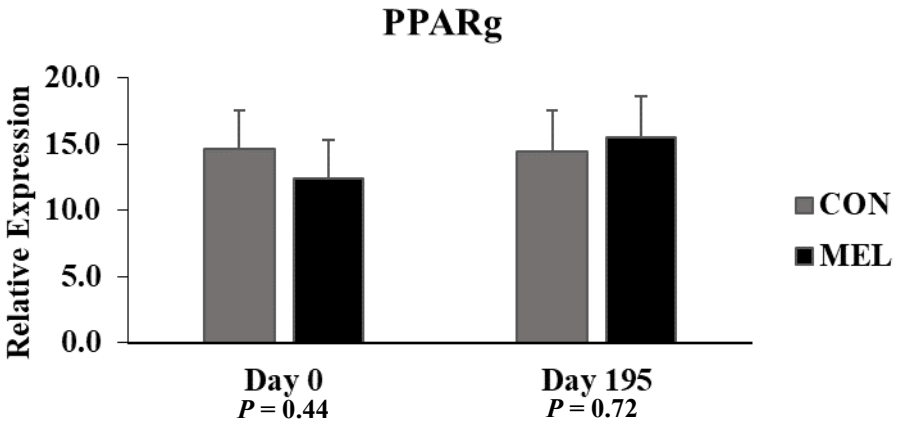

Figure 4.12 Relative expression (mRNA abundance) of peroxisome proliferator activated receptor gamma in Longissimus dorsi from day 0 and day 195 offspring born from CON (n=15) or MEL (n=12) treated dams.

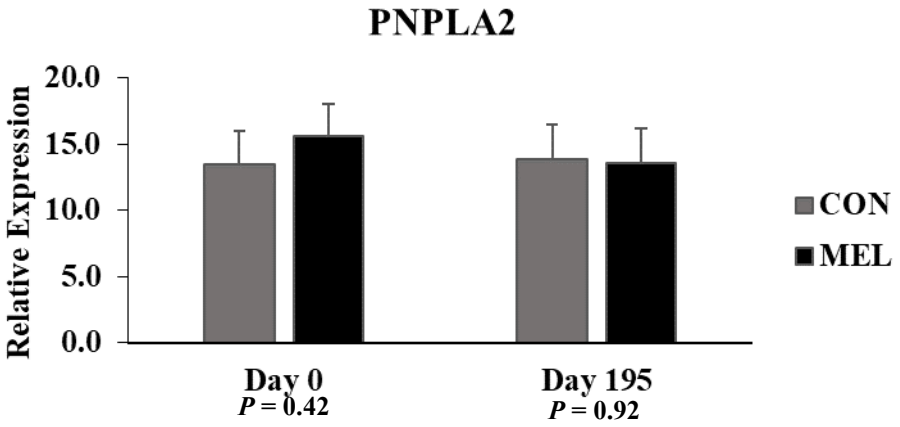

Figure 4.13 Relative expression (mRNA abundance) of patatin-like phospholipase domain containing 2 in Longissimus dorsi from day 0 and day 195 offspring born from CON (n=15) or MEL (n=12) treated dams.

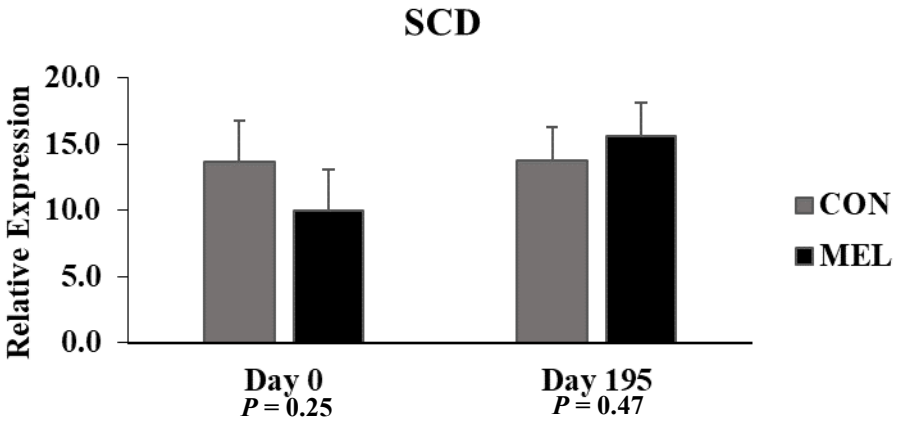

Figure 4.14 Relative expression (mRNA abundance) of stearoyl-CoA desaturase in Longissimus dorsi from day 0 and day 195 offspring born from CON (n=15) or MEL (n=12) treated dams.

4.6 References

Barton-Davis ER , Shoturma DI , Sweeney HL .Contribution of satellite cells to IGF-I induced hypertrophy of skeletal muscle.Acta Physiol Scand 167: 301-305, 1999

Bass, J., J. Oldham, M. Sharma, and R. Kambadur. 1999. Growth factors controlling muscle development. Dom. Ani. Endo. 17: 191-197

Beilhartz MW, Lareu R, Garrett KL, Grounds MD, Fletcher S. Quantitation of muscle precursor cell activity in skeletal muscle by Northern analysis of MyoD and myogenin expression: Application to dystrophic (MDX) mouse muscle. Mol. Cell. Neurosci. 1992;3:326–333

Braxton, L., Hollingshead P, Warburton C, Dowd M, Pitts-Meek S, Dalton D, Gillett N, Stewart T A. 1993. IGF-I is required for normal embryonic growth in mice. Genes Dev 7:2609–2617, pmid:8276243

Brockus, K. E., C. G. Hart, B. O. Fleming, T. Smith, S. H. Ward, C. O. Lemley. 2016. Effects of Supplementing Holstein Heifers with Dietary Melatonin during Late Gestation on Growth and Cardiovascular Measurements of their Offspring. Reprod. Dom. Anim. 51: 240-247; doi: 10.1111/rda.12672

Buonanno A, Apone L, Morasso MI, Beers R, Brenner HR, Eftimie R. The MyoD family of myogenic factors is regulated by electrical activity: Isolation and characterization of a mouse Myf-5 cDNA. Nucleic Acids Res. 1992;20:539–544.

Clark, D. L., Clark, D. I., Hogan, E. K., Kroscher, K. A. and Dilger, A. C. (2015). Elevated insulin-like growth factor 2 expression may contribute to the hypermuscular phenotype of myostatin null mice. Growth Horm. IGF Res. 25, 207-218

Dai N., Rapley J., Angel M., Yanik M. F., Blower M. D., Avruch J. (2011) mTOR phosphorylates IMP2 to promote IGF2 mRNA translation by internal ribosomal entry. Genes Dev. 25, 1159–1172

Dhawan, J., T.A. Rando Stem cells in postnatal myogenesis: molecular mechanisms of satellite cell quiescence, activation and replenishment Trends Cell Biol., 15 (2005), pp. 666-673

Du., M., J. Tong, J. Zhao, K. R. Underwood. M. Zhu, S. P. Ford, and P. W. Nathanielsz. 2010. Fetal programming of skeletal muscle development in ruminant animals. J. Anim. Sci. 88:E51–E60. doi:10.2527/jas.2009-2311

Duarte, M. S., M. P. Gionbelli, P. V. R. Paulino, N. V. L. Serão, C. S. Nascimento, M. E. Botelho, T. S. Martins, S. C. V. Filho, M. V. Dodson, S. E. F. Guimarães, and M. Du. 2014. Maternal overnutrition enhances mRNA expression of adipogenic markers and collagen deposition in skeletal muscle of beef cattle fetuses. J. Anim. Sci. 92:3846–3854. https://doi.org/10.2527/jas.2014-7568

Dubocovich, M.L., Yun, K., Al-Ghoul, W.M., Benloucif, S., Masana, M.I., 1998. Selective MT2 melatonin receptor antagonists block melatonin-mediated phase advances of circadian rhythms. FASEB J. 12, 1211–1220.

Dubocovich, M.L., Delagrange, P., Krause, D.N., Sugden, D., Cardinali, D.P., Olcese, J., 2010. International Union of Basic and Clinical Pharmacology. LXXV. Nomenclature, classification, and pharmacology of G protein-coupled melatonin receptors. Pharmacol. Rev. 62, 343–380.

Eftimie R, Brenner HR, Buonanno A. Myogenin and MyoD join a family of skeletal muscle genes regulated by electrical activity. Proc. Natl. Acad. Sci. USA. 1991;88:1349–1353.

Elliott JA, Bartness TJ, Goldman BD. Effect of melatonin infusion duration and frequency on gonad, lipid, and body mass in pinealectomized male Siberian hamsters. J Biol Rhythms 1989; 4: 439–455.

Erbay E., Park I. H., Nuzzi P. D., Schoenherr C. J., Chen J. (2003) IGF-II transcription in skeletal myogenesis is controlled by mTOR and nutrients. J. Cell Biol. 163, 931–936

Florini, J. R., K. A. Magri, D. Z. Ewton, P. L. James, K. Grindstaff, and P. S. Rotwein. 1991. "Spontaneous" differentiation of skeletal myoblasts is dependent upon autocrine secretion of insulin-like growth factor-II. J. Biol. Chem. 266:15917–15923

Funston, R. N., D. M. Larson, and K. A. Vonnahme. 2010. Effects of maternal nutrition on conceptus growth and offspring performance: Implications for beef cattle production. J. Anim. Sci. 88:E205-E215. doi:10.2527/jas.2009-2351

Ge, Y., J. Chen Mammalian target of rapamycin (mTOR) signaling network in skeletal myogenesis J Biol Chem, 287 (2012), pp. 43928-43935

Gardan, D., F. Gondret, M.K. Van den, N. Buys, S. De Smet, I. Louveau Lipid metabolism and cellular features of skeletal muscle and subcutaneous adipose tissue in pigs differing in IGF-II genotype Domest Anim Endocrinol, 34 (2008a), pp. 45-53

Gardan, D., Mourot, J., Louveau, I. Decreased expression of the IGF-II gene during porcine adipose cell differentiation. Mol Cell Endocrinol. 2008b;292:63–68

Glass D. J. (2010) Signaling pathways perturbing muscle mass. Curr. Opin. Clin. Nutr. Metab. Care 13, 225–229

Gluckman, P. D., Catherine S. Pinal; Regulation of Fetal Growth by the Somatotrophic Axis, The Journal of Nutrition, Volume 133, Issue 5, 1 May 2003, Pages 1741S–1746

Gonzalez, J. M., L. E. Camacho, S. M. Ebarb, K. C. Swanson, K. A. Vonnahme, AA. M. Stelzleni, and S. E. Johnson. 2013. Realimentation of nutrient restricted pregnant beef cows supports compensatory fetal muscle growth. J Anim. Sci. 91:4797–4806

Grand F. L. and M. A. Rudnicki. 2007. Skeletal muscle satellite cells and adult myogenesis.Curr Opin Cell Biol 19: 628-633

Ha E, Yim SV, Chung JH et al. Melatonin stimulates glucose transport via insulin receptor substrate-1/phosphatidylinositol 3-kinase pathway in C2C12 murine skeletal muscle cells. J Pineal Res 2006; 41:67–72.

Haig, D., and C. Graham. 1991. Genomic imprinting and the strange case of the insulin-like growth factor II receptor. Cell. 64:1045–1046

Hornberger T. A. (2011) Mechanotransduction and the regulation of mTORC1 signaling in skeletal muscle. Int. J. Biochem. Cell Biol. 43, 1267–1276

Huang Y. Yan X. Zhu M. J. McCormick R. J. Ford S. P. Nathanielsz P. W. Du M. 2010. Enhanced transforming growth factor-β signaling and fibrogenesis in ovine fetal skeletal muscle of obese dams at late gestation. Am. J. Physiol. Endocrinol. Metab. 298:E1254–E1260.

Hutcheson, D. A., J. Zhao, A. Merrell, M. Haldar, and G. Kardon. 2009. Embryonic and fetal limb myogenic cells are derived from developmentally distinct progenitors and have different requirements for beta-catenin. Genes Dev. 23:997–1013.

Karunaratne, J. F., C. J. Ashton, and N. C. Stickland. 2005. Fetal programming of fat and collagen in porcine skeletal muscles. J Anat. 207: 763-768

Koishi K , Zhang M , McLennan IS , Harris AJ. .MyoD protein accumulates in satellite cells and is neurally regulated in regenerating myotubes and skeletal muscle fibers..Dev Dyn 202: 244-254, 1995

Korhonen T, Mustonen AM, Nieminen P, Saarela S. Effects of cold exposure, exogenous melatonin and short-day treatment on the weight-regulation and body temperature of the Siberian hamster (Phodopus sungorus). Regul Pept 2008; 149: 60–66

Krauchi K., Cajochen C., Mori D., Graw A.T., Wirz-Justice A. (1997) Early evening melotonin and S20098 advance circadian phase and nocturnal regulation of core body temperature. Am J Physiol 272:R1178–R1188

Le Gouic S, Atgie C, Viguerie-Bascands N, Hanoun N, Larrouy D, Ambid L, Raimbault S, Ricquier D, Delagrange P, Guardiola-Lemaitre B, Pénicaud L, Casteilla L. Characterization of a melatonin binding site in Siberian hamster brown adipose tissue. Eur J Pharmacol 1997; 339: 271–278.

Le Roith, D., C. Bondy, S. Yakar, J. L. Liu, and A. Butler. 2001. The somatomedin hypothesis: 2001. Endocr. Rev. 22:53-57

Lemley, C. O., A. M. Meyers, L. E. Camacho, T. L. Neville, D. J. Newman, J. S. Caton, K. A. Vonnahme. 2012. Melatonin supplementation alters uteroplacental hemodynamics and fetal development in an ovine model of intrauterine growth restriction. Am. J. Physiol. Regul. Integr. Comp. Physiol. 302: 454–467; doi:10.1152/ajpregu.00407.2011

Lemley, C. O., L. E. Camacho, and K. A. Vonnahme. 2013. Uterine Infusion of Melatonin or Melatonin Receptor Antagonist Alters Ovine Feto-Placental Hemodynamics During Midgestation. Bio. of Repro. 89:41-49

Livak, K. J. and T. D. Schmittgen. 2001. Analysis of Relative Gene Expression Data Using Real-Time Quantitative PCR and the 2−ΔΔCT Method. Methods. 25:402-408

Machida S, Booth FW .Insulin-like growth factor 1 and muscle growth: implication for satellite cell proliferation.Proc Nutr Soc 63: 337-340, 2004

Nathanielsz, P. W., L. Poston, and P. D. Taylor. 2007. In utero exposure to maternal obesity and diabetes: Animal models that identify and characterize implications for future health. Clin. Perinatol. 34:515–526.18063102

Nixon, A. J., Choy, V. J., Parry, A. L., Pearson, A. J. (1993) Fiber growth initiation in hair follicles of goats treated with melatonin. J. Exp. Zool. 267,47-56

Pechanova O, Paulis L, Simko F. Peripheral and central effects of melatonin on blood pressure regulation. Int J Mol Sci 2014; 15:17920–17937

Puchalski SS, Green JN, Rasmussen DD. Melatonin effect on rat body weight regulation in response to high-fat diet at middle age. Endocrine 2003; 21: 163–167

Raskind MA, Burke BL, Crites NJ, Tapp AM, Rasmussen DD. Olanzapine-induced weight gain and increased visceral adiposity is blocked by melatonin replacement therapy in rats. Neuropsychopharmacology 2007; 32: 284–288

Rehfeldt, C. and Kuhn, G. Consequences of birth weight for postnatal growth performance and carcass quality in pigs as related to myogenesis. J. Anim. Sci. 2006; 84: 113–123

Richter, H. G., J. A. Hansell, S. Raut, and D. A. Giussani. 2009. Melatonin improves placental efficiency and birth weight and increases the placental expression of antioxidant enzymes in undernourished pregnancy. J. Pineal. Res. 46:357–364.

Stratos I, Richter N, Rotter R et al. Melatonin restores muscle regeneration and enhances muscle function after crush injury in rats. J Pineal Res 2012; 52:62–70.

Wang, B., X. Fu, X. Liang, Z. Wang, Q. Yang, W. Nie, J. Zhao, P. Gao, M.J. Zhu, J.M. De Avila, J.W. Maricelli, B.D. Rodger, and M. Du. 2017. Maternal retinoids increase PDGFRα progenitor population and beige adipogenesis in progeny by stimulating vascular development. E. Bio. Medicine. 18:288–299. doi:10.1016/j.ebiom.2017.03.041

Wang XH, Mitch WE. Mechanisms of muscle wasting in chronic kidney disease. Nature reviews Nephrology. 2014;10(9):504–516

Yablonka-Reuveni, Z. (1995). Development and Postnatal Regulation of Adult Myoblasts. Microscopy Research and Technique, 30(5), 366–380. http://doi.org/10.1002/jemt.1070300504

Zhu, M. J., S. P. Ford, W. J. Means, B. W. Hess, P. W. Nathanielsz, and M. Du. 2006. Maternal nutrient restriction affects properties of skeletal muscle in offspring. J. Physiol. 575:241–250.16763001